EVALUATION OF HIGH STRENGTH LIGHTWEIGHT CONCRETE PRECAST, PRESTRESSED BRIDGE GIRDERS

A Thesis
Presented to
The Academic Faculty

By

Jennifer Dunbeck

In Partial Fulfillment
Of the Requirements for the Degree
Master of Science in Civil and Environmental Engineering

Georgia Institute of Technology
May 2009

EVALUATION OF HIGH STRENGTH LIGHTWEIGHT CONCRETE

PRECAST, PRESTRESSED BRIDGE GIRDERS

Approved by:

Dr. Lawrence F. Kahn, Advisor
School of Civil and Environmental Engineering
Georgia Institute of Technology

Dr. Kimberly E. Kurtis
School of and Environmental Engineering
Georgia Institute of Technology

Dr. Reid W. Castrodale
Director of Engineering
Carolina Stalite Company

Date Approved: April 1, 2009

ACKNOWLEDGEMENTS

No accomplishment is the result of a single person, but rather the collective work of a body of people all pushing the one to succeed. This thesis could not have been accomplished without these wonderful people, whom I am honored to thank.

My husband, Andrew, was the first one to encourage me to pursue another degree. Thank you for believing in me, for enjoying every stage of life with me, and encouraging me when I felt defeated. I could not have finished without you.

My parents cannot be thanked enough. They have sacrificed for me and encouraged me in everyway. Thanks to my Mom, who is my endless cheerleader, and to my Dad, who is always ready to help me in any way he can. You two have modeled for me what it means to live a Christian life, and have always encouraged my ceaseless questions. Thank you for your unconditional love.

I would like to thank many of my fellow graduate students here at Georgia Tech. Thanks to Brett Holland for his countless hours on this research that we shared. Enjoy the next two years of it. Thanks to Robert Moser, Jonathan Hurff, Victor Garas, and Kennan Crane for helping in so many ways. Thanks for coming to the concrete pours, and for helping with the testing in the lab. Thanks for letting me ask dozens and dozens of questions. Thanks to my office mates, Ben Deaton, Mustafa Can Kara, Jong Han Lee, Jennifer Modugno, Efe Guney, and Katherine Snedecker. Y'all have always been so encouraging and made this a happy place to work.

Thanks to Standard Concrete Products for their willingness to work with us. They were always willing to help us, even when we delayed their schedule. Thank you for helping us accomplish this research.

Many thanks to Dr. Reid Castrodale who was an invaluable committee member. His recommendations not only improved the content of the thesis, but also its quality as a complete work. Thank you for being so generous with your time and detailed in your remarks. Your comments turned this thesis into a valuable source of information. I can't thank you enough.

Dr. Kimberly Kurtis was also generous enough to be on my committee. Thank you for your suggestions and remarks even during such a busy time for you and your staff.

I would especially like to thank my advisor, Dr. Lawrence Kahn, for giving me this opportunity. His wisdom and insight have been the most educational parts of my degree. His patience with me has been amazing. Thank you for your open door policy and for helping me to succeed. I cannot tell you how much I appreciate your generosity.

TABLE OF CONTENTS

LIST OF TABLES

LIST OF FIGURES

SUMMARY

This thesis evaluates the use of High Strength Lightweight Concrete (HSLW) in bridge girders for the I-85 Ramp "B" Bridge crossing SR-34 in Cowetta County, Georgia. This bridge consisted of four spans; all girders were constructed using lightweight expanded slate aggregate. Spans 2 and 3 had a design strength of 10,000 psi, and span 2 was chosen for this research. The BT-54 girders were 107 ft 11½ inches in length. The prestressing strands used in these girders were 0.6 in diameter, grade 270, low relaxation strands. Material properties and member properties were tested.

All 5 girders of span 2 were instrumented with vibrating wire strain gages at midspan, as well as with DEMEC inserts for transfer length measurements and with a deflection measurement system. Transfer length measurements found the transfer length of the girders to be 23% less than the values suggested by AASHTO and ACI equations. The deflection measurements showed 4.26 inches of camber at 56-days while the girders were stored at Standard Concrete Products. The camber measurements matched theoretical predictions within 5%. Mechanical property tests found the concrete to be within all design requirements.

A stiffness, load test was performed on each of the 5 girders at Standard Concrete Products. The average stiffness value of 8.428×10^6 kip ft^2 is recommend for use by GDOT engineers in designing the deck and road profile.

This thesis discusses all short term findings from construction to the end of storage. A later report will address long term issues such as creep and shrinkage, as well as the performance of the girders as part of the bridge.

CHAPTER 1

INTRODUCTION

High strength concrete is commonly used in pretensioned bridge girders to provide longer spans. However, these long girders often are too heavy to travel on current infrastructure and require a super-load permit for transportation between the precasting plant and the bridge site. High Strength Lightweight (HSLW) concrete girders can provide the needed length at a reduced load that does not require a super-load permit. (Meyer and Kahn, 2002) Longer spans, reduced transportation time, and reduced expense lead to more economical girders and bridges, and in some cases provide girders to regions where only lightweight girders can be delivered.

1.1 Purpose and Objectives

The overall purpose of this research is to evaluate the behavior of a highway bridge constructed with precast prestressed girders made using HSLW concrete. Specific objectives are to (1) assist Georgia Department of Transportation (GDOT) materials engineer in developing specific conventional specifications for high strength lightweight concrete, (2) instrument prestressed bridge girders and composite bridge deck, (3) evaluate the girder concrete short and long-term properties, (4) measure the short and long-term bridge deflection and girder strain behavior, (5) determine prestress losses, and (6) determine the stiffness of the girders so the deck can be properly profiled.

1.2 Scope

The results of this research will be presented in two reports. This report will address the short-term results of the research including the construction and instrumentation of the girders, the evaluation of short-term properties, and measuring of short-term deflections. A later report will address the long-term properties and long-term deflections and strains as well as the prestress losses of the girders. Both reports will be useful for development of GDOT specifications for HSLW concrete.

1.3 Bridge Description

GDOT selected the I-85 Ramp "B" Bridge over SR-34, Bullsboro Drive, in Cowetta County as a bridge to be constructed using HSLW concrete girders. This GDOT designed bridge called for lightweight concrete in all four spans. Spans 1 and 4 had a design strength of 5,000 psi, while spans 2 and 3 had a design strength of 10,000 psi. Research was conducted on the 5 girders of span 2 of this bridge, which are shown in Figures 1.1 and 1.2. Figure 1.3 shows the elevation view of the bridge and Figure 1.4 shows the cross-section view of the bridge and girders. The bridge had a skew angle of 39.86˚.

The span 2 girders were all BT-54, and were 107 feet 11½ inches in length, with a bearing length of 106 feet 8-7/8 inches. The girders rested on elastomeric bearing pads that were 10"x 20"x 2-3/8". All diaphragms were cast in place. The prestressing strands were harped at a single point in the middle of each girder. The strand layout of the girders is shown in Figure 1.5. Girders were numbered by GDOT as shown in Figure 1.2

from top to bottom 2.1, 2.2, 2.3, 2.4, and 2.5. For this report these girders will be referred to as girders 1, 2, 3, 4, and 5 respectively.

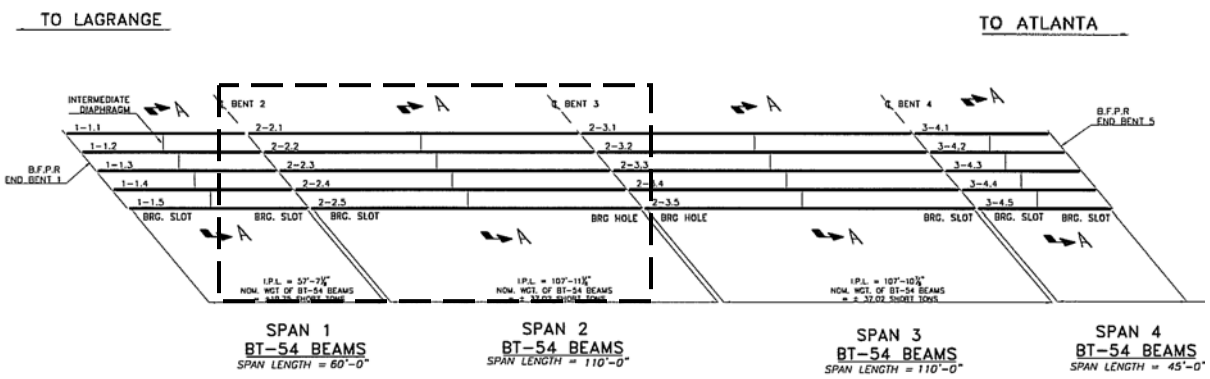

Figure 1.1 I-85 Ramp "B" Bridge over SR-34, Bullsboro Drive

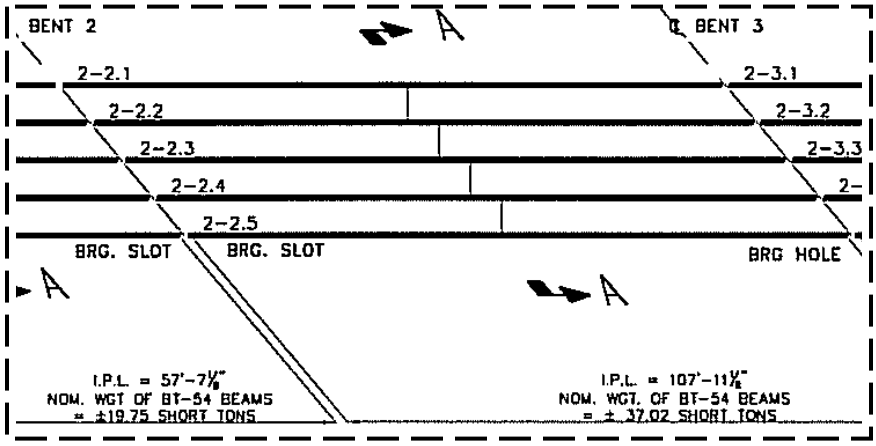

Figure 1.2 Magnified view of Figure 1.1 detailing Span 2

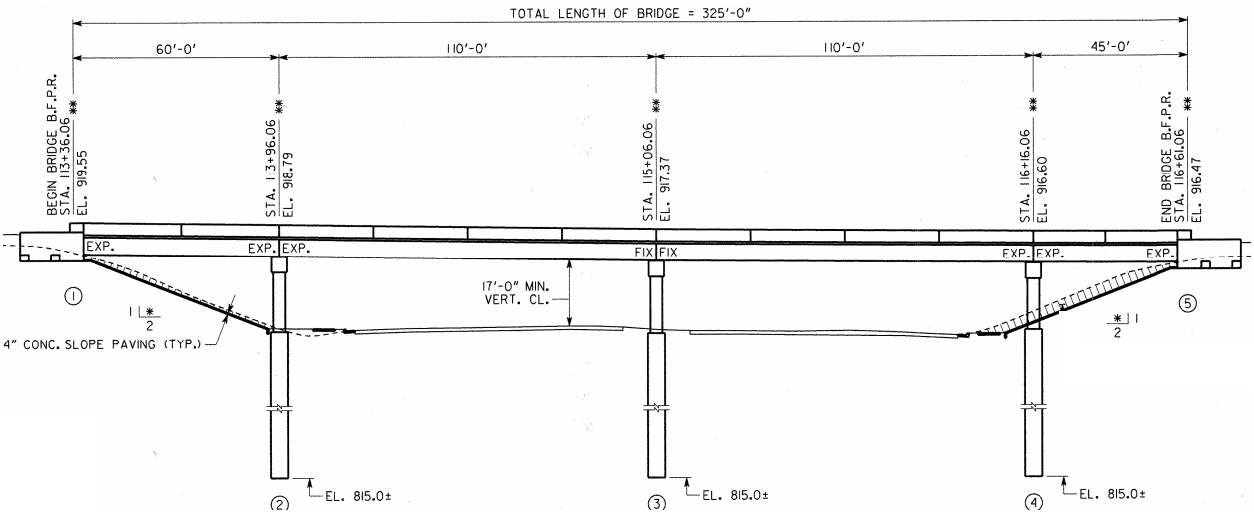

Figure 1.3 Elevation view of bridge

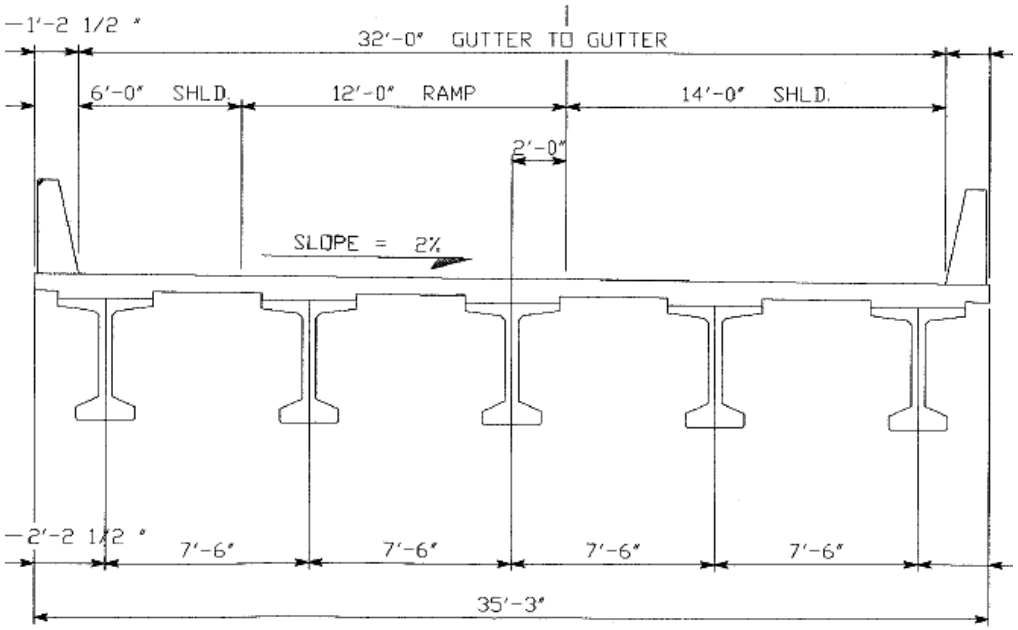

Figure 1.4 Bridge cross section showing all 5 girders

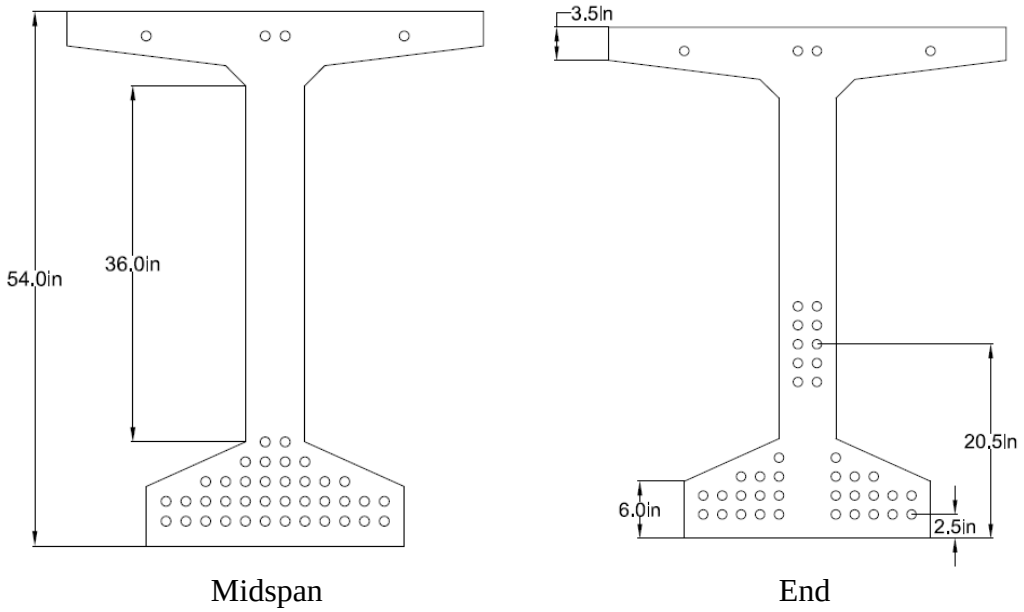

Figure 1.5 Strand layouts at midspan and end for AASHTO BT-54 girders

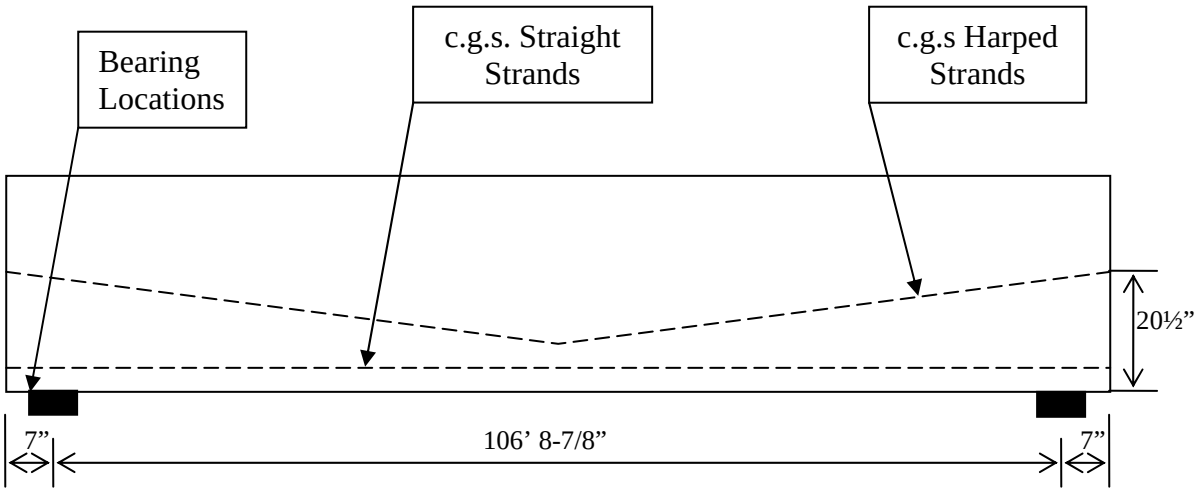

Figure 1.6 Elevation view of prestressing strands in girder

1.4 Research and Organization

This paper first reviews past research related to HSLW concrete, primarily previous research conducted as part of the "Lightweight Concrete for High Strength/High Performance Precast Prestressed Bridge Girders" project sponsored by the GDOT. Chapter 3 discusses the instrumentation used; the discussion of girder construction in Chapter 4. Chapters 5 through 7 discuss data collected from the girders. A testing of all 5 girders to determine stiffness is discussed in Chapter 8. Chapters 9 through 11 cover several issues that arose during the research as well as the results, conclusions and recommendations of this report.

CHAPTER 2

BACKGROUND

2.1 Introduction

The Georgia Department of Transportation (GDOT) sponsored the research project "Lightweight Concrete for High Strength/High Performance Precast Prestressed Bridge Girders" at the Georgia Institute of Technology. This research was conducted in several phases, and the results were published in various journals and research project reports. This chapter discusses this research and its findings. It also discusses the choice and trial batch of the mix design used for this research and research by Castrodale and Harmon (2007).

2.2 Need for HSLW Concrete

Meyer and Kahn (2002) performed an analytical study to investigate the possible benefits of High Strength Lightweight (HSLW) concrete. The goal of the research was to achieve a 150 foot girder with a gross vehicle weight, being the weight of the girder plus the weight of the tractor trailer, less than 150 kips. Loads over this 150 kips limit require super-permits in the state of Georgia. A second goal of the research was to have a girder spacing of at least 7 feet. This increased spacing could reduce the number of girders required for a bridge.

The study considered AASHTO girders Types II through V, AASHTO-PCI bulb-tee sections BT54, BT63, and BT72 as well as the modified bulb-tee sections where the

depths are increased 2-inches. Concrete strengths of 8,000, 10,000, and 12,000 psi were considered using expanded slate lightweight aggregate. Using and modifying GDOT bridge design software, Meyer and Kahn were able to analyze each section, while making minimal assumptions.

The conclusions of the study were as follows. The use of HSLW concrete has the potential to increase AASHTO girder lengths by up to 4% and AASHTO-PCI bulb-tee girders by up to 3%. For spans between 125 and 155 feet, HSLW concrete can be used to reduce the gross vehicle weight to less than 150 kips when a similar normal weight section would have exceeded this limit. The use of HSLW concrete has no appreciable benefit for AASHTO Type II and III girders. The use of HSLW can extend modified bulb-tee girder lengths by up to 10 feet over that of a normal weight bulb-tee of the same size. Lastly, for girders over 105 feet in length, AASHTO-PCI bulb-tees, both standard and modified, provided longer spans at less weight than standard AASHTO girders.

2.3 Mix Design and Resulting Material Characteristics

Buchberg (2002) investigated and developed high-strength lightweight mix designs made with materials available in Georgia. His three recommended mixes were for 8,000, 10,000, and 12,000 psi concrete made with expanded slate aggregate. He investigated over 75 mixes, which were then narrowed down using conditions favorable to HSLW concrete. The final three mix designs were batched both in the laboratory and at Tindall Precast Company for comparison. The 3 mix designs are shown in Table 2.1. Using samples from these batches the mechanical properties of the mixes were determined. Properties considered included: compressive strength, modulus of elasticity,

Poisson's ratio, modulus of rupture, rapid chloride permeability, drying shrinkage, creep, and coefficient of thermal expansion. Buchberg also considered curing temperature, specimen dimensions, and curing method in this study. Test results from field batch, ASTM cured concrete specimens are shown in Table 2.2.

Table 2.1 Three mix designs found by Buchberg

Material	Units	8,000 psi	10,000 psi	12,000 psi
Type III cement	lbs	783	765	740
Class "F" flyash	lbs	142	146	150
Silica fume	lbs	19	49	100
Normal weight fine aggregate	lbs	947	955	955
½ inch Stalite aggregate	lbs	1022	1030	1030
Water	gallons	32.1	29.9	27.3
Water/Cementitious Ratio	W/CM	0.28	0.26	0.23
Water reducer	fl oz	57	58	59
Superplasticizer	fl oz	57	65	139
Air entrainer	fl oz	9.4	9.6	7.5
Theoretical Wet Unit Weight	pcf	115.6	116.2	116.6

Table 2.2 Field batched ASTM cured concrete mechanical properties at 56 days

	Units	8,000 psi	10,000 psi	12,000 psi
Compressive Strength	psi	11,090	11,300	11,620
Elastic Modulus	ksi	4,130	4,260	4,400
Poisson's Ratio	-	0.1869	0.1856	0.1852
Chloride Permeability	coulombs category	664 Very Low	300 Very Low	99 Negligible
Plastic Unit Weight	lb/ft^3	118.6	121.0	124.0

Buchberg first concluded that silica fume was effective in increasing the early strengths of lightweight concrete as well as the late strengths. Second, chloride permeability of HSLW concrete made with Stalite expanded slate lightweight aggregate

was very low as defined by ASTM C1202. Third, the 8,000 and 10,000 psi mixes were obtainable in the laboratory and in the field, but the 12,000 psi mix was not.

Meyer (2002) expanded Buchberg's research by applying these mix designs to construct six AASHTO Type II prestressed girders using 0.6-inch diameter low relaxation strands. These girders were made with the 8,000 and 10,000 psi mixes using expanded slate lightweight concrete. Meyer tested the flexural and shear behavior of the girders, as well as the transfer length and development length of the strands.

Meyer concluded that the transfer length of strands in HSLW concrete did not differ from those in normal weight high performance concrete with initial strengths over 6,000 psi. He found that both ACI and AASHTO overestimated transfer lengths by more than 40% each. Meyer developed equations for both transfer length and modulus of elasticity to better fit HSLW concrete.

2.4 Mix Selection and Test Batch at SCP

Although the 12,000 psi mix used in both Buchberg's and Meyer's research did not meet the goal strengths, it did produce the highest strengths of the 3 mixes. For this reason it was chosen as the mix design for this research, with a goal strength set at 10,000 psi. Table 2.3 shows the volumes of materials needed for this mix and the resulting unit weight.

Table 2.3 Materials needed to make one cubic yard of HSLW concrete

Material	Units	12,000 psi
Type III cement	lbs	740
Class “F” flyash	lbs	150
Silica fume	lbs	100
Normal weight fine aggregate	lbs	955
½ inch Stalite aggregate	lbs	1030
Water	gallons	27.3
Water/Cementitious Ratio	W/CM	0.23
Water reducer	fl oz	59
Superplasticizer	fl oz	139
Air entrainer	fl oz	7.5
Theoretical Wet Unit Weight	pcf	116.6

In preparation for the casting of the girders for this research, two test batches of HSLW concrete were produced at Standard Concrete Products (SCP). The mix design was slightly adjusted for use at SCP, as given in Table 2.3. A key difference was the use of a different brand of admixtures. Research by Buchberg and Meyer used Grace Construction Products for all admixtures and silica fume. SCP used Sika admixtures and silica fume for this test batch as well as in the girders. Table 2.3 shows the materials used in the trial batches, and Table 2.4 shows the aggregate specific gravities. SCP batch reports are shown in Appendix A.

Table 2.4 Materials used at SCP to make one cubic yard of HSLW concrete

Material	Units	SCP HSLW Mix
Type III cement	lbs	740
Class “F” flyash	lbs	150
Silica fume	lbs	100
Normal weight fine aggregate	lbs	931.6
½ inch Stalite aggregate	lbs	980
Water	gallons	32
Water/Cementitious Ratio	W/CM	0.27
Water reducer	fl oz	29.7
Superplasticizer	fl oz	59.4
Air entrainer	fl oz	2
Accelerator	fl oz	148.5
Actual Wet Unit Weight	pcf	121

Table 2.5 Specific Gravity of products used at SCP

Material	Specific Gravity
Normal weight fine aggregate	2.60
½ inch Stalite aggregate	1.50

Compression specimens were taken from these concrete batches and tested at 18 hours, 7, 28, and 56 days by SCP Quality Control personnel. These tests showed actual wet unit weights of 122 and 120 lbs per cubic foot, and compressive strengths as listed in Figure 2.1. The water-to-cement ratio was higher in the trial batch than in Buchberg’s research, but the mix design was approved due to the adequate strengths achieved by the compression tests.

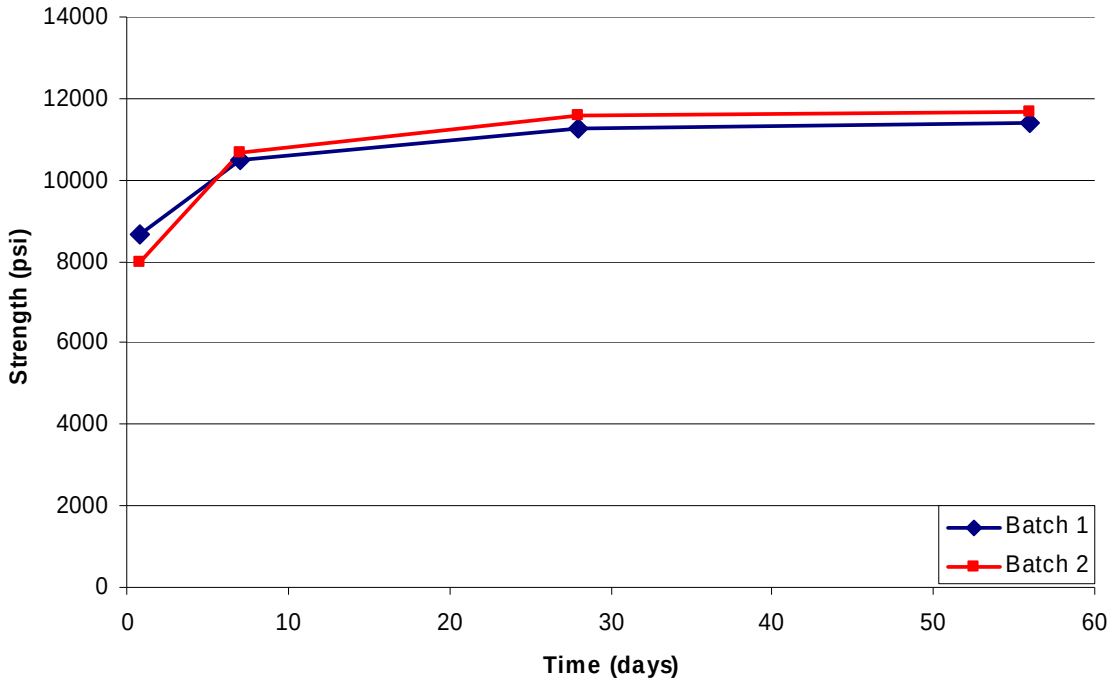

Figure 2.1 Compressive strengths of SCP test batches

2.5 Bridge Elements Constructed with Lightweight Concrete

Castrodale and Harmon (2007) summarized past performance of bridge elements constructed with lightweight aggregate. Their report discussed several recent projects that used lightweight concrete, and the main benefit in its use. Bridge girders are discussed as well as columns and pier caps.

CHAPTER 3

INSTRUMENTATION

3.1 Introduction

The girders were instrumented to collect information on camber and deflection, internal strains, internal temperatures, prestressing force, and transfer length. Four main systems were used to gather this information: vibrating wire strain gages for internal strain and temperature, external load cells for prestressing force verification, taut wire system for initial camber measurements, and a prestressing strand transfer length system.

3.2 Vibrating Wire Strain Gages

Geokon Vibrating Wire Strain Gages (VWSG) were used to determine strains inside the girders. The internal strains were needed to determine long-term prestress concrete losses, such as creep and shrinkage. These gages use a small wire held taut inside a dog bone shaped steel cylinder, shown in Figure 3.1. The wire is excited by a signal sent from a computer, and the change in vibration shows the relative change in strain surrounding the gage. Five VWSG were used at midspan of each girder. They were arranged with two gages in the bottom flange, one in the web, and two in the top flange, as shown in Figure 3.2. The numbering system used for the gages is also shown in Figure 3.2. Each gage was numbered by the girder it was located in followed by its location in the girder. For example, gages 2-1 through 2-5 were located in girder 2 according to Figure 3.2 placement. The end of the wire coming from each gage was

labeled with a small green flag containing the gage number, shown in Figure 3.3. Also, a series of lines were drawn on the wire itself to show its number in the event that the flag was lost.

In the future, two more VWSG will be place in the deck directly above midspan of each girder. These final two gage locations will be called D1 and D2, preceded by the beam number, as shown in Figure 3.2.

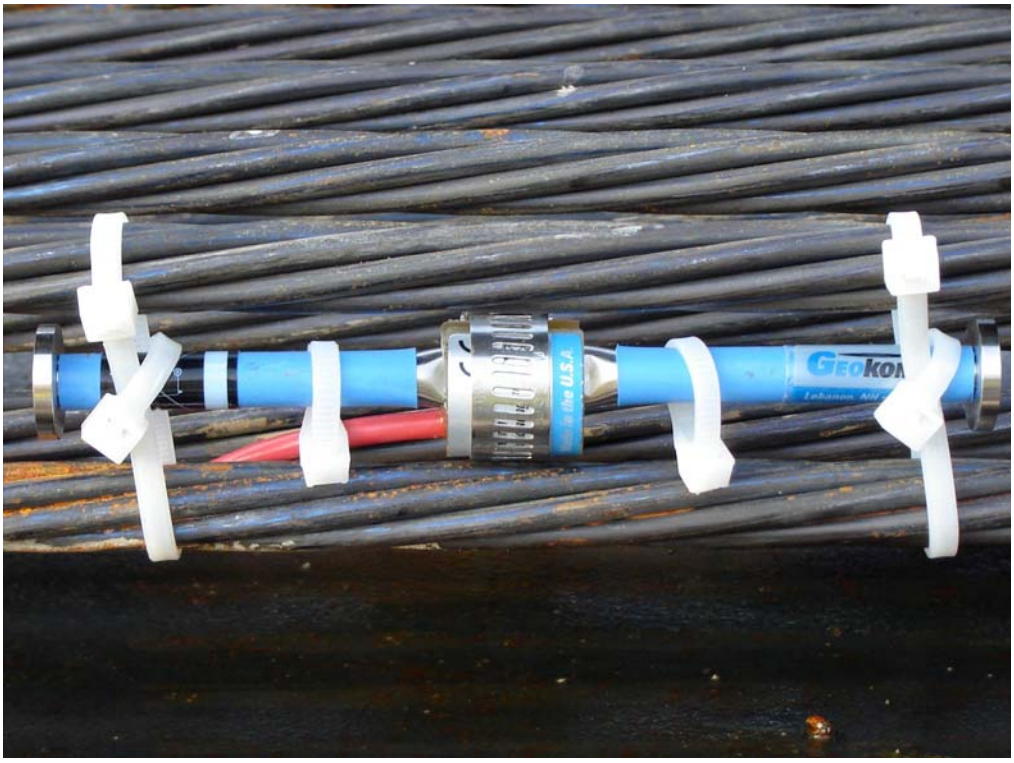

Figure 3.1 VWSG used in girders

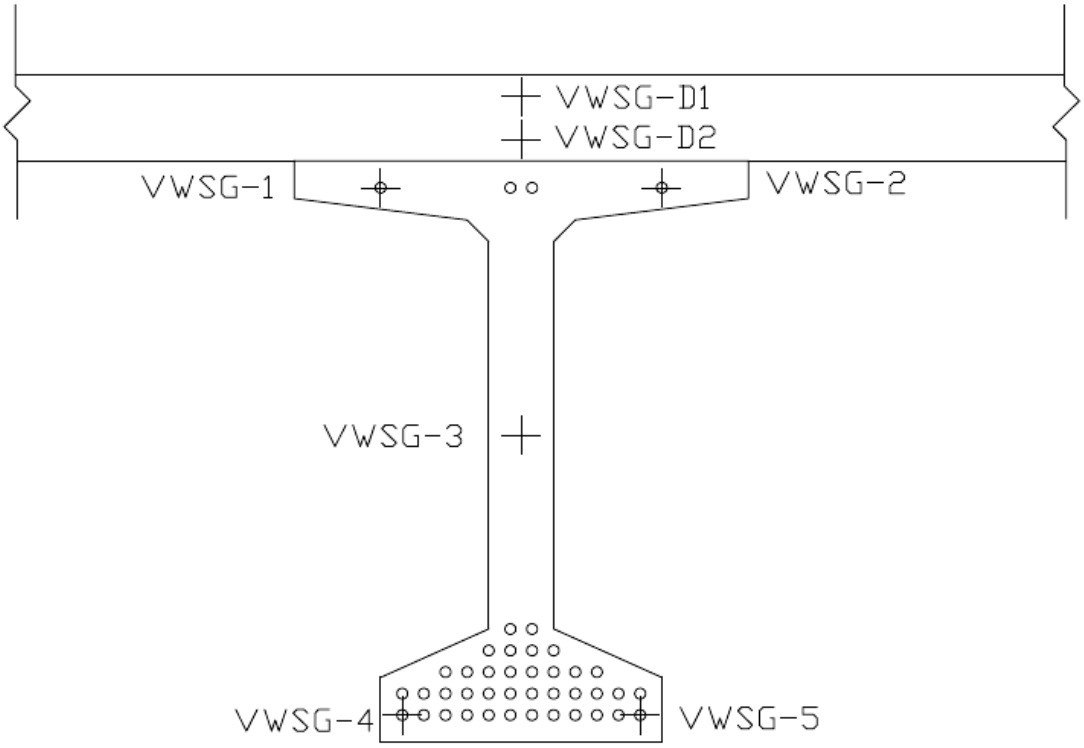

Figure 3.2 VWSG locations inside BT-54 girder and in deck above

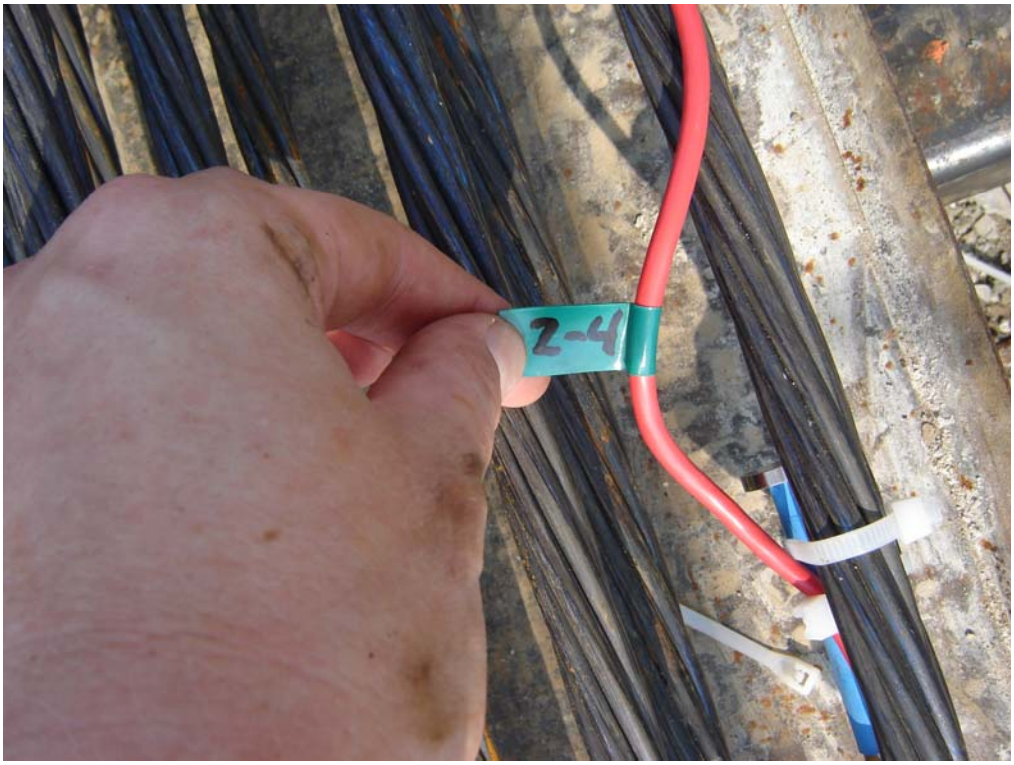

Figure 3.3 Green flag labeling gage 2-4

The VWSG were placed in their locations during the construction of the girders. Each gage was secured between two prestressing tendons, or directly to a prestressing tendon with plastic zip ties. The wires were run to the center of the girder and up and out the top of the beam in one bundle. The majority of the wires were left on spools. Each spool was also labeled with the corresponding gage number. The spools were organized together on a single rod directly above the sensors during construction. Figures 3.4 through 3.6 show the final placement of gages.

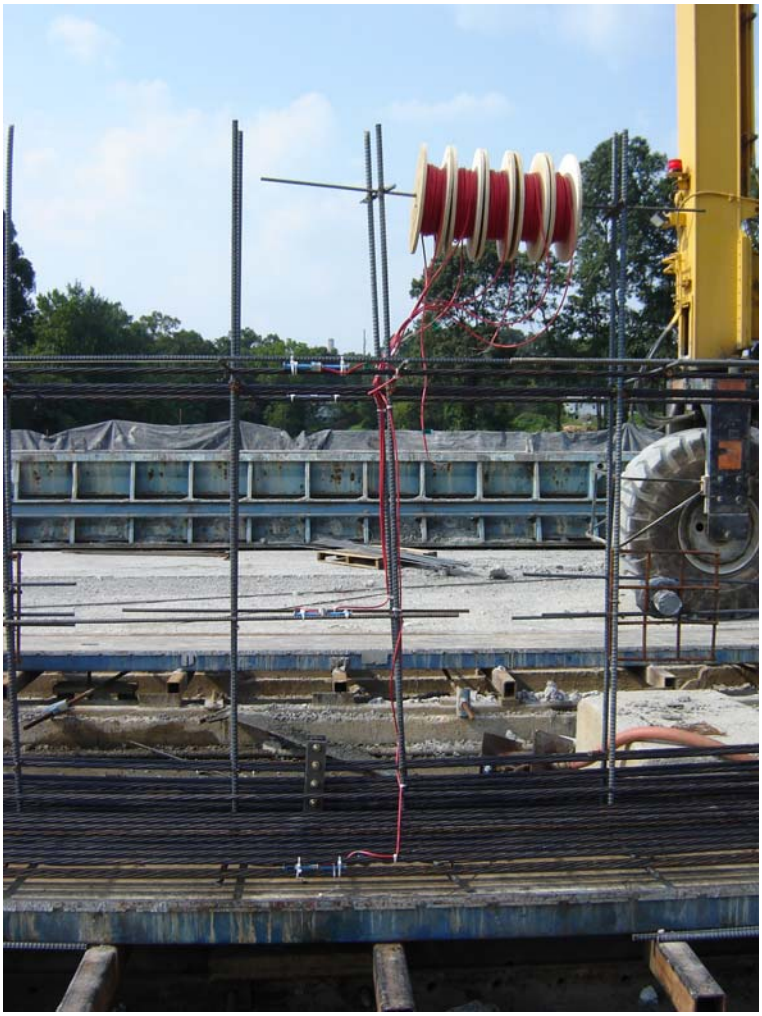

Figure 3.4 Gages in place with wires running up to bundled spools of wires above

Figure 3.5 VWSG secured with one side of forms placed

Figure 3.6 Researcher Brett Holland securing VWSG at midheight of girder

3.3 Load Cells

The first pour was for girders 1, 2, and 3 in the layout shown in Figure 3.7. For this pour load cells were used to measure the force in 8 prestressed tendons as shown in Figure 3.8. These load cells were calibrated prior to use on a calibrated MTS Universal testing machine. The load cells were aluminum cylinders with a hollow core large enough for the prestressing strand to fit through. The load cells were placed on the dead end of the prestressing strand between the chuck and the anchor abutment, as shown in Figures 3.9 and 3.10.

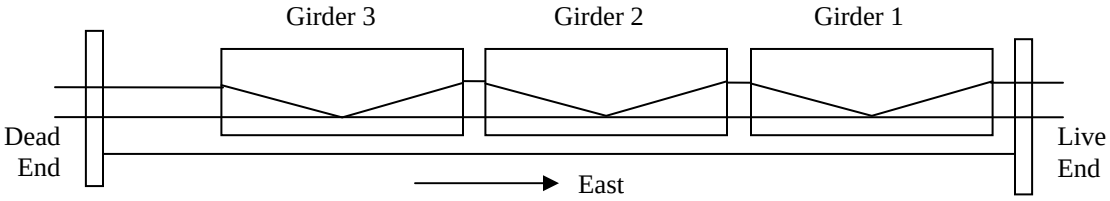

Figure 3.7 Pour 1 layout of girders

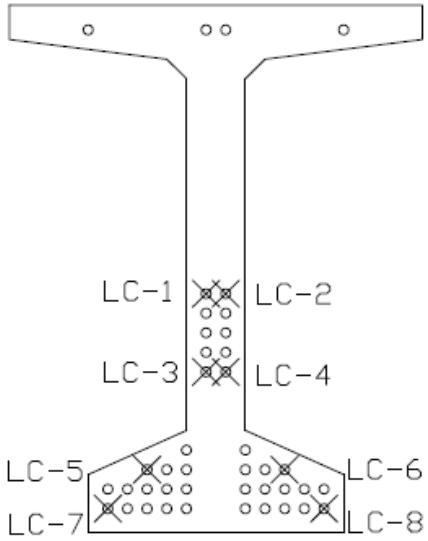

Figure 3.8 Load cell locations

Figure 3.9 Dead end abutment with prestressing strands and load cells in place

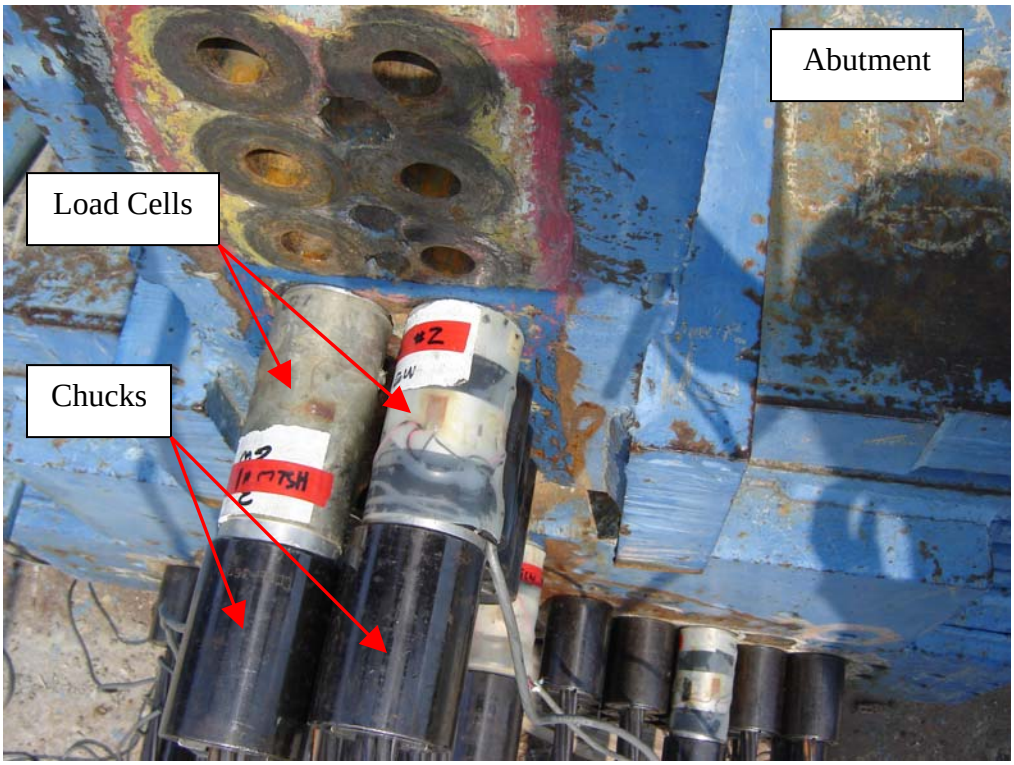

Figure 3.10 Load cells placed between chuck and abutment

All load cell readings were taken with a strain indicator box. Readings were taken before the load cell was placed on the strand, to acquire a zero reading. The strands were pulled, and readings were taken upon completion of all prestressing. The data collected from the load cells was processed to find resulting strand load values. These values are compared with jacking values recorded by SCP in Table 3.1. Figure 3.11 displays the numbering convention used by SCP. The black dots represent strands that also had load cells. Table 3.2 highlights the strands monitored with load cells during pour 1.

Table 3.1 Load on strands from initial pull as recorded by load cells and SCP

	Pour 1	
	SCP Report	Load Cell
	(kips)	(kips)
1A	44.50	40.11
1B	45.00	
1C	45.00	
1D	44.50	
1E	44.50	
1H	45.00	
1I	44.50	
1J	44.50	
1K	45.00	
1L	44.50	37.95
2A	44.50	
2B	44.50	
2C	44.50	
2D	44.00	
2E	45.00	
2H	44.50	
2I	44.50	
2J	44.50	
2K	44.50	
2L	44.00	
3C	44.50	40.60
3D	44.50	
3E	44.50	
3H	44.50	
3I	44.50	
3J	44.50	37.86
4E	44.50	
4H	44.50	
6F	45.00	38.24
6G	45.50	38.67
7F	45.00	
7G	45.00	
8F	45.50	
8G	45.00	
9F	45.50	
9G	45.50	
10F	45.50	37.86
10G	45.50	39.10

	Pour 2	
	SCP Report	Load Cell
	(kips)	(kips)
1A	45.50	38.02
1B	44.00	
1C	44.00	
1D	44.00	
1E	44.20	
1H	44.50	
1I	44.50	
1J	44.80	
1K	44.80	
1L	45.50	37.05
2A	44.20	
2B	44.50	
2C	44.20	
2D	44.20	
2E	44.00	
2H	44.00	
2I	44.00	
2J	43.80	
2K	43.90	
2L	43.90	
3C	45.00	39.98
3D	44.00	
3E	44.00	
3H	43.90	
3I	44.00	
3J	44.00	31.52
4E	44.50	
4H	44.50	
6F	44.00	
6G	44.00	
7F	44.00	
7G	44.50	
8F	44.50	
8G	44.80	
9F	44.80	
9G	44.50	
10F	44.80	
10G	44.80	

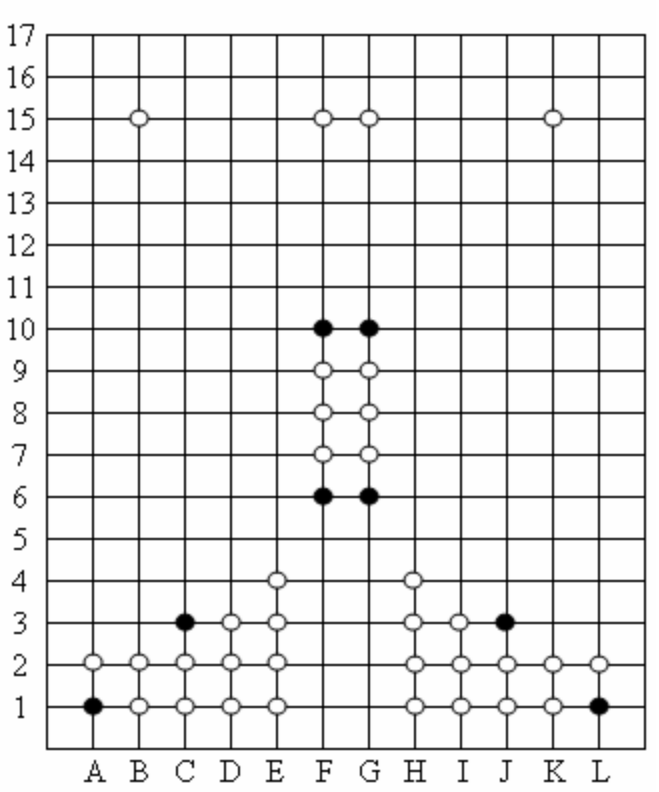

Figure 3.11 SCP naming convention for prestressing strand locations

Table 3.2. Load on strands from initial pull as recorded by load cells and SCP for pour 1.

SCP Number	Load Cell Number	Load Cell (kips)	SCP Report (kips)	Load Cell / SCP Report
10F	1	37.86	45.50	0.83
10G	2	39.10	45.50	0.86
6F	3	38.24	45.00	0.85
6G	4	38.67	45.50	0.85
3C	5	40.60	44.50	0.91
3J	6	37.86	44.50	0.85
1A	7	40.11	44.50	0.90
1L	8	37.95	44.50	0.85
	Average	38.80	44.94	0.86

Load cell readings were also taken several times after the pour until cut-down. The change in the force in the strands over time can be seen in Figure 3.12. Appendix B contains all load cell readings recorded.

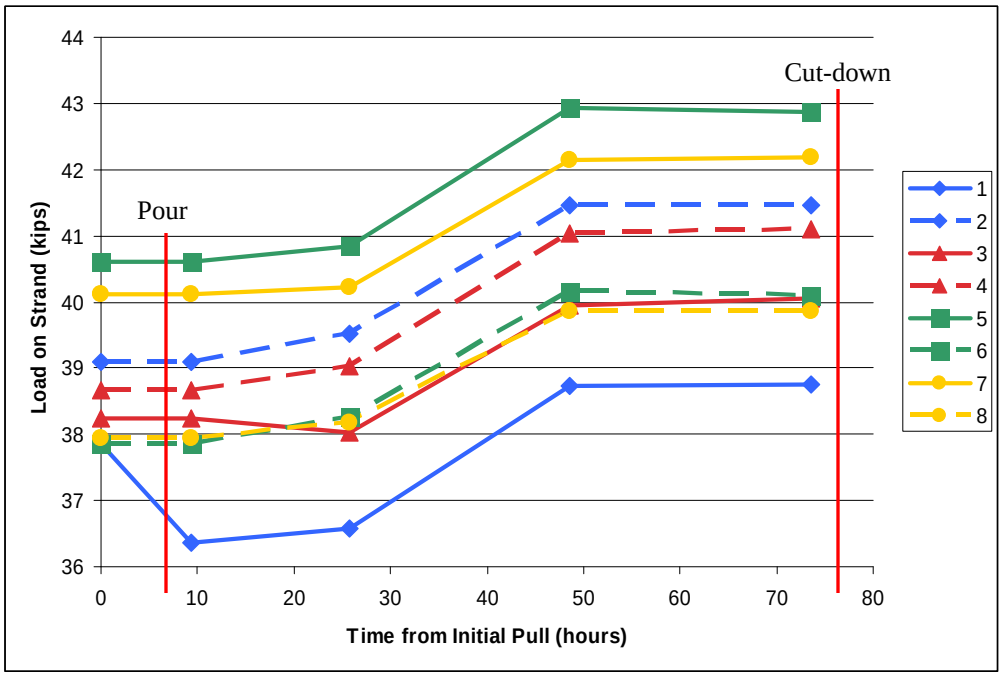

Figure 3.12 Change in prestressing load over time for pour 1

The second pour consisted of girders 4 and 5, which were arranged as shown in Figure 3.13. For this pour only four load cells were available to use on the strands. These four were placed at locations 5, 6, 7 and 8 on Figure 3.8. Table 3.3 shows the comparison of load on the strands between SCP and the load cells. Figure 3.14 shows the change in prestress force over time. For pour 2, the load cell in position 5 malfunctioned and the data were not used for analysis.

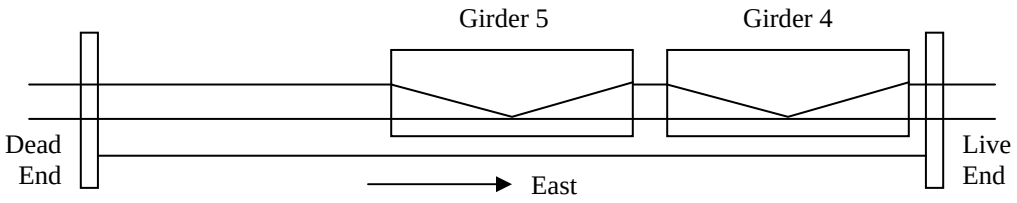

Figure 3.13 Pour 2 girder layout

Table 3.3 Load on strands from initial pull as recorded by load cells and SCP for pour 2

SCP Number	Load Cell Number	Load Cell (kips)	SCP Report (kips)	Load Cell / SCP Report
3J	6	31.52	44.00	0.72
1A	7	38.02	45.50	0.84
1L	8	37.05	45.50	0.81
	Average	35.53	45.00	0.79

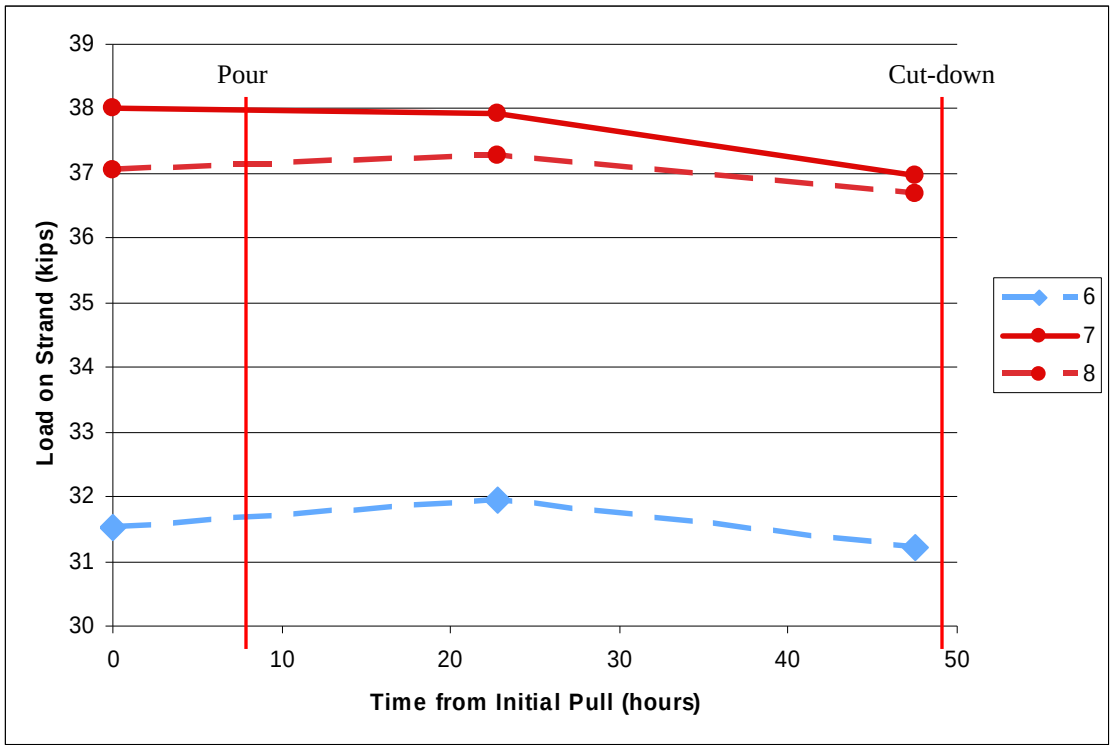

Figure 3.14 Change in prestressing load over time for pour 2

The initial prestressing strand loads showed significant discrepancies between the values given by SCP and the values resulting from the load cells. For the first pour, the load cells showed loads that were 86% of the loads reported by SCP, and 79% for the second pour. The load cell readings were not taken at the exact time that the strand was pulled. Due to the dangers involved in the prestressing process, all readings were taken immediately after all strands had been prestressed and anchored. Because the readings were taken after the pull and set of the strand, the anchorage losses were included in the load cell value. This slip of the strand as it set in the anchor released some of the tension that the SCP value included. Also, the SCP value was taken at the live end of the strand with a pressure gage, while the load cell reading was taken at the dead end of the strand. Between these two points friction losses may have occurred as the harped strands were stressed through the harping devices. Another possible source of error between the two values could come from small movements of the abutments during prestressing. Strands that were stressed first could lose some of their tension if the abutment moved in during the stressing of a subsequent strand.

Figures 3.12 and 3.14 show some conflicting information. Figure 3.14 shows that as expected the prestressing strands in pour 2 displayed some relaxation over time. This decrease in force is typically due to relaxation of the prestressing strand itself. However, the increasing loads on the prestressing strands in pour 1 deviate from this principle. Strands 1 and 3 showed an initial decline in tension during the first 26 hours after the pull, but the other 6 strands did not. After this point all load cells showed increasing loads. This increase in load may be a result of the ambient temperature affecting the tension of the strand due to the time of day that the readings were taken. Table 3.4 shows

the time of day readings were taken and the resulting loads for strand 2 of pour 1. These data suggest that an increase in load resulted from the change in temperature between 5:37pm the day of the pour and 10:01am the following morning and then at 8:50am on the next day. The cooler mornings caused contraction of the strands, resulting in higher forces. The last load recorded by the load cells was used for all further calculations.

It is also important to note that the forms were removed from the pour 1 girders two days after the pour. The increased load cell force was recorded after these forms had been removed. The exposed concrete could have cooled, and therefore given larger stress values. The pour 1 girders sat on the beds for 5 days, while the pour 2 girders were only on the beds for 3 days.

A final point to note is that there were significant amounts of exposed strand at the end of each bed. The pour 1 setup had approximately 70 feet of free strand, and pour 2 had approximately 190 feet. All free strand was on the dead end of the bed, which was also the end from which the load cell readings were taken. This free strand would change in temperature differently from that in the girder.

Table 3.4 Load values and time of day reading taken for strand 2 of pour 1

Time	Date	Load (kips)
8:15am	August 6	39.096
5:37pm	August 6	39.096
10:01am	August 7	39.521
8:50am	August 8	41.466
9:45am	August 9	41.469

3.4 Deflection Measurement System

The taut wire system was used to monitor the camber of the girders. This system was used from the time of construction, through field stiffness test, and throughout storage in the yard. The system measured deflection or camber using a taut wire strung down the length of the girder. At midspan a ruler was affixed to the girder and a mirror was affixed just beside it. A researcher would look directly at the wire and read the ruler. The mirror was used to make sure the researcher was looking directly at the wire and not at an angle. When looking at the wire in the mirror at an angle, the wire and a reflection of the wire could be seen, looking like 2 wires. When looking at the same level of the wire, no reflection of the wire could be seen. Once the researcher saw only one wire, then the reading was taken off of the ruler. Figure 3.15 shows a researcher reading the taut wire system. The system was attached to the girder while it was still on the bed, before release of the prestressing strands. The initial zero reading was taken before cut-down. This camber system was used on both sides of girders 2, 3, and 4, and on the inside faces of girders 1 and 5. The exterior of the bridge was not marred with testing equipment.

Figure 3.15 Researcher Jennifer Dunbeck reading taut wire system

Construction of this system required embedded anchor systems. These embedments were placed during the construction of the girders. Before the forms were set in place, several holes were drilled through the forms at measured locations. A ¼ inch bolt was placed on the outside of the form, and a threaded sleeve was attached on the inside of the form along with another ¼ inch bolt. The threaded sleeve and interior bolt were the considered the anchor system. This assembly is shown in Figure 3.16. Nylon washers were used between the bolt and the outside face of the form. The forms were then set and the concrete was placed. Before removal of the forms, the exterior screws were removed, leaving the threaded sleeve inside, secure in the concrete. After removal of the forms, screws were put back into the holes and used as needed to attach the taut

wire system. Figure 3.17 shows an embedment in a steel form. Figure 3.18 shows an embedment in a constructed girder with a machine screw inserted afterward.

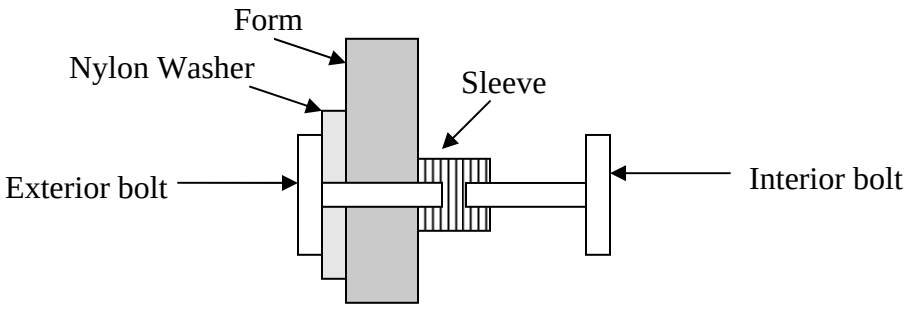

Figure 3.16 Embedment anchor assembly attached to steel form

Figure 3.17 Embedments in bottom flange of steel forms for attachment of angles

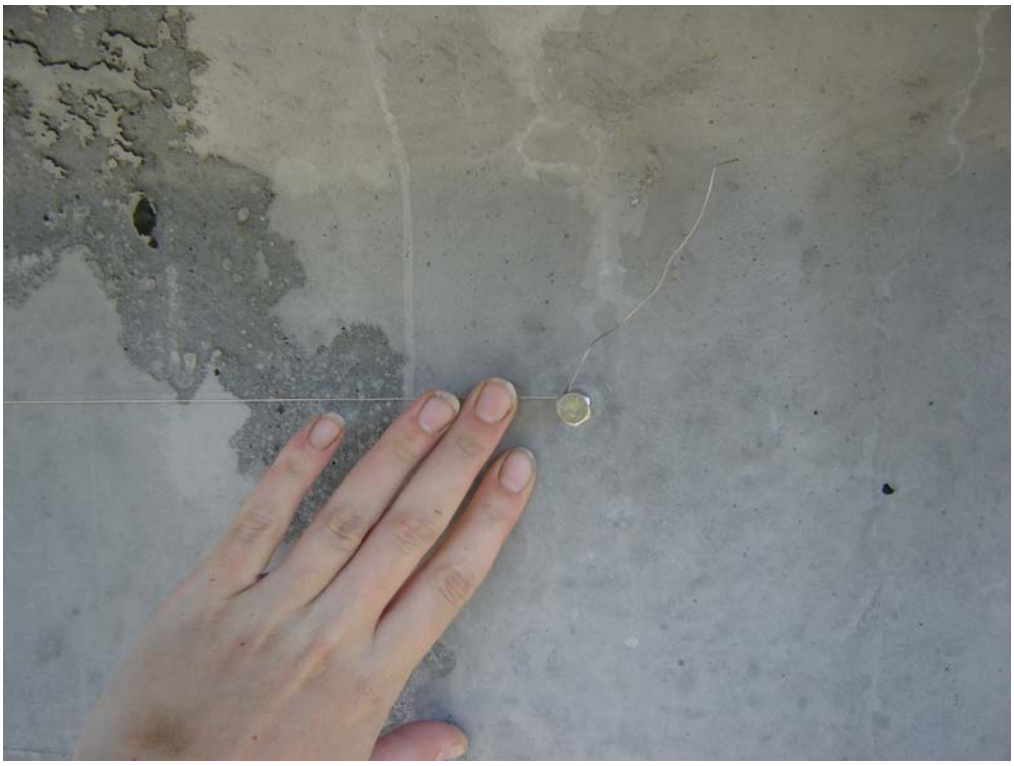

Figure 3.18 Bolt screwed into embedment in girder face with taut wire tied around it

The construction of the taut wire system required ¼ inch bolts embedded at each end of the girder in the web, approximately 3 inches below the top flange, in line with the girder center-of-bearing. A 0.02 inch diameter stainless steel piano wire was tied around the bolt on the southwest end and then strung down the length of the girder over a pulley wheel attached to the girder with the second bolt. The pulley was used to allow free movement of the wire as the girder adjusted. A 15-pound weight was tied to the end of the wire to keep it taut. At midspan a third embedment and bolt were located to support a stainless steel ruler, and ensure that it remained perpendicular to the ground. Once the ruler was in place it was also epoxied to the face of the girder to prevent movement and variable readings. A mirror was epoxied directly beside the ruler, as shown in Figure 3.19.

Initial measurements were taken before cut-down, and then the next reading was taken immediately after cut-down. The second reading showed more camber than was originally expected and longer rulers were required. Secondary rulers were then glued directly beside the primary one. The bottom inch of the primary ruler was lined up with the top inch of the secondary ruler, and measurements continued.

Figure 3.19 Primary ruler with mirror adjacent and taut wire running across

3.5 Transfer Length Measurement System

The transfer length of the prestressing strands was measured using embedments in the bottom flange of the girder. These embedments were spaced 2 inches apart from the end of the beam moving toward the center for at least 48 inches. The distance between these holes was measured with a DEMEC gage, which reads to accuracy of 0.0001 inches. The DEMEC gage has two conical points spaced 8 inches apart, with one point

on a spring, which can adjust. DEMEC gage readings were taken before cut-down of strands for an initial zero reading.

The DEMEC embedment points were placed using a piece of steel 1 inch wide by 4 feet long, or longer depending on the piece used, which was fitted with holes at 2 inches apart. The holes were filled with countersunk screws on the outside and a threaded anchor on the inside, similar to the setup for the camber system embedments. This entire steel piece was then bolted to the inside of the steel forms, as shown in Figure 3.20. After the concrete had set, the exterior nuts were removed from the bolts, and the forms were removed. Each screw used in the 2 inch spaced holes was then removed, followed by the steel piece itself. The anchors were left in the concrete for the DEMEC gage to use. This assembly was installed on both ends of each girder, with both assemblies being on the same side of the girder. Figure 3.21 shows researchers taking DEMEC gage readings.

Figure 3.20 Transfer length embedments attached to forms

Figure 3.21 Researchers taking DEMEC gage readings on girder end before cut-down

CHAPTER 4

HSLW GIRDER CONSTRUCTION

4.1 Introduction

All 5 HSLW BT-54 girders were constructed at Standard Concrete Products in Atlanta, Georgia. Girders 1, 2, and 3 were all poured on August 6, 2008 on bed 4. Girders 4 and 5 were poured on August 8, 2008 on bed 3, adjacent to bed 4.

4.2 Prestressing Strands

The same prestressing strand layout was used for all 5 girders. For each girder 42 0.6-inch diameter prestressing strands were used. Of these 42, 4 were placed in the top flange, 10 strands were in the web, which were harped at the midspan, and 28 strands were in the bottom flange of the girder. Girders 1, 2, and 3 were built end to end between abutments on bed 4, as illustrated in Figure 4.1. Prestressing strands were run through the live end abutment, through all 3 girders, and secured at the dead end abutment. Load cells were placed on strands as they were secured into the dead end. Girders 4 and 5 were built on bed 3 as shown in Figure 4.2.

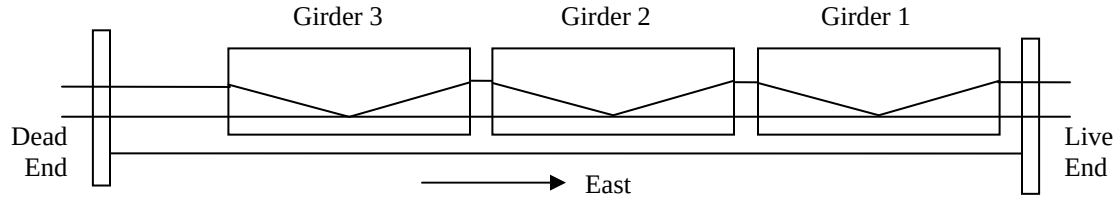

Figure 4.1 Pour 1 girder layout on bed 4

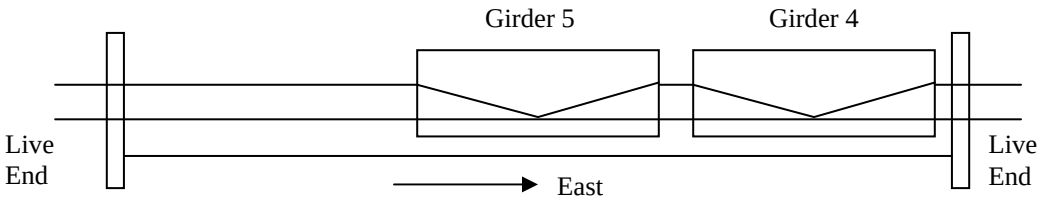

Figure 4.2 Pour 2 girder layout on bed 3

Once the prestressing strands were in place, SCP workers placed the shear and bursting reinforcement, shown in Figures 4.3 and 4.4. Quality control personnel checked locations of all prestress cables and reinforcing bars before proceeding, shown in Figure 4.5.

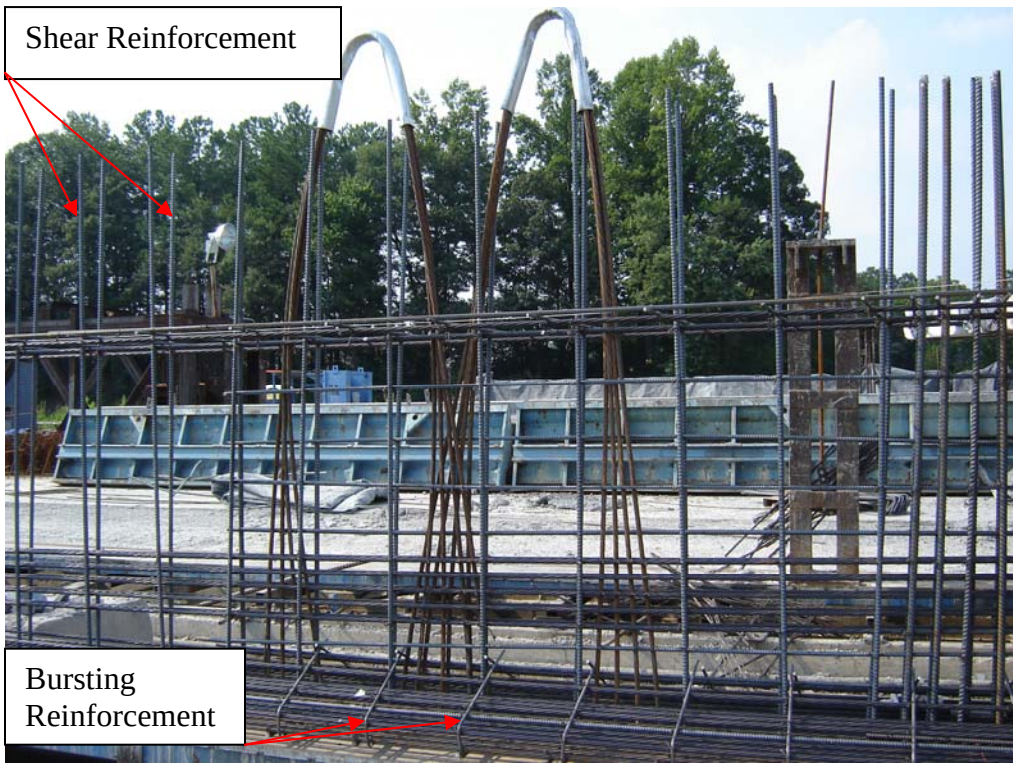

Figure 4.3 Reinforcing bars around prestressing cables

Figure 4.4 Reinforcing bars across 2 girders

Figure 4.5 Quality Control checking reinforcing bar placement

The Vibrating Wire Strain Gages (VWSG) were put into place and secured to the prestressing strands as described in Chapter 3. The wires were kept on their spools, and were secured at the top of the girder between vertical reinforcing bars, as shown in Figure 4.6. The spools were each covered with a bag during the pour to keep concrete away from the wires.

Figure 4.6 VWSG locations and wire secured above girder

Once the reinforcement was in place, and the VWSG were secure, the metal forms were moved onto the construction bed. The forms were previously fitted with the

embedments discussed in Chapter 3. The forms were lifted in panels by the straddle-lift, shown in Figure 4.7, and carefully placed along the bed edge. After both sides were in place, a clamp was positioned to hold the edge of the form to the bed on either side. A rod ran under the bed, connecting the two clamps, and the entire assembly was tightened with an air-compressor drill. This assembly kept the forms in place and at the correct dimensions along the bottom. Also, a metal brace was fitted across the top to keep the top a consistent width.

Figure 4.7 Straddle-lift placing form around reinforcing bars

4.3 Concrete Batching

SCP has a batch plant onsite which was used to produce the HSLW concrete for these girders. The batching operation was controlled and monitored by a computer. Silica fume was manually added to the mixer. Pour 1 consisted of 19 batches: six batches each in girders 2 and 3 and seven batches in girder 1. Each batch was labeled by the girder into which it was placed and the order it was placed. For example, the third batch placed into girder 1 was labeled 1-3. Batch properties for each girder in pour 1 are listed in Table 4.1. The ambient temperature for this pour was 89 degrees Fahrenheit.

Table 4.1 Concrete properties for Pour 1 from SCP Quality Control

Girder	Slump (in)	Temp (deg F)	Air Content (%)	Unit Weight (lb/ft^3)
1	5.75	91.5	3	120.7
2	6.5	95	2.25	122.4
3	6.5	94	2.25	data not collected

Pour 2 consisted of 13 batches: seven in girder 4 and six in girder 5. Data for pour 2 is shown in Table 4.2.

Table 4.2 Concrete properties for Pour 2 from SCP Quality Control

Girder	Slump (in)	Temp (deg F)	Air Content (%)	Unit Weight (lb/ft3)
4	4.75	92	3.5	data not collected
5	5	95.2	2.5	118

During both pours, several batches of concrete were found to be too hot and had to be thrown out. Ice was used with the water in subsequent batches to lower the temperature to an acceptable level of 95˚ F or less.

The quantities of each ingredient are shown in Table 4.3 along with the designed quantities. These are the ingredients required to make 3.5 cubic yards of concrete, which was the standard batch size. Table 4.4 shows the provider of each material and the type used. Appendix C contains batch report summaries for each girder.

Table 4.3 Average quantities of ingredient for girders compared to design

	units	Design	Girder 1	Girder 2	Girder 3	Girder 4	Girder 5
Number of Batches			7	6	6	7	6
Cement	lbs	2590	2589.43	2587.67	2603.67	2584.33	2584.17
Flyash	lbs	525	524.57	527.00	524.00	526.00	525.00
Silica Fume	lbs	350	350	350	350	350	350
Sand	lbs	3262	3290.71	3259.33	3265.67	3285.50	3239.17
Lightweight Aggregate	lbs	3430	2996.86	3421.67	3524.33	3441.50	3403.17
Water	gallons	87.9	87.43	86.17	84.33	89.40	88.00
Water Reducer	ozs	126	125.71	126.33	126.33	126.00	126.00
HRWR	ozs	158	157.43	157.33	157.33	158.00	157.67
AEA	ozs	7	6.86	7.17	7.17	7.00	7.00

Table 4.4 Sources and type of materials used in these pours

Materials	Source	Type
Cement	LaFarge	III (II)
Flyash	Boral	Class “F”
Silica Fume	Sika SF	Silica Fume
Sand 1	Vulcon LS	Granite
Lightweight Aggregate	Stalite	ES
Water	County	
High Range Water Reducer	Sika	V-2100
Admix 2	Sika	Plastiment
Admix 3	Sika	RAPID 1
Air Entraining Agent	Sika	AEA-14

4.4 Concrete Sampling

Concrete cylinder samples were taken from each batch of concrete used in the girders. Georgia Tech graduate research assistants made the concrete specimens according to ASTM C 31 standards. Table 4.5 shows tests that required specimens and their number per batch. These numbers apply to 5 girders and a total of 32 batches. Table 4.6 shows the total number of specimens taken from each batch. Figure 4.8 shows graduate research assistants making concrete specimens.

Table 4.5 Concrete cylinder specimens cast for testing purposes

From Each Batch:

	4x8	6x12
Compressive Strength:		
56 days	3	
Modulus of Elasticity:		
56 days		1

From Center Batch:

	4x8	6x12
Compressive Strength:		
Release	3	
3 days	3	
7 days	3	
28 days	3	
56 days	3	
6 months	3	
2 years	3	
Modulus of Elasticity:		
Release		1
56 days		1
6 months		1
2 years		1
Split Cylinder:		
Release		1
56 days		1
6 months		1
2 years		1
Creep:		3
Thermal Expansion:		
Release		1
56 days		1
6 months		1
2 years		1
Chloride Permeability:		
56 days	2	
2 years	2	
Total	221	105

Table 4.6 Batches and number of cylinder specimens made from each

Batch	4x8	6x12
1-1	3	1
1-2	3	1
1-3	28	16
1-4	3	1
1-5	3	1
1-6	3	1
1-7	3	1
2-1	3	1
2-2	3	1
2-3	28	16
2-4	3	1
2-5	3	1
2-6	3	1
3-1	3	1
3-2	3	1
3-3	28	16
3-4	3	1
3-5	3	1
3-6	3	1
4-1	3	1
4-2	3	1
4-3	3	1
4-4	28	16
4-5	3	1
4-6	3	1
4-7	3	1
5-1	3	1
5-2	3	1
5-3	28	16
5-4	3	1
5-5	3	1
5-6	3	1

Figure 4.8 Georgia Tech GRAs construct concrete cylinder specimens

Each cylinder was covered with a plastic cap and set on a flat crate for overnight storage at SCP. The specimens were covered with plywood to shade them from direct sunlight, as shown in Figure 4.9. Specimens were exposed to ambient temperature for the first 18 hours of curing in the same conditions as the girders. The day after the pour the cylinders were transported to the Structures Lab on Georgia Tech's campus where the forms were stripped, and each specimen was labeled with its batch number. Specimens were then stored in a 100% humidity room for curing at 73˚ F ± 2˚ F.

Several cylinders from each pour were monitored for temperature change during curing. Thermocouples were placed in these cylinders and a temperature reading was taken every 30 minutes. The resulting data are shown in Figures 4.10 and 4.11.

Figure 4.9 Researchers cover concrete specimens with plywood for shade

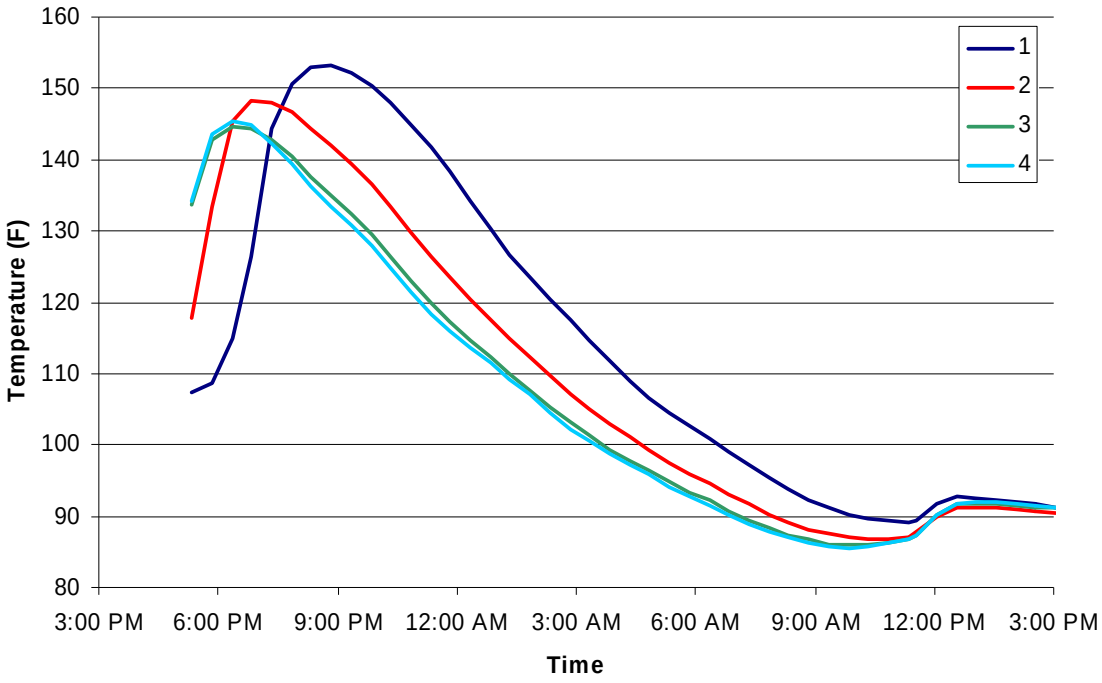

Figure 4.10 Thermocouple temperature readings from cylinders in Pour 1

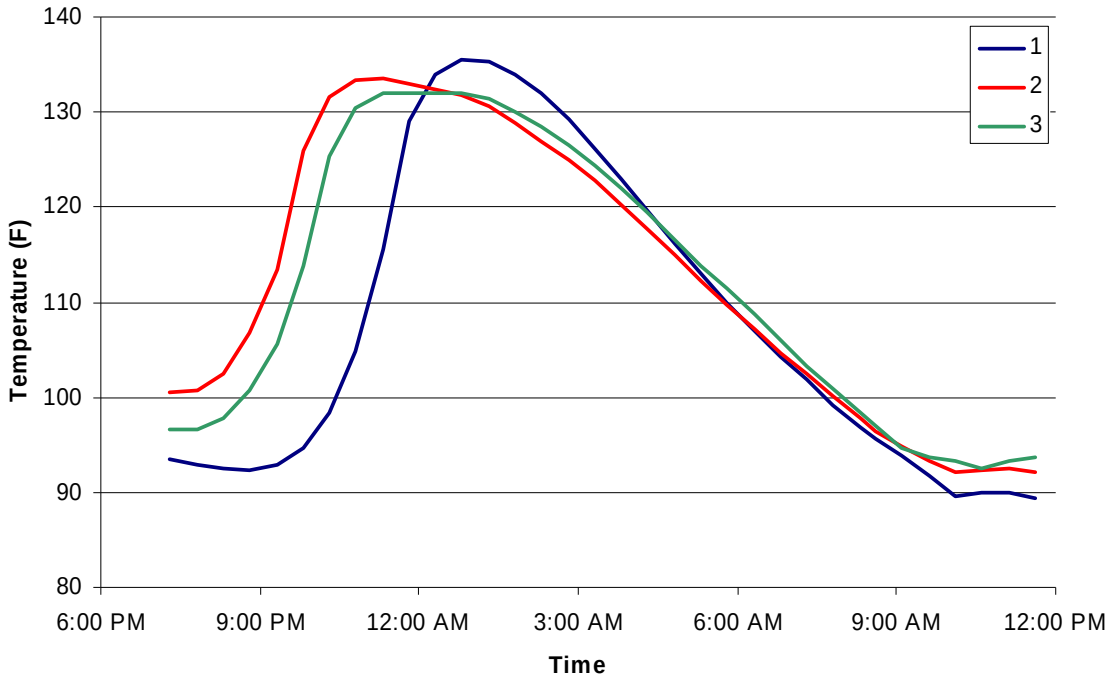

Figure 4.11 Thermocouple temperature readings from cylinders in Pour 2

4.5 Concrete Placement

Batches were dropped from the batch plant into Tuckerbilt Tractors which transported the concrete to the beds. Concrete was placed into the forms, and workers used internal and external vibrators to release air and ensure consolidation, shown in Figures 4.12- 4.14. The forms had a track in which the external vibrator could slide along the form, and workers came behind the pour to vibrate. Care was taken to avoid vibrations exactly on the VWSG, as this could severely damage them. Workers finished the top of the girders and pulled tarps over them to let them cure as shown in Figure 4.15. Due to the high ambient temperature on the pour days, steam was not needed to ensure quick curing, and no steam was used on the beds.

Figure 4.12 Tuckerbilt delivering concrete to forms

Figure 4.13 Tuckerbilt placing concrete into forms with worker using vibrator

Figure 4.14 Workers vibrating concrete in the web of the girder

Figure 4.15 Tarps cover the girders to aid in curing

4.6 Curing, Release and Storage

SCP took sample cylinders of concrete from each beam to test for desired strengths. The concrete was required to attain 7,000 psi compressive strength before forms could be taken off, and 8,000 psi before the strands could be cut-down. Girders 1, 2, and 3 were slow to gain strength. Forms were removed 2 days after pour, but cut-down was not until the 5th day after the pour, since the 3rd and 4th days were over a weekend. Girders 4 and 5 had forms removed and strands cut-down on the 3rd day after the pour.

Several initial measurements were taken on the girders after the forms were removed, but prior to cut-down. First, initial VWSG readings were taken for all girders. Secondly, the taut wire deflection system discussed in Chapter 3 was installed, and an initial reading was taken. Thirdly, DEMEC readings were taken for transfer length calculations. Finally, load cell readings were taken just before cut-down.

Cut-down of strands was performed with torches. A SCP worker with a torch was located at each end of the bed and at the space between each girder. The workers would all cut the same strand at the same time to minimize any shifting the girder might have due to transfer of energy. Figures 4.16 and 4.17 show workers cutting down strands. The cut-down sequence is shown in Figure 4.18, which was closely followed. The harp holding down the draped prestressing strands was held to the bed by a threaded rod. This rod was cut after the draped strands were released prior to cut-down of strands in bottom flange.

Figure 4.16 Two SCP workers look to the lead worker to signal the next cut

Figure 4.17 Lead worker examines next strand to be cut

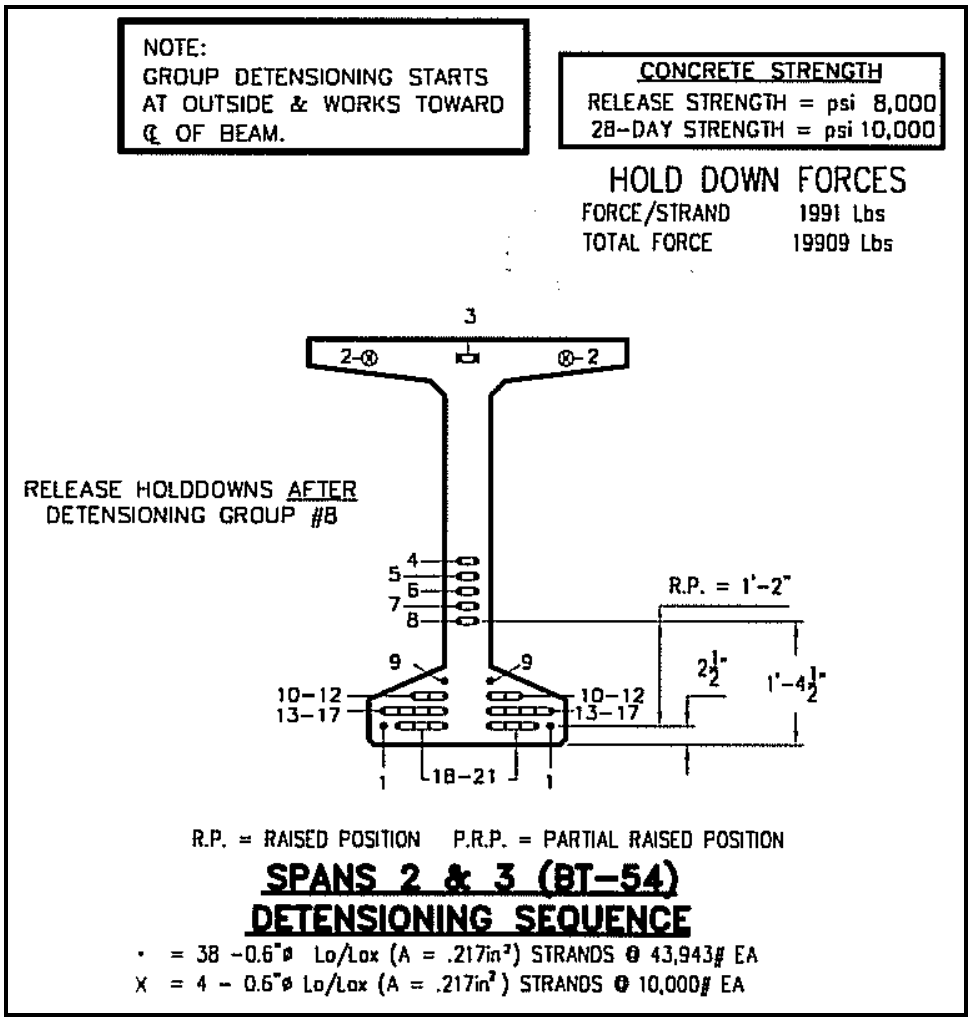

Figure 4.18 Cut-down sequence for all girders

After cut-down, the girders were transferred into the yard at SCP for further curing. Each girder was moved individually using the straddle-lift, shown in Figures 4.19 and 4.20, and all 5 girders were placed side by side for continued research, shown in Figure 4.21.

Figure 4.19 Straddle-lift picks girder up off construction bed

Figure 4.20 Straddle lift moves through the yard to store girder

Figure 4.21 Girders stored together in SCP yard

CHAPTER 5

CONCRETE MATERIAL DATA

5.1 Introduction

Concrete samples were taken from every batch of concrete used in the construction of the girders. Concrete cylinder specimens were made at SCP and were transported to the Structures Lab at Georgia Tech for curing and testing as discussed in Chapter 4. Several types of tests were used to analyze the concrete, including compression tests, modulus of elasticity and Poisson's ratio tests, splitting tension tests, and coefficient of thermal expansion tests.

5.2 Specimen Numbering System

For this research a large number of concrete specimens were made. A four digit numbering system was developed to track individual cylinders. The first two digits corresponded to the girder and batch number of the concrete respectively. The third digit was the diameter of the specimen: either 4 or 6 inches. The fourth and final number was simply the order in which the specimen was tested. For instance, the label 3-1-6-2 would refer to a cylinder from batch 1 of girder 3 that is 6 inches in diameter, and therefore 12 inches tall, and is the second 6"x 12" to be tested from this batch. This numbering system was used for all cylinders and did not vary based on the test for which it was used.

5.3 Testing Procedures and Results

5.3.1 Compression Tests

All compression tests were conducted according to ASTM C 39. Cylinders were stored in the 100% humidity room at 73˚ F ± 2˚ F until testing. Compression tests were conducted at 3, 5, 7, 28, and 56 days after the pour. Tests performed after 56 days will be discussed in a future report. Compression tests were conducted on the SATEC Systems compression testing machine, which is calibrated annually and has a capacity of 800,000 pounds.

Figures 5.1 through 5.6 show strength of concrete against time, and the average strength gain curve. The concrete needed to reach 8,000 psi before the strands were released and 10,000 psi at 56 days. Girders 2 and 3 met the required average strength for strand release, but the other 3 girders did not, showing a slower strength gain than expected. A possible cause of this slow gain is discussed in Chapter 9. All girders reached 10,000 psi by 56 days.

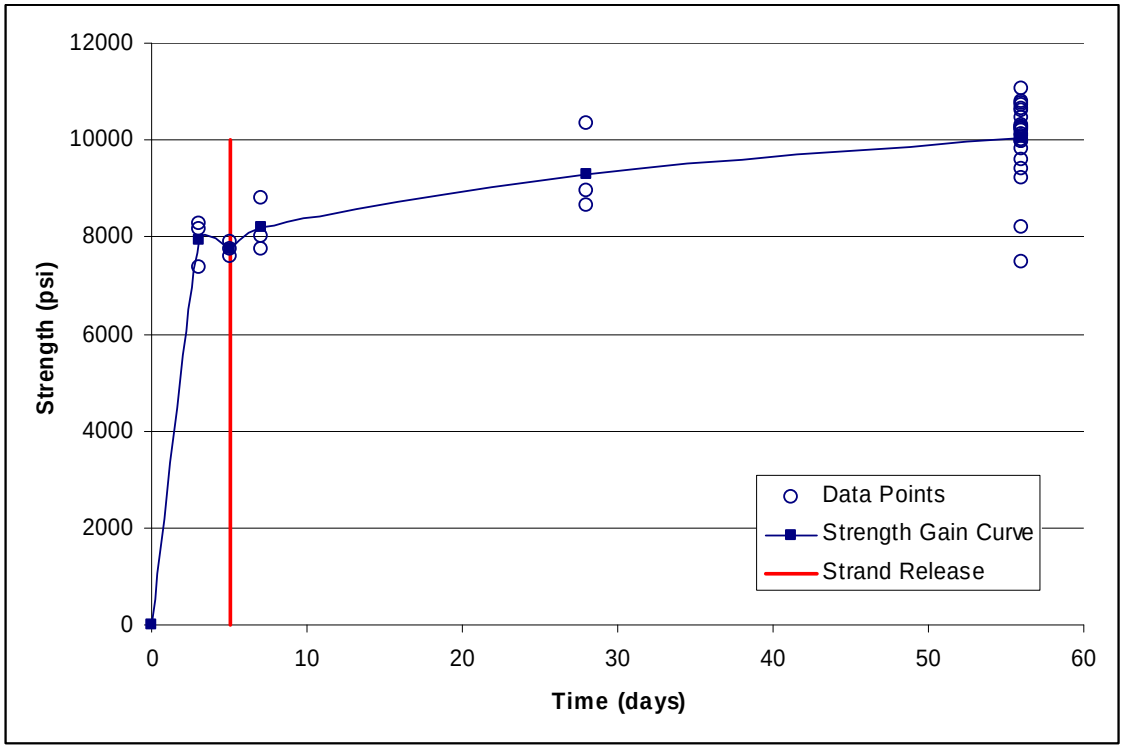

Figure 5.1 Compression test values and strength gain of girder 1 up to 56 days

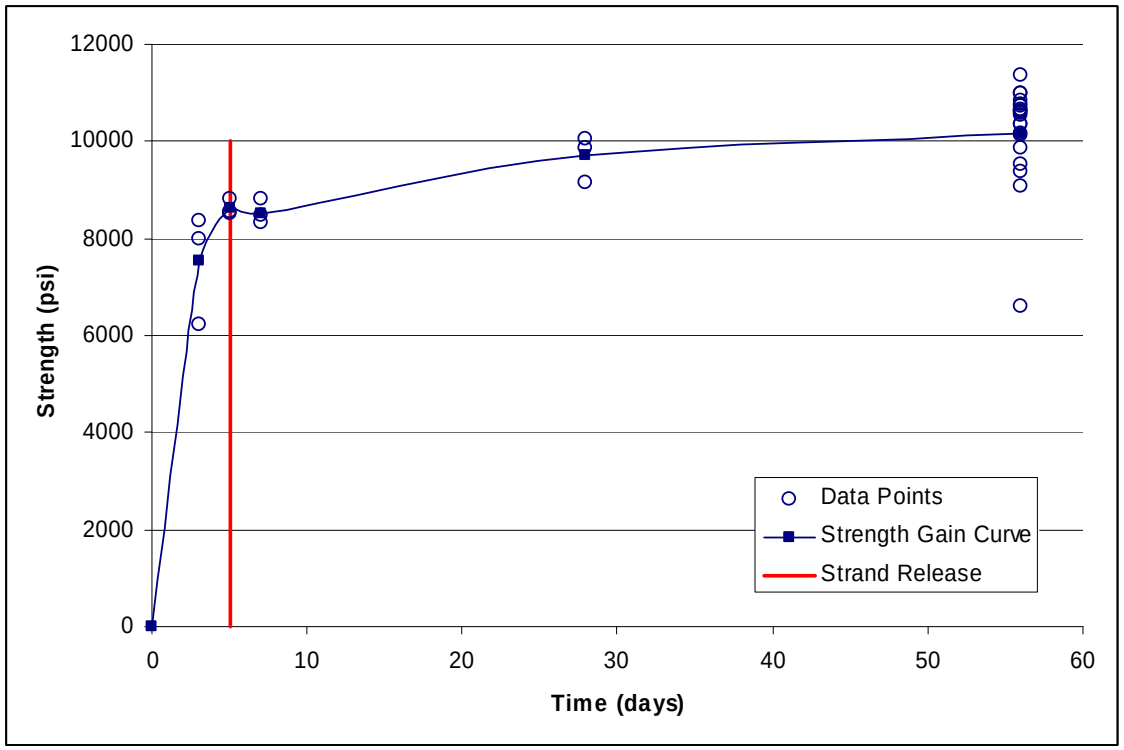

Figure 5.2 Compression test values and strength gain of girder 2 up to 56 days

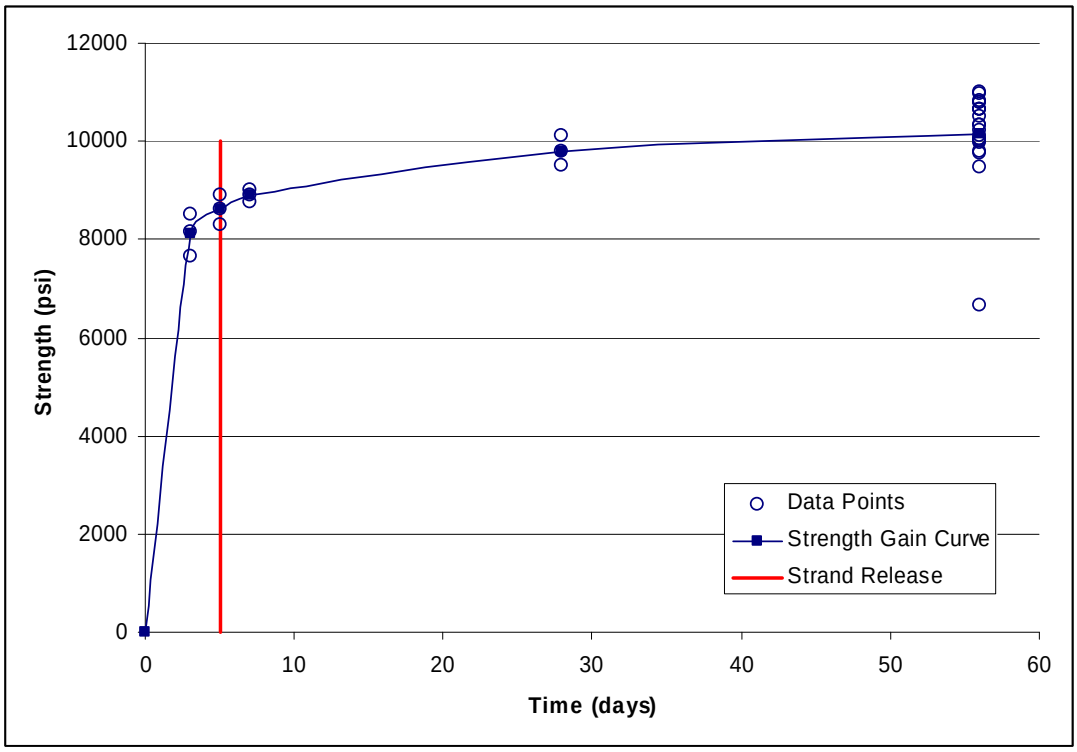

Figure 5.3 Compression test values and strength gain of girder 3 up to 56 days

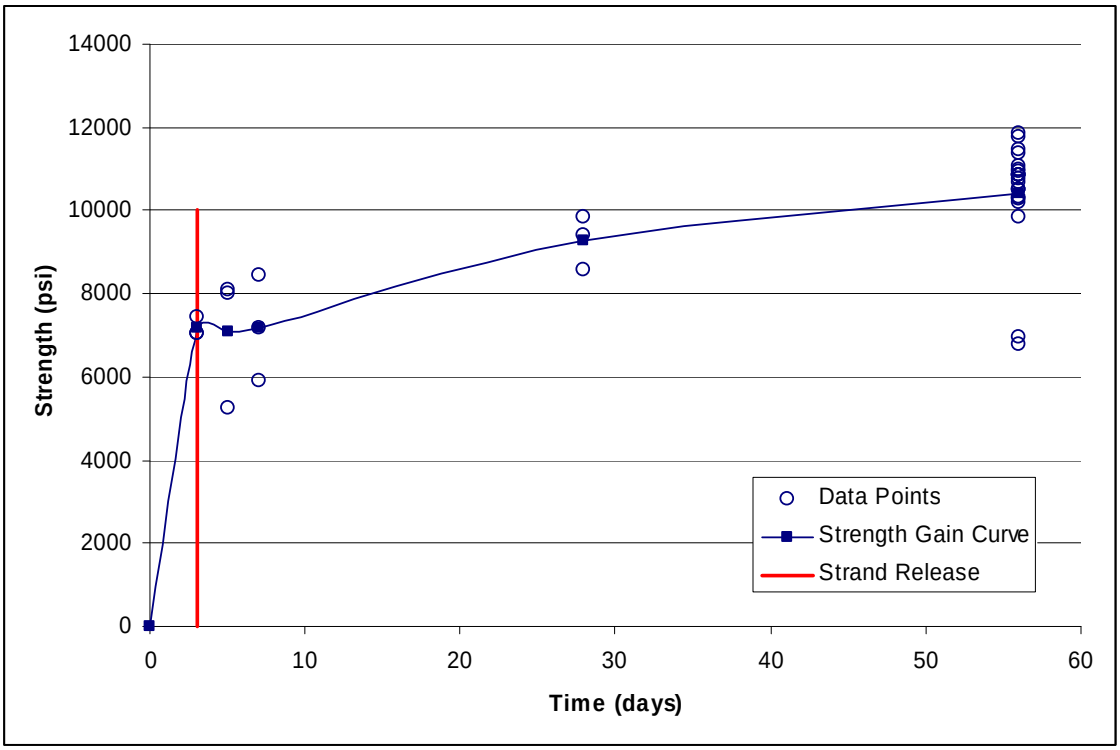

Figure 5.4 Compression test values and strength gain of girder 4 up to 56 days

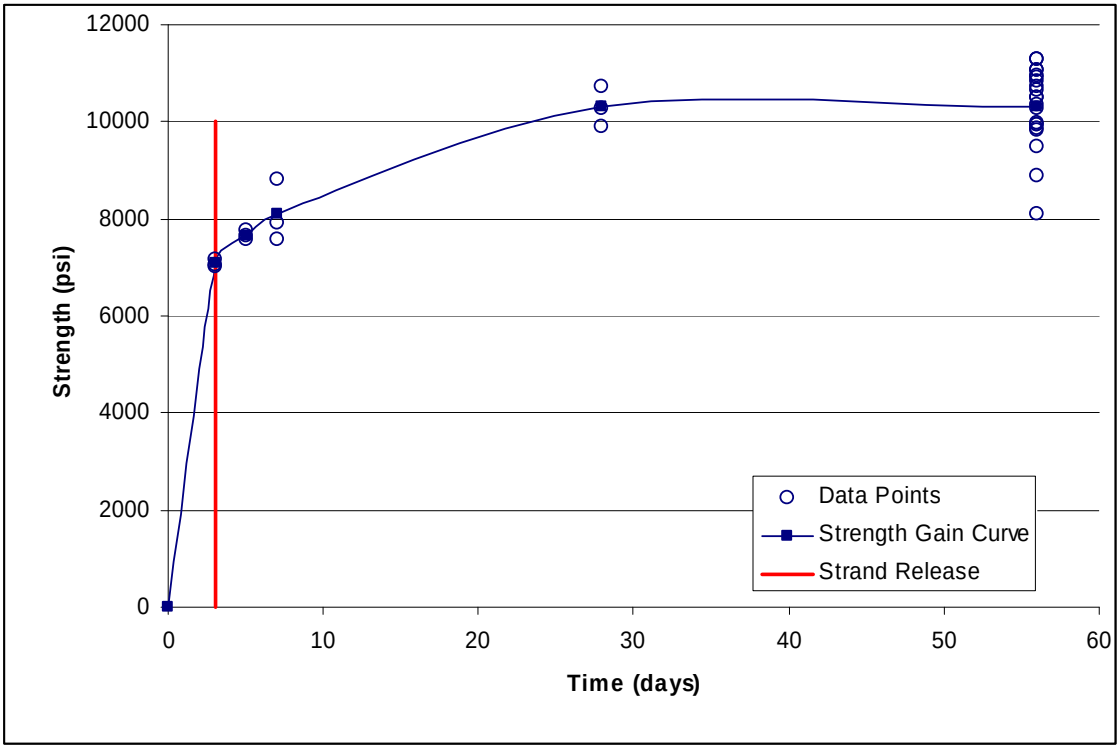

Figure 5.5 Compression test values and strength gain of girder 5 up to 56 days

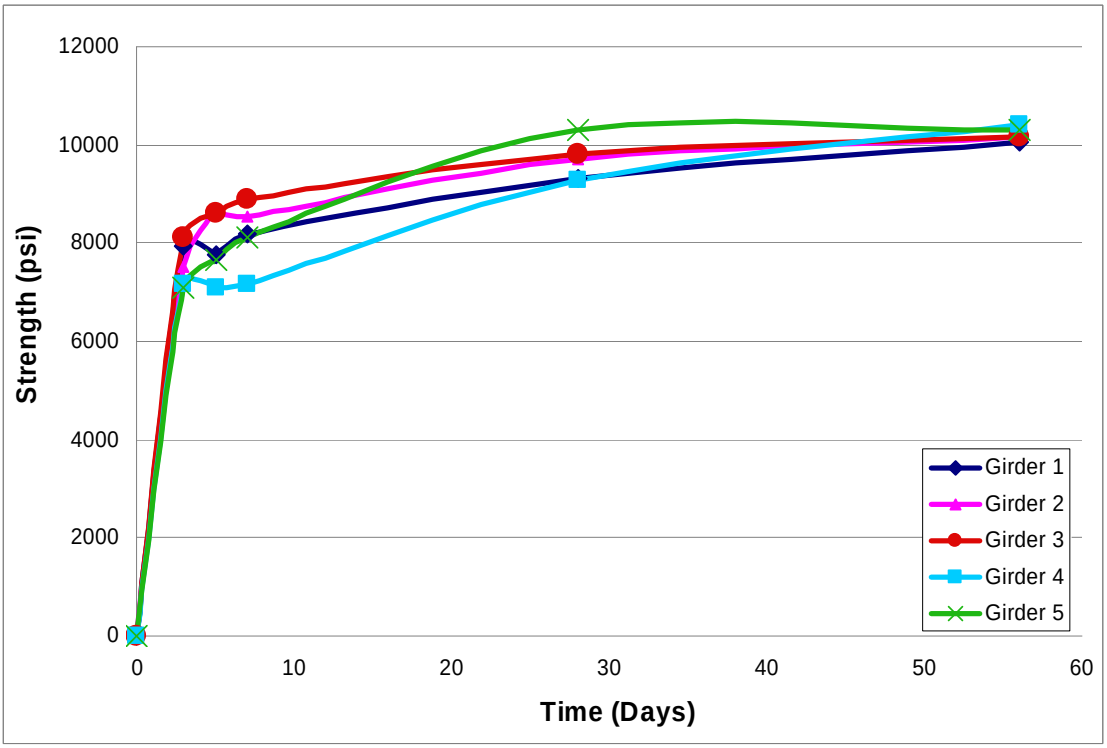

Figure 5.6 Strength gain of girders 1, 2, 3, 4, and 5 up to 56 days

Mean compression strengths for each day of testing are shown in Tables 5.1(a) and (b). Statistical analysis was done on the 56 day tests to determine (1) if all batches of the same girder could be considered statistically equal within a 95% confidence interval, and (2) if the concrete from all five girders could be considered statistically equal within a 95% confidence interval.

The statistical tests showed that all batches within girders 1, 3, 4, and 5 could be considered equal, but that the concrete within girder 2 could not. By removing one outlier point in compression tests from girder 2, the girder passed the statistical analysis and all batches could be considered equal within a 95% confidence interval.

The analysis of all concrete between the girders showed that all girders could be considered statistically equal within a 95% confidence interval.

Table 5.1(a) Mean compressive strength of concrete (psi)

Day	Girder 1	Girder 2	Girder 3	Girder 4	Girder 5	Mean	Standard Deviation	Coefficient of Variation
3	7,946	7,520	8,103	7,177	7,088	7,567	451	0.0596
5	7,757	8,617	8,607	7,104	7,667	7,950	654	0.0822
7	8,190	8,531	8,890	7,169	8,107	8,177	643	0.0786
28	9,304	9,694	9,799	9,277	10,304	9,676	420	0.0434
56	10,016	10,224	10,171	10,472	10,307	10,238	168	0.0164

Table 5.1(b) Mean compressive strength of concrete (MPa)

Day	Girder 1	Girder 2	Girder 3	Girder 4	Girder 5	Mean	Standard Deviation	Coefficient of Variation
3	54.78	51.85	55.87	49.49	48.87	52.17	3.11	0.0596
5	53.48	59.41	59.34	48.98	52.86	54.82	4.51	0.0822
7	56.47	58.82	61.29	49.43	55.89	56.38	4.43	0.0786
28	64.15	66.84	67.56	63.97	71.04	66.71	2.90	0.0434
56	69.06	70.49	70.13	72.20	71.07	70.59	1.16	0.0164

The compressive strength of the cylinders did not reach the 11,620 psi found by Buchberg (2002) using a similar mix design. This could have resulted from a low moisture content of the lightweight aggregate. Moisture content of the aggregate was not measured the days of the pours, so this speculation cannot be confirmed. Appendix D contains recommendations from the manufacturer for moisture conditioning of Stalite expanded slate lightweight coarse aggregate prior to batching.

5.3.2 Modulus of Elasticity and Poisson's Ratio Tests

Modulus of elasticity tests were conducted according to ASTM C 469, in which both modulus of elasticity and Poisson's ratio were calculated on the 2nd loading to $0.40f_c'$ using the chord modulus. The tests were conducted on the same SATEC Systems testing machine used for previous tests. Modulus of elasticity tests were conducted the day the strands were released and at 56 days. Tables 5.2 through 5.4 show the data from the tests.

Table 5.2 Elastic Modulus and Poisson's Ratio results at release

Day	Batch	Cylinder Number	Elastic Modulus (ksi)	Elastic Modulus (GPa)	Poisson's Ratio
Release	1-3	1-3-6-1	3656	25.21	0.2155
Release	2-3	2-3-6-1	3715	25.61	0.3260
Release	3-3	3-3-6-1	3678	25.36	0.2297
Release	4-4	4-4-6-1	3378	23.29	0.1772
Release	5-3	5-3-6-1	3217	22.18	0.2078

Table 5.3 Elastic Modulus and Poisson's Ratio results at day 56

Day	Batch	Cylinder Number	Elastic Modulus (ksi)	Elastic Modulus (GPa)	Poisson's Ratio
56	1-1	1-1-6-1	3905	26.92	0.2308
56	1-2	1-2-6-1	4230	29.16	0.2455
56	1-3	1-3-6-3	3591	24.76	0.1992
56	1-3	1-3-6-4	3881	26.76	0.2238
56	1-4	1-4-6-1	4211	29.03	0.2462
56	1-5	1-5-6-1	3868	26.67	0.2308
56	1-6	1-6-6-1	3526	24.31	0.1735
56	1-7	1-7-6-1	3598	24.81	0.2166
56	2-1	2-1-6-1	3951	27.24	0.2238
56	2-2	2-2-6-1	3738	25.77	0.2166
56	2-3	2-3-6-3	3672	25.32	0.2074
56	2-3	2-3-6-4	3587	24.73	0.2094
56	2-4	2-4-6-1	3888	26.81	0.2310
56	2-5	2-5-6-1	3342	23.04	0.1545
56	2-6	2-6-6-1	3695	25.48	0.2380
56	3-1	3-1-6-1	3280	22.61	0.2027
56	3-2	3-2-6-1	3783	26.08	0.2310
56	3-3	3-3-6-3	3510	24.20	0.2716
56	3-3	3-3-6-4	3787	26.11	0.2244
56	3-4	3-4-6-1	3522	24.28	0.2001
56	3-5	3-5-6-1	3458	23.84	0.2108
56	3-6	3-6-6-1	3154	21.75	0.1888
56	4-1	4-1-6-1	3892	26.83	0.2380
56	4-2	4-2-6-1	3760	25.92	0.2249
56	4-3	4-3-6-1	3734	25.75	0.2176
56	4-4	4-4-6-3	3767	25.97	0.2176
56	4-4	4-4-6-4	4173	28.77	0.2539
56	4-5	4-5-6-1	3442	23.73	0.2113
56	4-6	4-6-6-1	3585	24.72	0.2101
56	4-7	4-7-6-1	3935	27.13	0.2060
56	5-1	5-1-6-1	4296	29.62	0.2224
56	5-2	5-2-6-1	3835	26.44	0.1949
56	5-3	5-3-6-3	3747	25.83	0.2108
56	5-3	5-3-6-4	3705	25.55	0.2210
56	5-4	5-4-6-1	3678	25.36	0.2310
56	5-5	5-5-6-1	3642	25.11	0.2278
56	5-6	5-6-6-1	3609	24.88	0.2210

Table 5.4 Average elastic modulus and Poisson's values at 56 days for each girder

Girder	Average Elastic Modulus (ksi)	Standard Deviation (ksi)	Average Elastic Modulus (GPa)	Average Poisson's Ratio
1	3,851	271	26.55	0.2208
2	3,696	201	25.48	0.2115
3	3,499	236	24.13	0.2185
4	3,786	222	26.10	0.2224
5	3,787	236	26.11	0.2184
Final Average	3,729	254	25.71	0.2185

These values differ from the results found by Buchberg (2002) using a similar mix design. Values found by that research were 4,400 ksi and 0.1852 for elastic modulus and Poisson's ratio. This research found elastic modulus values 15% lower than Buchberg's results and Poisson's ratio values 18% higher.

AASHTO uses Equation 5.1 to calculate modulus of elasticity from Section 8.4.2.4 of the code. This is the standard equation for unit weights between 0.90 and 0.155 kips per cubic foot. This equation is similar to the one used by ACI for normal weight concretes.

$$E_c = 33{,}000 K_1 w_c^{1.5} \sqrt{f_c'} \qquad (5.1)$$

where,

E_c = Modulus of elasticity, ksi

K_1 = Correction factor for source aggregate; equal to 1.0 unless noted

w_c = Weight of concrete, kips/ft^3

f_c' = Compressive strength of concrete, ksi

ACI uses equation 5.2 when predicting modulus of elasticity for high strength concrete. This equation a modified version of the ACI 363-97 report equation.

$$E_c = \left(40{,}000\sqrt{f_c'} + 1.0\times10^6\right)\left(\frac{w_c}{145}\right)^{1.5} \tag{5.2}$$

where,

E_c = Modulus of elasticity, psi

w_c = Weight of concrete, lbs/ft^3

f_c' = Compressive strength of concrete, psi

Meyer (2002) developed a new equation specifically for high strength lightweight concrete, shown in equation 5.3.

$$E_c = 44{,}000\sqrt{f_c'\frac{w_c}{145}} \tag{5.3}$$

where,

E_c = Modulus of elasticity, psi

w_c = Weight of concrete, lbs/ft^3

f_c' = Compressive strength of concrete, psi

Cook and Meyer developed another equation in 2006 for lightweight aggregates, as shown in equation 5.4.

$$E_c = w_c^{2.687} f_c'^{0.24} \tag{5.4}$$

where,

E_c = Modulus of elasticity, psi

w_c = Weight of concrete, lbs/ft^3

f_c' = Compressive strength of concrete, psi

The National Cooperative Highway Research Program uses an equation recently developed by Rizkalla shown in equation 5.5.

$$E_c = 310{,}000 K_1 w_c^{2.5} f_c'^{0.33} \quad (5.5)$$

where,

E_c = Modulus of elasticity, ksi

w_c = Weight of concrete, kip/ft^3

f_c' = Compressive strength of concrete, ksi

Figure 5.7 shows the modulus of elasticity data from this experiment and the five equations shown, along with the trendline of the data. The average wet density of 120.4 lb/ft^3 was used for the equations. Note that Meyer's equation is significantly closer than the ACI 318 equation. The ACI 363 equation is the closest match to the trendline of the data. Both Cook & Meyer's equation and Rizkalla's equation give values less than the trendline. Previous research suggested that the elastic modulus was dependent on the type of lightweight aggregate used even when compressive strengths were the same. Variations between equations could be resulting from this principle.

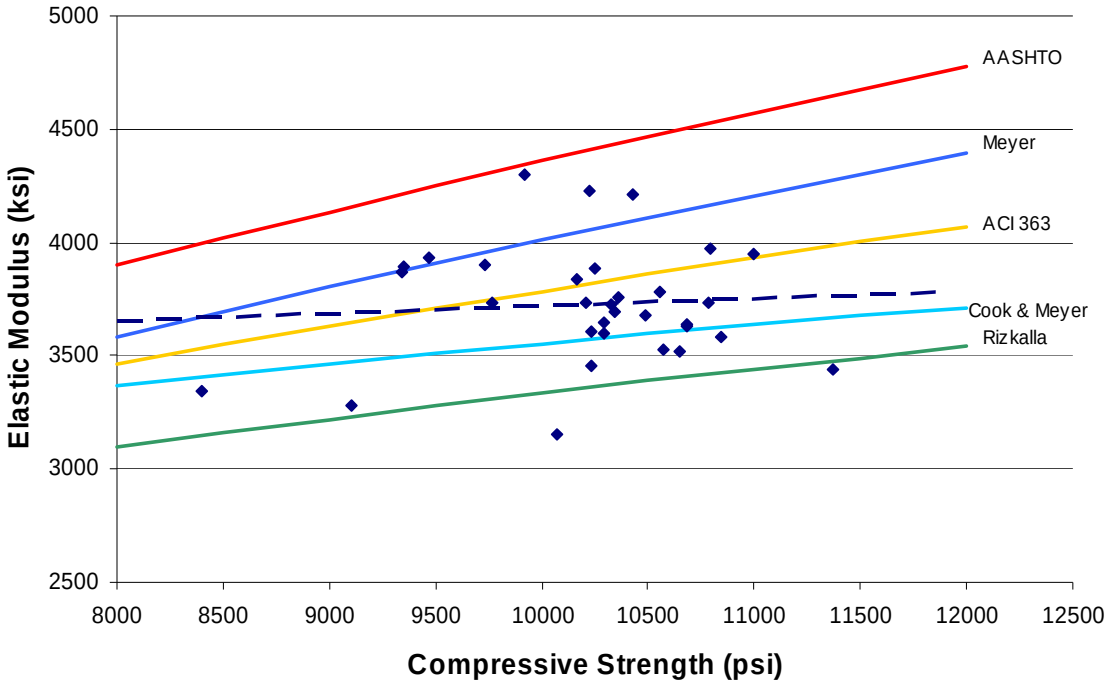

Figure 5.7 Elastic Modulus and Compressive Strength compared to standard equations

5.3.3 Splitting Cylinder Tests

Splitting cylinder tests were conducted according to ASTM C 496. The tests were conducted on the same SATEC Systems testing machine used for previous tests. Splitting cylinder tests were conducted the day the strands were released and at 56 days. Data from these tests are shown in Tables 5.5 and 5.6.

AASHTO estimates the tensile strength for most normal weight concretes using equation 5.6 from the Bridge Design Specifications section 5.4.2.7. For sand-lightweight concrete, as used in this mix design it recommends equation 5.7 from section 5.4.2.6. ACI 318-08 uses equation 5.8 for sand-lightweight concrete.

$$f_r = 0.23\sqrt{f_c'} \tag{5.6}$$

$$f_r = 0.20\sqrt{f_c'} \tag{5.7}$$

where,

f_r = Modulus of rupture, ksi

f_c' = Compressive strength of concrete, ksi

$$f_r = 0.85\left(7.5\sqrt{f_c'}\right) \tag{5.8}$$

where,

f_r = Modulus of rupture, psi

f_c' = Compressive strength of concrete, psi

Table 5.5 Split cylinder values

Date	Batch	Cylinder Number	Splitting Cylinder Strength (psi)	Splitting Cylinder Strength (MPa)
Release	1-3	1-3-6-2	687	4.74
Release	2-3	2-3-6-2	588	4.06
Release	3-3	3-3-6-2	444	3.06
Release	4-4	4-4-6-2	404	2.78
Release	5-3	5-3-6-2	614	4.23
56	1-3	1-3-6-5	729	5.03
56	2-3	2-3-6-5	714	4.92
56	3-3	3-3-6-5	516	3.56
56	4-4	4-4-6-5	783	5.40
56	5-3	5-3-6-5	657	4.53

Table 5.6 Average splitting cylinder strengths and sand-lightweight standards

Date	Splitting Cylinder Strength (psi)	AASHTO (psi)	ACI 318 (psi)
Release	547.45	640	645
56	679.80	640	645

The 56 day splitting cylinder exceeded the values suggested by AASHTO LRFD (4^{th} Edition) and ACI 318-08. The equations produced close, but conservative estimates in both cases at 56 days.

5.3.4 Coefficient of Thermal Expansion Tests

Coefficient of thermal expansion tests were conducted according to CRD-C 39. The tests were conducted on a Thermotron SE-1200 machine. Coefficient of thermal expansion tests were conducted the day the strands were released and at 56 days. Data from these tests are shown in Table 5.7. The mean 56 day coefficient was 3.24×10^{-6} strain/˚F at 100% humidity.

Table 5.7 Coefficient of thermal expansion results

			Coefficient of Thermal Expansion (strain/degree Fahrenheit)	
Batch	T_{cold} (˚F)	T_{hot} (˚F)	7-14 day	56 day
1-3	41	140	4.57×10^{-6}	3.96×10^{-6}
2-3	41	140	4.82×10^{-6}	3.33×10^{-6}
3-3	41	140	3.46×10^{-6}	2.80×10^{-6}
4-4	41	140	3.06×10^{-6}	2.60×10^{-6}
5-3	41	140	3.41×10^{-6}	3.48×10^{-6}
Average	41	140	3.86×10^{-6}	3.24×10^{-6}

5.3.5 Chloride Ion Permeability Tests

The rapid chloride ion permeability tests were conducted by Robert Moser 56 days after the pour. These tests were conducted according to ASTM C1202. Figures 5.8 through 5.12 show those tests. The resulting data are shown in Table 5.8.

Figure 5.8 Vacuum saturation in desiccator

Figure 5.9 Concrete specimens soaking in vacuum desiccator

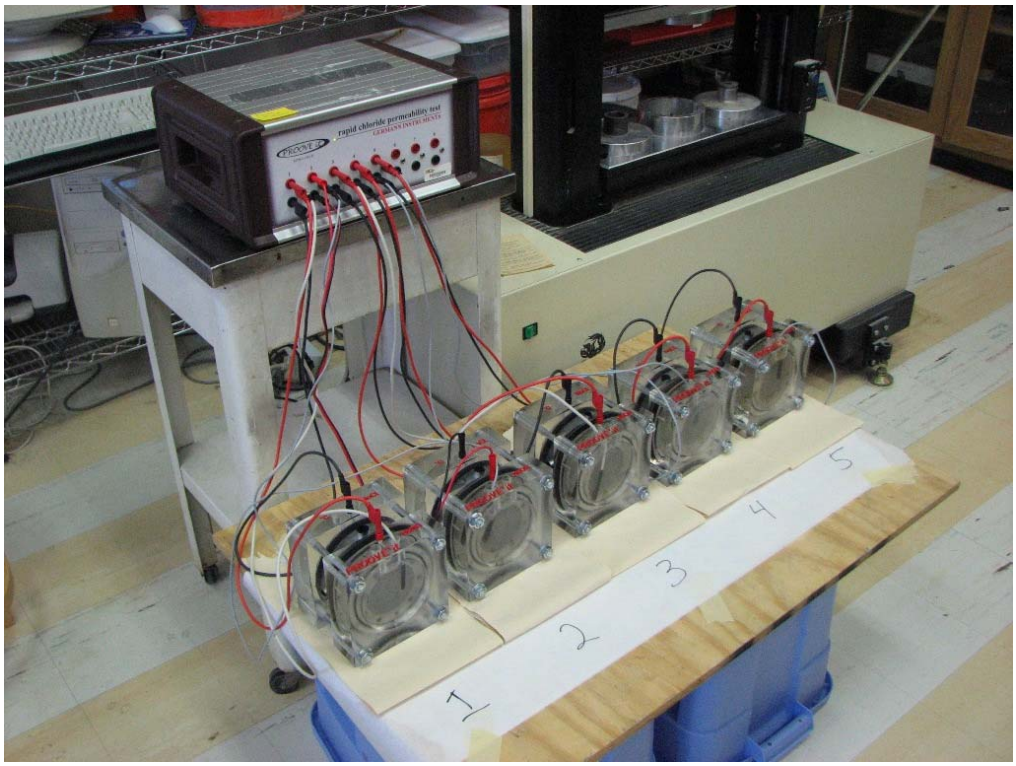

Figure 5.10 Specimens mounted in frames with current running through concrete

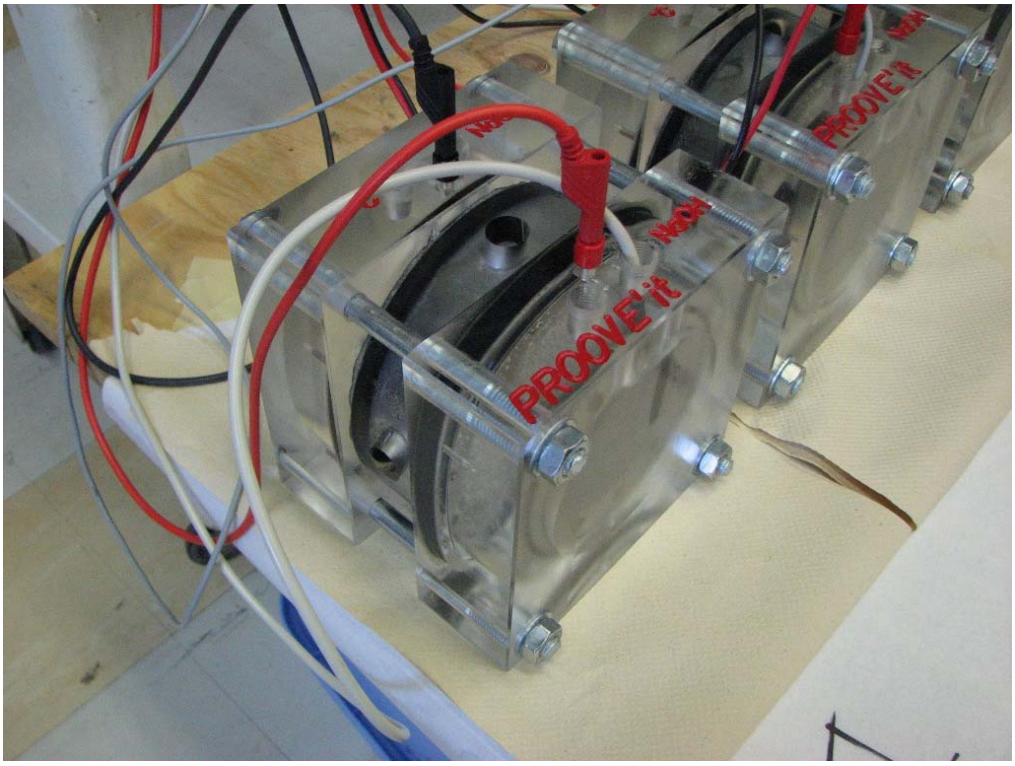

Figure 5.11 Wires connecting frame to power source

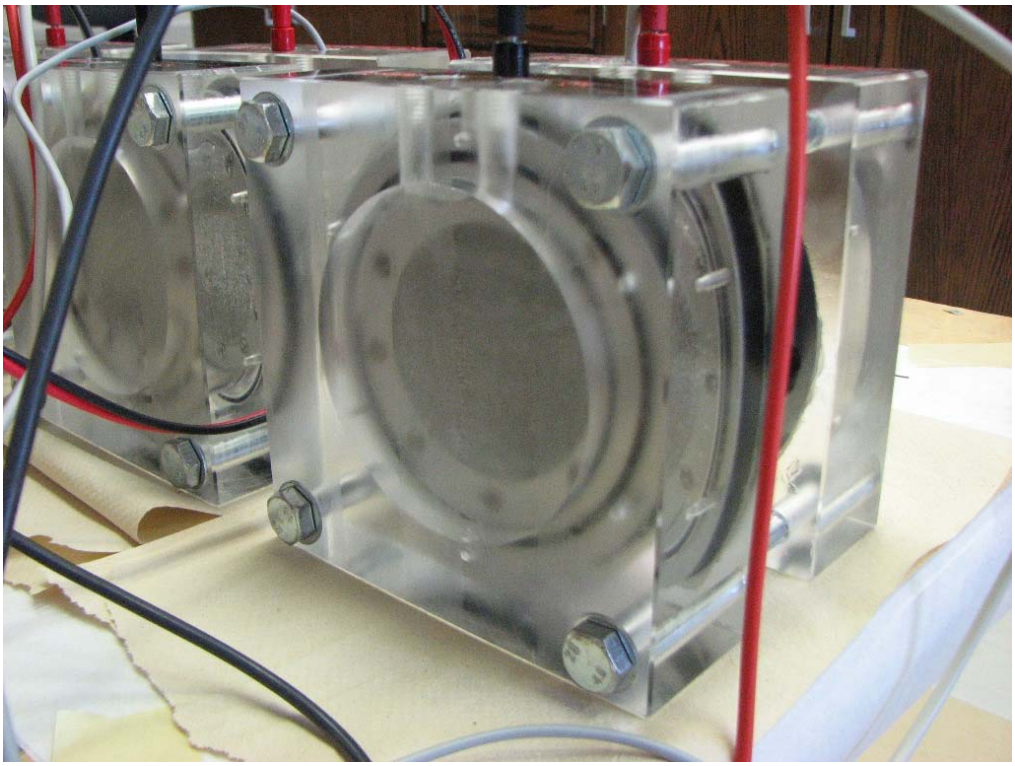

Figure 5.12 Magnified view of specimen mounted in frame

Table 5.8 Chloride ion permeability results at 56 days

Concrete Age (days)	Batch	Chloride Ions Permeability (coulombs)
56	1-3	284
56	2-3	289
56	3-3	297
56	4-4	359
56	5-3	360
Average		318

The test results for all the specimens fell in the "Very Low Chloride Ion Permeability" range. The values were well under the maximum value set by GDOT as 3,000 coulombs. Moser noted that results from girders 1 through 3 correlated well to each other, all of which were poured on the same day. The same was true for girders 4 and 5, which were poured together. The higher results from girders 4 and 5 could be due to a larger amount of superplasticizer used in the mix. This superplasticizer may increase the conductivity of the pore solution itself, leading to artificially high measurements.

Results found from these tests were similar to previous research done by Mauricio Lopez (2005). Lopez found a mean chloride ion value of 227 coulombs at 56 days for the same 10 ksi HSLW concrete mix used in these girders.

5.3.6 Dry Unit Weight Tests

The dry unit weight of the concrete was measured using two methods. Three 6 inch by 12 inch cylinders were dried in a oven at 100° C for 24 hours. These cylinders then were weighed in their dried state. The first method involved measuring the volume

using a water displacement method. The second method measured volume by taking physical dimensions of a cylinder and averaging the results. The two methods found different unit weights, shown in Table 5.9. The water displacement method produced a more reasonable number, and the unit weight of 116.12 lb/ft^3 was used.

Table 5.9 Dry unit weight calculations

		Water Displacement Results		Physical Measurement Results	
	Dry Weight (lb)	Volume (ft^3)	Unit Weight (lb/ft^3)	Volume (ft^3)	Unit Weight (lb/ft^3)
1-3	23.17	0.1963	118.03	0.1915	120.99
2-3	23.34	0.1927	121.14	0.1915	121.87
4-4	23.02	0.2108	109.18	0.1888	121.90
		Average	116.12	Average	121.59

CHAPTER 6

TRANSFER LENGTH

6.1 Introduction

Transfer length of prestressed girders is discussed in this chapter. The definition of transfer length is discussed along with current code provisions required by both ACI and AASHTO. These standards are compared with the experimental transfer lengths values found for the HSLW girders.

6.2 Definition

Transfer length is defined by Russell (1992) as "the distance required to transfer the fully effective prestressing force from the strand to the concrete." The transfer length is measured from the end of the girder to the point where the concrete around the strand is carrying the effective prestressing force. Figure 6.1 shows an idealized view of transfer length as a function of steel stress along the length of the beam.

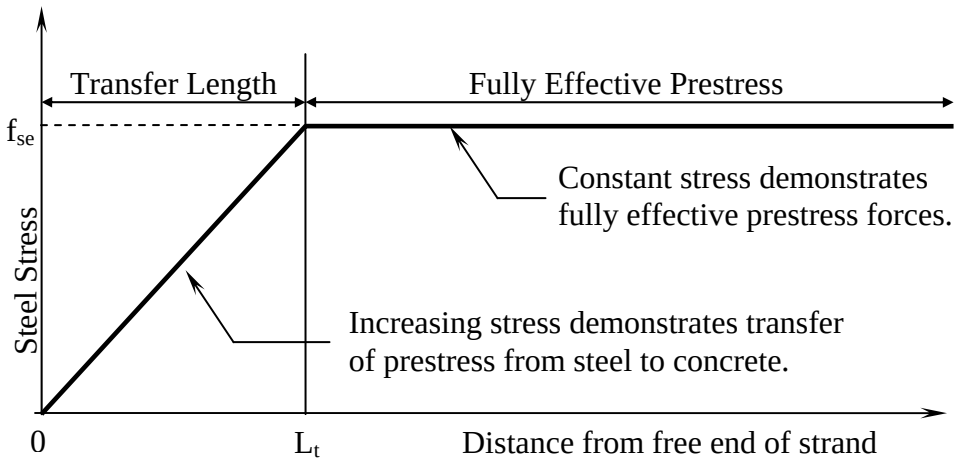

Figure 6.1 Idealized stress in steel strand in a prestressed concrete member

6.3 Current Code Provisions

Currently both ACI and AASHTO have recommended values for transfer length. ACI 318-08 uses the effective prestressing stress, f_{se}, and the diameter of the bar, d_b, or in this case strand, to calculate transfer length, shown in Equation 6.1.

$$l_t = \frac{f_{se} d_b}{3} \tag{6.1}$$

AASHTO (2007) currently only used the strand diameter to define the transfer length, shown in Equation 6.2.

$$l_t = 60 d_b \tag{6.2}$$

Previous research (Meyer, 2002) has shown both of these equations to be conservative.

6.4 Test Specimens

All five HSLW girders were instrumented to measure transfer length. DEMEC embedments were placed at the North and South ends of each girder, with North and

South referring to final bridge positions. These embedments were placed over length of at least 48 inches on the same side of the girder along the bottom flange as pictured in Figure 6.2.

Figure 6.2. Grey boxes indication location of embedments spaced at 2 inches over a length of at least 48 inches.

All 5 girders used 0.6 inch diameter 7-wire low-relaxation strand. The strands were stressed to approximately the same prestressing force of 45 kips. Due to the early age of the girders during the transfer length measurements, the initial stress of the strands was used for effective stress, f_{se}, in calculations. The initial stress was found to be 178.8 ksi using load cell data of tension in the strand just before cut-down.

6.5 Measurement of Transfer Length

The concrete surface strain (CSS) method was used to calculate the transfer length. This method uses the assumption that as the prestressing strand develops a bond with the surrounding concrete, the concrete will move in the same way the strand does. Changes in strain in the strand are then the same as the change in compressive strain in the concrete. Using this idea, the change in length can be measured at the surface and directly correlated to the strand inside the girder.

A DEMEC gage was used to take the CSS measurements monitoring the relative change in distance between points on the girder, and thus the strain in the concrete.

Embedments in the concrete were used as reference points for the DEMEC gage, shown in Figure 6.3. These embedments were spaced 2 inches apart from the end of the beam moving toward the center for at least 48 inches. The distance between these holes was then measured with the DEMEC gage, which reads to accuracy of 0.0001 inches. The DEMEC gage has two conical points spaced 8 inches apart, with one point on a spring, which can adjust. Figure 6.4 shows a researcher taking DEMEC readings with a second researcher recording values.

Figure 6.3 DEMEC gage used for this research

Figure 6.4 Researchers Jennifer Dunbeck and Brett Holland taking DEMEC readings

Several steps were taken to ensure accurate usage of the DEMEC gage. First, the same DEMEC gage was used for all readings. Second, the DEMEC gage was zeroed before each use. A steel bar with conical holes spaced at 8 inches was provided by the manufacturer. This bar and the gage were allowed to reach ambient temperature before the tool was zeroed and then used to take readings. Third, the same researcher took all DEMEC readings, with another research present to record the data. Care was taken to hold the gage in the same manner each time. Finally, all readings were taken close to 8:00am before direct sunlight hit the girders. This prevented thermal effects from playing a factor in the results.

6.6 Determination of Transfer Length

The strains in the concrete were measured by finding the difference between the initial CSS reading, which was before cut-down, and the reading of a given day. These strains were already partly "smoothed out" due to the nature of taking the readings. Using an 8 inch gage length allowed each reading to cover 5 embedment points: one at each point of the DEMEC gage and 3 in the middle. This averaged any change in length over 8 inches rather than only over 2 inches. A second tool was used to further "smooth out" the data. Using a spreadsheet, the strains for a given point were averaged using a 3 point floating average, shown in Equation 6.3.

$$\varepsilon_x = \frac{\varepsilon_{(x-1)} + \varepsilon_{(x)} + \varepsilon_{(x+1)}}{3} \tag{6.3}$$

These smoothed out values were then plotted against their distance from the girder end. The "95% Average Maximum Strain" method was used to calculate the transfer length, developed by Russell (1992). This method uses a "strain plateau", which ideally is the constant strain value in the concrete once full transfer of effective prestress is reached. This plateau is used to determine the "Average Maximum Strain" of all values inside the plateau. 95% of this average is taken and plotted against the data. The transfer length is then determined by the intersection of the 95% line with the "smoothed" strain profile.

This method is considered to be conservative when compared to the "idealized" transfer length. The idealized transfer length would be located at the intersection of the strain plateau and a trendline of the smoothed strains. This idealized transfer length is

typically less than the measured transfer length. However, a different result was found for much of this data when using this method. Some graphs were similar to expectations, such as the graph shown in Figure 6.5, but some were far from standard, such as Figure 6.6. These atypical graphs resulted in a measured transfer length less than the idealized transfer length. All transfer length graphs are shown in Appendix E.

Another anomaly of the data was that several data sets showed negative strains at the end of the girder. This was probably the result of small cracks, such as thermal cracks, that occurred after the initial readings were taken on the bed. The negative values were not used in creating the trendlines.

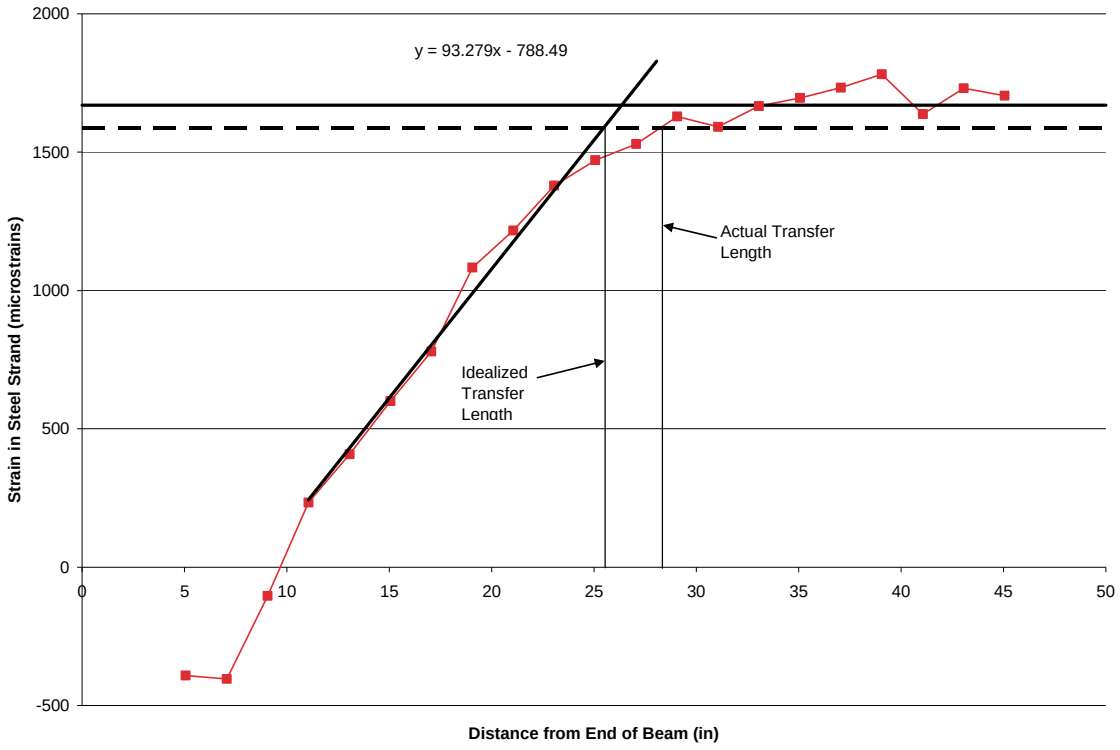

Figure 6.5 Smoothed CSS readings for the South end of Girder 1 at day 8

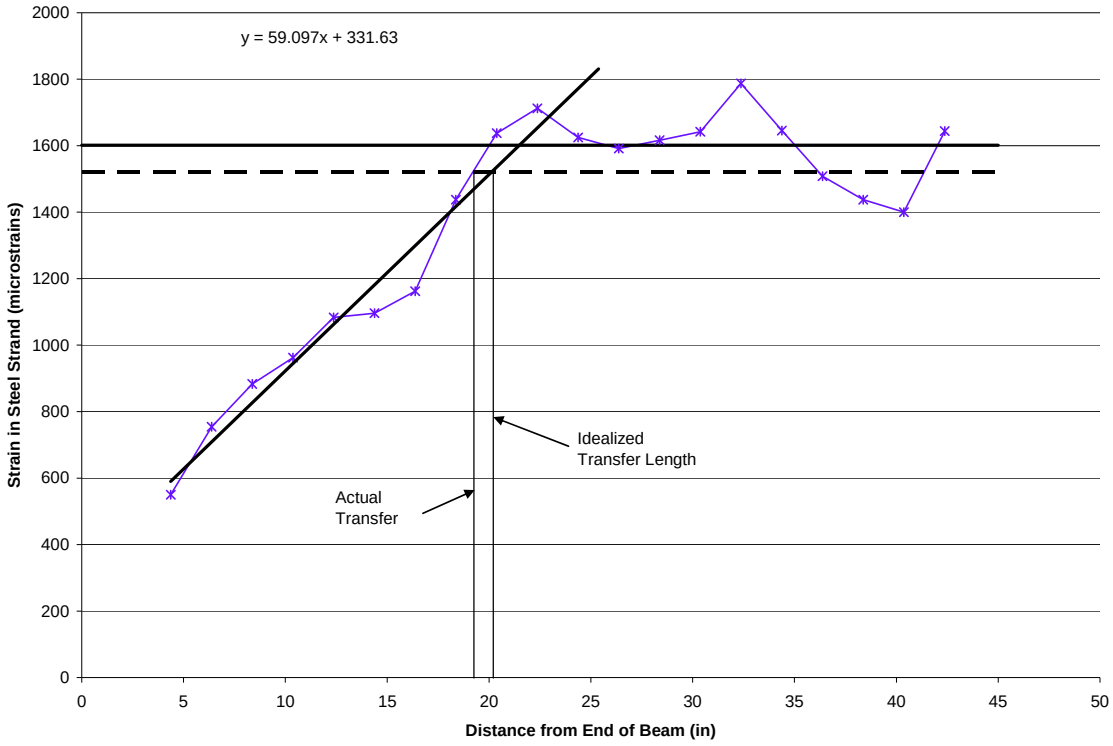

Figure 6.6 Smoothed CSS readings for the South end of Girder 5 at day 80

6.7 Transfer Length Results

Table 6.1 shows all values found, except for those of the North end of Girder 4. These data points had to be thrown out due to error readings obtained by the DEMEC gage. Tables 6.2-6.6 show the average measured and idealized transfer lengths for each reading day. Table 6.7 summarizes these averages for comparison.

Table 6.1. Measured and idealized transfer lengths for all girders.

Girder	Days after Cut-down	Measured Transfer Length (in)	Idealized Transfer Length (in)
1 South	5d	33.06	27.13
	8d	28.10	26.36
	14d	28.20	26.49
	28d	33.20	29.32
	80d	32.25	29.42
1 North	5d	27.00	31.40
	8d	27.56	31.82
	14d	27.50	34.44
	28d	30.40	31.22
	80d	21.50	24.52
2 South	5d	25.25	25.45
	8d	25.80	23.55
	14d	24.33	24.81
	28d	18.25	19.34
	80d	25.80	28.18
2 North	5d	16.80	19.93
	8d	25.00	27.89
	14d	25.40	28.68
	28d	24.75	26.16
	80d	24.60	28.75
3 South	5d	25.00	35.07
	8d	26.20	24.94
	14d	26.70	44.44
	28d	26.20	30.49
3 North	5d	34.50	39.57
	8d	30.20	30.89
	14d	30.40	35.42
	28d	29.60	29.47
	80d	33.80	33.55
4 South	5d	23.20	25.13
	8d	25.40	26.24
	14d	23.60	25.51
	28d	24.75	26.76
5 South	5d	18.00	14.59
	8d	25.20	23.33
	14d	18.50	19.34
	28d	19.30	20.35
	80d	19.20	21.48
5 North	5d	33.60	32.61
	8d	35.05	38.06
	14d	32.10	34.00
	28d	32.13	35.62
	80d	35.75	38.60

Table 6.2. Average transfer lengths at 5 days.

Girder	Measured Transfer Length (in)	Idealized Transfer Length (in)
1 South	33.06	27.13
1 North	27.00	31.40
2 South	25.25	25.45
2 North	16.80	19.93
3 South	25.00	35.07
3 North	34.50	39.57
4 South	23.20	25.13
5 South	18.00	14.59
5 North	33.60	32.61
5 Day Average	26.27	27.87
Standard Deviation	6.50	7.72

Table 6.3. Average transfer lengths at 8 days.

Girder	Measured Transfer Length (in)	Idealized Transfer Length (in)
1 South	28.10	26.36
1 North	27.56	31.82
2 South	25.80	23.55
2 North	25.00	27.89
3 South	26.20	24.94
3 North	30.20	30.89
4 South	25.40	26.24
5 South	25.20	23.33
5 North	35.05	38.06
8 Day Average	27.61	28.12
Standard Deviation	3.26	4.75

Table 6.4. Average transfer lengths at 14 days.

Girder	Measured Transfer Length (in)	Idealized Transfer Length (in)
1 South	28.20	26.49
1 North	27.50	34.44
2 South	24.33	24.81
2 North	25.40	28.68
3 South	26.70	44.44
3 North	30.40	35.42
4 South	23.60	25.51
5 South	18.50	19.34
5 North	32.10	32.10
14 Day Average	26.30	30.14
Standard Deviation	4.01	7.39

Table 6.5. Average transfer lengths at 28 days.

Girder	Measured Transfer Length (in)	Idealized Transfer Length (in)
1 South	33.20	29.32
1 North	30.40	31.22
2 South	18.25	19.34
2 North	24.75	26.16
3 South	26.20	30.49
3 North	29.60	29.47
4 South	24.75	26.76
5 South	19.30	20.35
5 North	32.13	35.62
28 Day Average	26.51	27.64
Standard Deviation	5.33	5.19

Table 6.6. Average transfer lengths at 80 days.

Girder	Measured Transfer Length (in)	Idealized Transfer Length (in)
1 South	32.25	29.42
1 North	21.50	24.52
2 South	25.80	28.18
2 North	24.60	28.75
3 North	33.80	33.55
5 South	19.20	21.48
5 North	35.75	38.60
80 Day Average	27.56	29.22
Standard Deviation	6.41	5.63

Table 6.7. Summary of average transfer lengths.

Averages	Measured Transfer Length (in)	Idealized Transfer Length(in)
5 Day	26.27	27.87
8 Day	27.61	28.12
14 Day	26.30	30.14
28 Day	26.51	27.64
80 Day	27.56	29.22

6.8 Discussion of Results

The values from day 8 were selected to be used as the transfer lengths for these girders. The day 8 values had the lowest standard deviations, and therefore the best agreement between numbers. Also, when compared to the averages from other days in Table 6.7 the measured transfer length from day 8 is the longest length. Using this value is conservative.

The transfer length of the HSLW girders was 27.61 inches. This number is 23% less than the values suggested by AASHTO and ACI, confirming that the equations are conservative. Table 6.8 compares the three values.

Table 6.8. HSLW transfer length compared to code requirements.

Source	Equation	Transfer Length (in)
HSLW Girders		27.61
ACI	$\frac{f_{se} d_b}{3}$	35.76
AASHTO	$60\ d_b$	36.00

The variations in transfer length between girders ends were more than expected. Previous research (Meyer, 2002 and Russell, 1992) has suggested that girders constructed at the free end, or dead end, of the bed have longer transfer lengths. Typically multiple beams are constructed on a bed starting at the live end and moving toward the dead end. There is often a space left at the dead end of the bed between the last beam and the abutment. From this research, Girder 3 was on the free end of pour 1 with approximately 79 feet of free prestressing cable, and Girder 5 was on the free end of pour 2 with approximately 190 feet of free prestressing cable. The average transfer length of the Girder 3 was 4.09 inches greater than the average transfer length for all the girders of 27.61 inches. Girder 5's average transfer length was 6.12 inches greater than the average for all the girders. These values indicate that long lengths of free strand increase transfer length of the nearest girder end.

CHAPTER 7

CAMBER

7.1 Introduction

The concept of prestressing beams puts a large amount of compression in the bottom of the beam relative to the top. This variation in forces causes the beam to camber upwards. During use of the beam, the camber lessens as dead and live loads are added to it.

This chapter discusses the camber of the five HSLW girders from construction to the end of the storage period (226 days). Equations used to predict camber are discussed and compared to actual results.

7.2 Measurement of Camber

The camber of all five HSLW girders was monitored with the deflection measurement system discussed in Chapter 3. This taut wire system was placed on the southeast side of Girder 1, and the northwest side of Girder 5. Girders 2, 3, and 4 had taut wire systems attached to both sides. For these latter three girders, the results of the two sides were averaged.

Taut wire readings were always taken around 8:00 am to minimize the camber resulting from the heating of the beam due to direct sunlight. Before each reading was taken, the weight attached to the taut wire would be pulled away from the face of the

beam, and allowed to move freely. This prevented any interaction between the weight and the face of the beam from affecting the readings.

The camber data are shown in Table 7.1. The first reading after cut-down was taken while the girder was still on the bed. The second reading on that same day was taken after the girders were placed in the yard for storage. All subsequent readings were also taken in the storage positions.

Two outliers were found, and were discarded: reading 3a on day 56, and reading 4a on day 73. These readings were both at least 15% higher than the other reading from the same girder. Figure 7.1 graphically displays the increasing camber over time, and does not include outlier data.

Table 7.1 Camber Data

	11 Aug	11 Aug	16 Aug	19 Aug	25 Aug	8 Sep	6 Oct	23 Oct	24 Jan
	After cut	7:00p	8:15a	8:05a	8:00a	8:00a	9:18a	8:30a	12:00p
	0	0.5	5	8	14	28	56	73	197
1	3.7500	4.1875	3.9844	4.0156	4.0313	4.0938	4.2656	4.4844	4.7656
2a	3.7031	4.0469	3.9531	3.9063	4.1250	4.1719	4.2188	4.3906	4.9219
2b	3.7188	4.0469	3.8906	3.9063	3.9375	4.1094	4.0469	4.2500	4.8281
3a	3.7188	4.0938	4.0781	4.0938	4.1563	4.2500	5.0000	4.4688	4.8438
3b	3.8594	4.0313	3.9063	3.9688	3.9375	4.2188	4.2656	4.5156	5.0313
4a	3.8125	4.3438	4.3281	4.3438	4.3750	4.4375	4.6094	5.1250	5.1406
4b	3.7031	4.1563	4.0938	4.1250	4.1250	4.3594	4.3125	4.4688	4.7031
5	3.5938	4.0313	3.9219	3.9219	3.9375	4.2344	4.1563	4.1719	4.7188

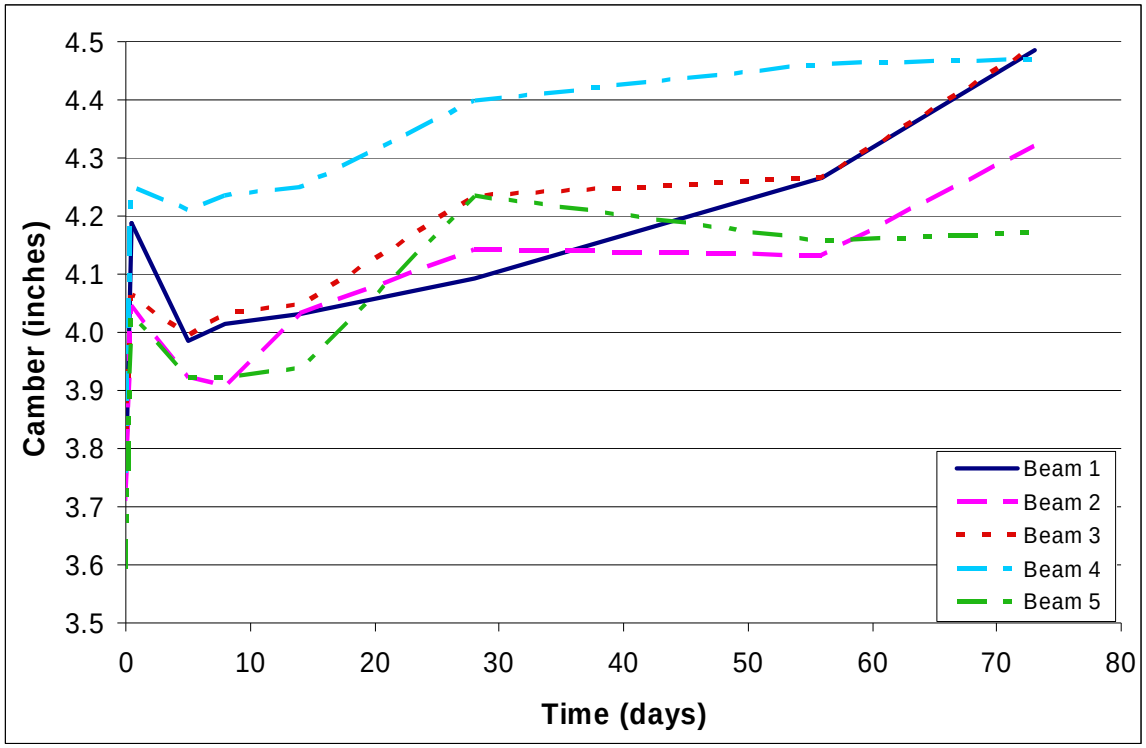

Figure 7.1 Camber of girders over time

The girders were stored at SCP in their yard for further curing. During storage the girders were set on 4x4 timber atop reinforced concrete dunnage pieces for support. These dunnage pieces were not directly underneath the bearing points of the girders, and this affected the camber value. Figure 7.2 shows the South ends of the girders resting on the timber and concrete dunnage. The distance to the bearing points was measured from each end of the girder. The distances and resulting span length are shown in Table 7.2.

Figure 7.2 South ends of girders set at varying lengths from the end

Table 7.2 Distances from end of girders to bearing points and resulting span length

Girder	North (in.)	South (in.)	Span Length (ft)
1	51.0	39.0	100.50
2	52.0	44.0	100.00
3	53.5	41.5	100.08
4	50.5	42.5	100.25
5	47.0	46.0	100.25

Washington State Department of Transportation (WSDOT) has developed a method for determining total camber of a beam not supported at its intended bearing locations. Equations 7.1 through 7.5 are from the WSDOT report. (2007)

$$\Delta = \Delta_{ps} - \Delta_{sw} \tag{7.1}$$

where,

Δ = Camber, in.

Δ_{ps} = Camber due to prestressing, in.

Δ_{sw} = Deflection due to self weight of girder, in.

$$\Delta_{ps} = \frac{PL^3}{8E_c I_g}\left[e_{mid} + (e_{end} - e_{mid})\frac{4a^2}{3L^2} \right] \tag{7.2}$$

where,

P = Total prestressing force, lbs

L = Length of beam, in.

E_c = Experimental modulus of elasticity at 56 days, psi

I_g = Measured moment of inertia, in.^{4}

e_{mid} = Eccentricity of strands at midspan, in.

e_{end} = Eccentricity of strands at end, in.

a = Distance from the end of the girder to the harping point, in.

$$\Delta_{sw} = \Delta_{overhang} + \Delta_{midspan} \tag{7.3}$$

where,

$\Delta_{overhang}$ = Deflection of overhang relative to the support, in.

$\Delta_{midspan}$ = Deflection at midspan relative to the support, in.

$$\Delta_{overhang} = \frac{\omega_{sw} L_c}{24 E_c I_g}\left[3L_c{}^2\left(L_c + 2L_n\right) - L_n{}^3\right] \tag{7.4}$$

where,

ω_{sw} = Weight per linear foot of girder, lb/ft

L_c = Overhanging length, in.

L_n = Distance between supports, in.

$$\Delta_{midspan} = \frac{\omega_{sw} L_n{}^2}{384 E_c I_g}\left(5L_n{}^2 - 24L_c{}^2\right) \tag{7.5}$$

Using these equations the expected camber for each girder was calculated. Table 7.3 compares the actual camber values at 56 days to the camber predicted by the WSDOT equations.

Table 7.3 Predicted camber and actual camber at 56 days

Girder	Actual	Predicted	Actual - Predicted / Actual	
	(in.)	(in.)	(in.)	%
1	4.2656	4.0600	0.2056	4.8%
2	4.1328	4.2600	-0.1272	-3.1%
3	4.2656	4.4460	-0.1804	-4.2%
4	4.4609	4.1150	0.3459	7.8%
5	4.1563	4.1040	0.0522	1.3%
Average	4.2563	4.1970	0.0592	1.4%

7.3 Discussion of Results

The average 56-day camber in the girders is 4.26 inches. The camber values are very close to the predicted values. The slight discrepancies may be due to slight errors in reading off the taut wire system and variations in modulus of elasticity values as compared to the average.

Camber and deflections of the girders will be monitored while the bridge is in use. These findings will be presented in a future report.

CHAPTER 8

GIRDER FIELD STIFFNESS TESTS

8.1 Introduction

In order to better predict the performance of the HSLW girders, a field test was performed at Standard Concrete Products (SCP) on all five BT-54 girders to be used in Span 2. By loading each girder and measuring its deflection, the stiffness of each beam could be calculated and then used by Georgia Department of Transportation (GDOT) designers to precisely design the deck and road profile.

8.2 Design of Test

The girder field stiffness test was designed to load each girder enough to obtain a stiffness measurement without damaging it in anyway. A primary concern was the method in which the load would be applied. When in use, the girder will carry distributed loads from the weight of the deck and traffic, however, a distributed load would have been difficult to generate in a large scale test, and raised some safety issues as well. A point load was chosen instead.

There were two options for locations to place the point load: on the top of the girder, or on the bottom. The bottom loading was chosen for two reasons. First, due to the length of the girders, there was concern that loading from the top would induce torsional buckling, causing the beam to fail, or be damaged. A bottom loading design was self-stabilizing. Secondly, these girders were constructed with a threaded rod

protruding from the bottom at midspan, which was used to hold down the harping device. Significant force was applied to this device during the pretensioning of the strands. Figure 1 shows the pretensioning forces which are resolved into the hold down force, W_B. The threaded rod was holding down W_B equal to 19.335 kips of force, which was calculated using Equation 8.1. Figures 8.2 and 8.3 show the harping device which was being held down by the threaded rod.

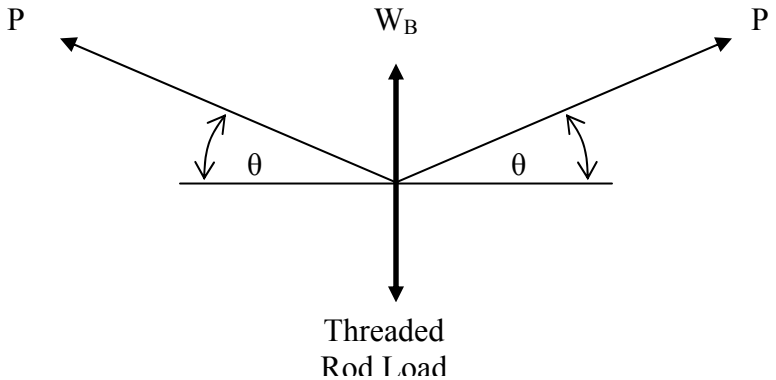

Figure 8.1 Model of forces induced on threaded rod by prestressing forces

$$W_B = P \times 2\theta \tag{8.1}$$

where,

P = Prestressing force, 439 kips

θ = Angle of strand, 0.022 radians

W_B = Hold down force, 19.335 kips

Figure 8.2 Strand harping device being held down to construction bed by a threaded rod

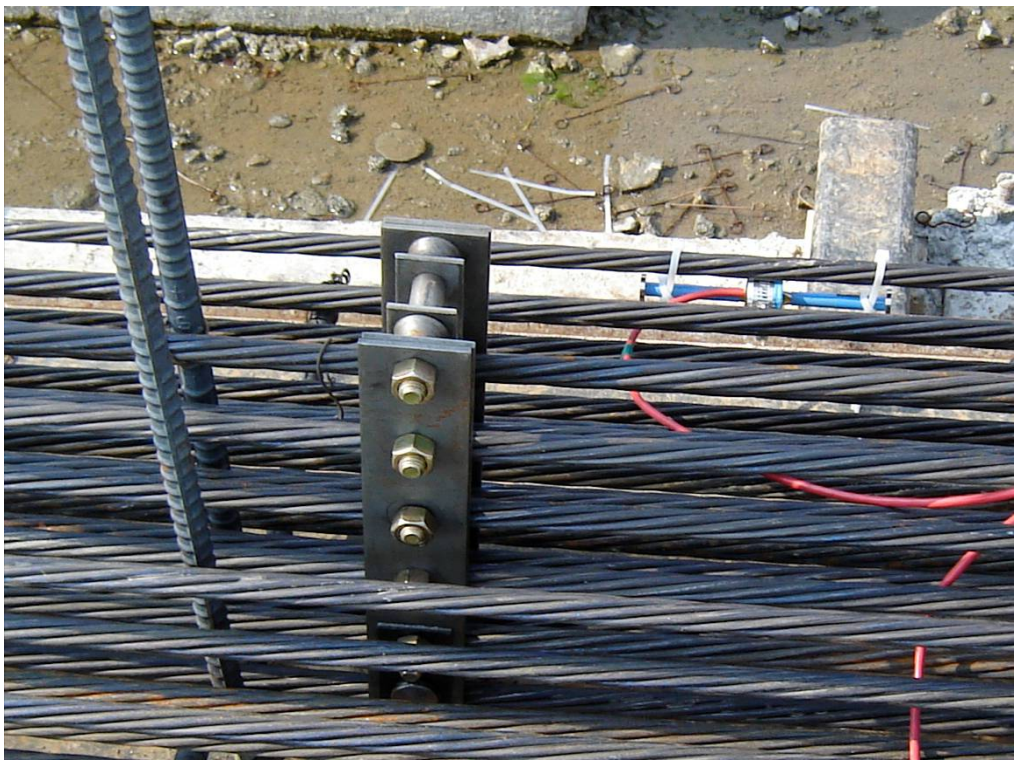

Figure 8.3 Strand harping device detail

The threaded rod supported 19.335 kips during construction, so loading the same threaded rod from the bottom of the girder with a lesser weight was a conservative loading scheme. This method was chosen to be used for this field test.

There was still some concern about the stability of the girders. The bottom loading should have prevented any torsional buckling, but two extra precautions were taken to ensure a safe loading. First, both ends of the girder were braced by strapping a chain across the top and securing on either side using concrete road barriers. Secondly, after setting the girder the crane's carrying hooks were left inside the pick-up loops, but were lowered so that no load was being carried. If the girder were to begin to fall, the hooks would quickly catch it.

8.3 Testing Procedures

Each girder was tested at the same staging area. Two stacks of dunnage were set up 106 feet 8 -7/8 inches from center to center to support the ends of the girders as shown in Figure 8.4. The dunnage used was large reinforced concrete blocks. These blocks were stacked and then shimmed to matching elevations. Three elastomeric bearing pads, 14"x 10"x 3¼", were placed side by side on top of each dunnage platform to match actual bridge conditions and to protect the integrity of the girders shown in Figure 8.5. Dial gages were used at both ends to monitor vertical deflections of elastomeric bearing pads, if there were any. Figure 8.6 shows one such dial gage.

Figure 8.4 Crane setting girder on dunnage supports

Figure 8.5 Girder end resting on elastomeric bearing pads; Friction between the beam and the construction bed during prestress strand cut-down caused the friction failure shown here, which was corrected in the field.

Figure 8.6 Dial gage measuring end support deflection

A reinforced concrete block was constructed at Standard Concrete Products to be used as the load for the tests. This 76in x 76in x 36in block was weighed using 2 different methods. Before the testing began, the block was weighed on 3 load cells set in a triangular formation on the ground, as shown in Figure 8.7. The values from the load cells were read using a strain indicator box. The second weight measurement came from the coupler used to attach the block to the threaded rod on the beam. Strain gages were attached to all 4 side-rods of the coupler device, and readings were taken while the weight of the block was being supported by the coupler. The coupler and load cells were calibrated in a laboratory testing machine which was itself calibrated. The load cell method found the weight of the block to be 17,893 lbs, and the coupler method found the

weight to be 17,895 lbs. The average value of 17,894 lbs was used in further calculations as the weight of the block.

Figure 8.7 Three load cells and strain indicator box used to weigh the load block

The block was moved using a forklift provided by SCP (Figure 8.8). The block had a threaded rod imbedded in the concrete that extended from the top of the block, to which a coupler was affixed. The block was then placed under midspan of the girder by the forklift, and the coupler was screwed up onto a matching threaded rod protruding from the bottom of the girder (Figures 8.9 and 8.10). This threaded rod is used during construction of the girder to hold the harping device that holds the prestressed strands down. Once the weight was in place, the forklift slowly lowered the forks until all the weight was carried by the girder.

Figure 8.8 Reinforced concrete block used to load girders

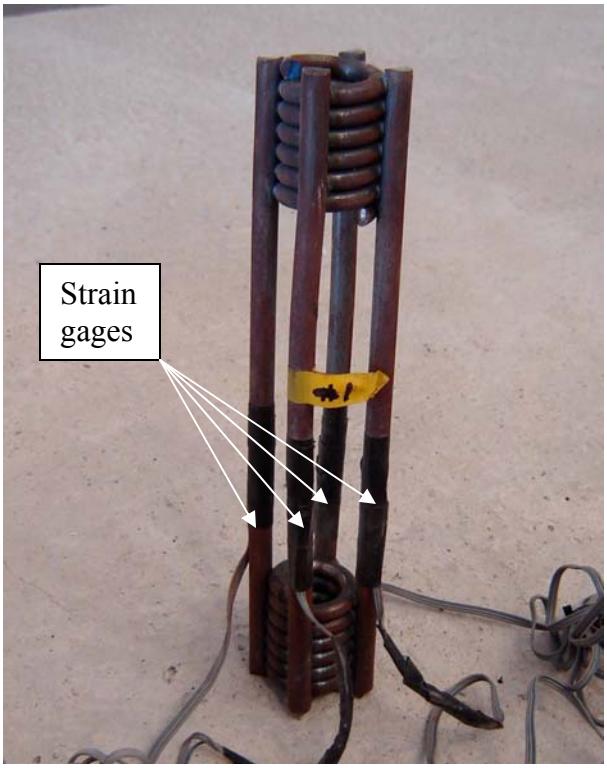

Figure 8.9 Coupler with strain gages attached on all 4 vertical pieces

Figure 8.10 Coupler connecting load onto girder

While the girder was loaded, camber measurements and VWSG measurements were taken as shown in Figure 8.11. The taut wire system was used to measure the deflection of the beams under the weight, and a secondary system was also used to check the reasonableness of the values. This secondary system was manual tape measurement taken from the bottom of the beam to the ground approximately 5 feet on either side of midspan, shown in Figure 8.12.

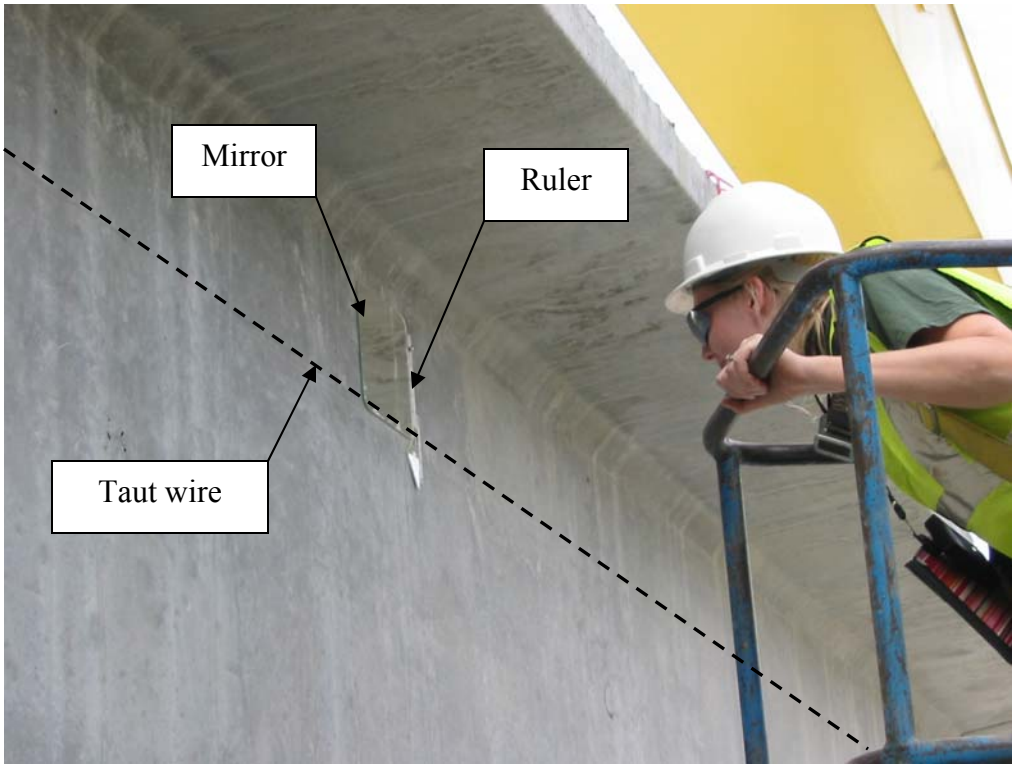

Figure 8.11 Researcher reading taut wire measurement; Dashed line is used to depict wire which is barely visible in photo. Accuracy 1/32 inch.

Figure 8.12 Researchers manually measuring beam deflection. Accuracy 1/8 inch.

8.4 Measured Data

Tables 8.1 and 8.2 and Figure 8.14 show resulting data. Girder numbering system is discussed in Chapter 4. VWSG locations are shown in Figure 8.13.

Table 8.1 Deflections from load test as measured from taut wire system

Girder	Initial Reading	Loaded Reading	Change = Deflection
1	1.594	2.281	0.688
2a	0.719	1.375	0.656
2b	2.625	3.266	0.641
3a	4.781	5.406	0.625
3b	8.688	9.313	0.625
4a	8.641	9.250	0.609
5	3.000	3.141	0.141
AVERAGE			0.641*

*Note that the average value does not include the reading from Girder 5, which was obviously in error.

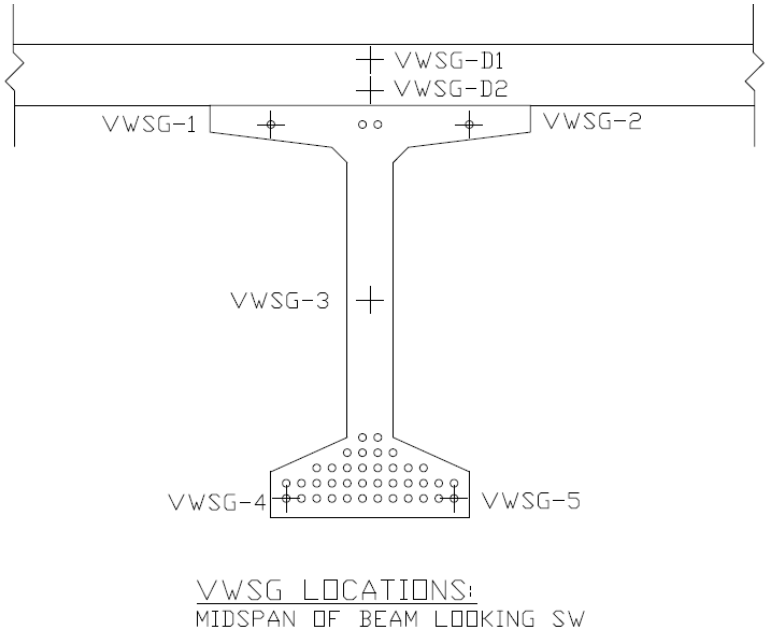

Figure 8.13 VWSG layout showing locations of each gage, and 2 future gages which will be place in the deck of the bridge.

Table 8.2 Vibrating Wire Strain Gage readings and change due to load

Girder - Gage	y (in)	Initial Reading (in/in)	Loaded Reading (in/in)	Strain from Loading (in/in)	Average Strains (in/in)	Expected Strain (in/in)
1-1	24.37	483.5 E-6	537.9 E-6	-54.4 E-6	-55.7 E-6	-116.6 E-6
1-2	24.37	458.5 E-6	515.5 E-6	-57.0 E-6		
1-3	-0.63	777.5 E-6	788.6 E-6	-11.1 E-6	-11.1 E-6	3.0 E-6
1-4	-24.63	1,481.1 E-6	1,266.1 E-6	214.9 E-6	278.8 E-6	117.8 E-6
1-5	-24.63	2,179.6 E-6	1,837.0 E-6	342.6 E-6		
2-1	24.37	466.2 E-6	522.4 E-6	-56.3 E-6	-62.0 E-6	-116.6 E-6
2-2	24.37	524.9 E-6	592.7 E-6	-67.8 E-6		
2-3	-0.63	683.4 E-6	719.8 E-6	-36.5 E-6	-36.5 E-6	3.0 E-6
2-4	-24.63	1,234.6 E-6	1,081.1 E-6	153.5 E-6	233.7 E-6	117.8 E-6
2-5	-24.63	1,991.0 E-6	1,677.1 E-6	313.9 E-6		
3-1	24.37	454.3 E-6	510.2 E-6	-55.8 E-6	-51.4 E-6	-116.6 E-6
3-2	24.37	456.8 E-6	503.8 E-6	-47.0 E-6		
3-3	-0.63	744.4 E-6	753.6 E-6	-9.3 E-6	-9.3 E-6	3.0 E-6
3-4	-24.63	1,492.4 E-6	1,300.0 E-6	192.4 E-6	290.6 E-6	117.8 E-6
3-5	-24.63	2,283.0 E-6	1,894.2 E-6	388.8 E-6		
4-1	24.37	546.2 E-6	612.4 E-6	-66.2 E-6	-56.5 E-6	-116.6 E-6
4-2	24.37	467.7 E-6	514.5 E-6	-46.8 E-6		
4-3	-0.63	889.0 E-6	899.4 E-6	-10.3 E-6	-10.3 E-6	3.0 E-6
4-4	-24.63	2,165.2 E-6	1,841.2 E-6	324.0 E-6	330.8 E-6	117.8 E-6
4-5	-24.63	2,083.4 E-6	1,745.8 E-6	337.7 E-6		
5-1	24.37	624.6 E-6	647.0 E-6	-22.4 E-6	-23.3 E-6	-116.6 E-6
5-2	24.37	569.9 E-6	594.2 E-6	-24.3 E-6		
5-3	-0.63	987.8 E-6	991.4 E-6	-3.6 E-6	-3.6 E-6	3.0 E-6
5-4	-24.63	1,673.5 E-6	1,582.1 E-6	91.4 E-6	108.2 E-6	117.8 E-6
5-5	-24.63	3,041.3 E-6	2,916.3 E-6	125.0 E-6		

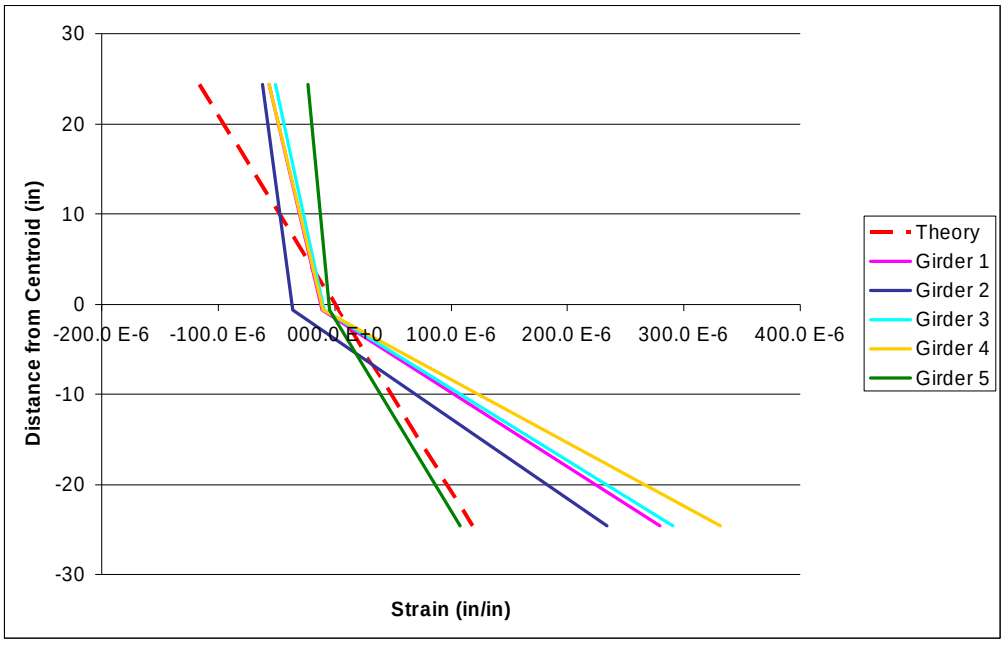

Figure 8.14 Strains of girders compared to theoretical strain induced by loading

The strain data from the beams showed that the average lower point for all 5 girders was 32% of the theoretical value, and the average upper point was 150% of the upper theoretical value.

8.5 Girder Stiffness

The deflections from Table 8.1 were used in Equation 8.2 to find the stiffness, combined EI, of each girder.

$$\Delta = \frac{PL^3}{48EI} \tag{8.2}$$

where,

Δ = Deflection, in

P = Concentrated Load, kips

L = Span Length of Girder, in

E = Modulus of Elasticity, ksi

I = Moment of Inertia, in^4

The theoretical EI was found using a modulus of elasticity, E, of 3,729 ksi as found by the experimental tests discussed in Chapter 5, and the standard I of an AASHTO BT-54 of 268,077 in^4. The results are given in Table 8.3.

Table 8.3 Stiffness values resulting from load test

Girder	Measured EI (kip ft^2)	Theory EI (kip ft^2)	EI Measured / EI Theory
1	7.883 x 10^6	6.942 x 10^6	1.14
2	8.258 x 10^6	6.942 x 10^6	1.19
3	8.671 x 10^6	6.942 x 10^6	1.25
4	8.899 x 10^6	6.942 x 10^6	1.28
5	1.387 x 10^7 *	6.942 x 10^6	2.00
Average	8.428 x 10^6	6.942 x 10^6	1.21

* Continued error in Girder 5. This value was not used.

The measured stiffness was about 21% larger than the theoretical stiffness. This can be accounted for by considering the actual moment of inertia and modulus of elasticity. The cross-section of the girders was found to be larger than that of a standard AASHTO BT-54. The end dimensions of the girders were measured according to Figure 8.15 to calculate the cross-sectional area and the moment of inertia, I (in^4). The end dimensions of the girders and resulting moment of inertia are shown in Table 8.4. Note that the new centroid for the cross-section was calculated for each end.

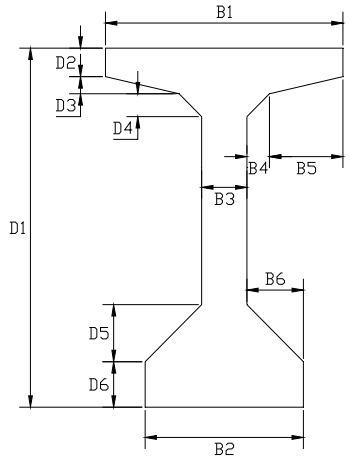

Figure 8.15 Dimension labels used compute I in Table 8.4

Table 8.4 Girder end dimensions and moment of inertia compared to typical BT-54

		Girder 1		Girder 2		Girder 3		Girder 4		Girder 5	
	BT-54	North End	South End	North End	South End	North End	South End	North End	South End	North End	South End
B1 =	42	42.313	42.313	42.375	42.25	42.25	42.25	42.25	42.313	42.313	42.313
B2 =	26	26.125	26.188	26.188	26.188	26.688	26.313	26	26.25	26.25	25.375
B3 =	6	6.2292	6.1875	6.2917	6.25	6.5625	6.2917	6	6.2292	6.2292	6.2708
B4 =	2	2	2	2	2	2	2	2	2	2	2
B5 =	16	16	16	16	16	16	16	16	16	16	16
B6 =	10	10	10.031	9.9688	10	9.9688	10.031	10	10.063	10.031	10.063
D1 =	54	54.25	54.5	54.5	54.25	54.563	54.313	54.75	54.375	54.75	54.5
D2 =	3.5	3.5313	3.5938	3.5313	3.6563	3.625	3.5938	3.625	3.6563	3.6563	3.6563
D3 =	2	1.9688	2.0313	2.0938	1.8438	2.125	1.9063	2.25	1.9063	1.9688	1.9688
D4 =	2	2	2	2.125	2	2	2	2	2.0625	2	2
D5 =	4.5	4.5	4.5	4.5	4.5	4.5	4.5	4.5	4.5	4.5	4.5
D6 =	6	6.5	6.6875	6.4375	6.4063	6.3125	6.375	6	6.7188	6.4063	6.4688
Area (in^2) =	659	683.0	690.6	689.4	684.3	705.8	685.8	673.9	692.7	689.8	685.8
y_{bottom} (in.) =	27.63	27.52	27.63	27.76	27.61	27.87	27.60	28.35	27.53	27.93	27.97
I_x (in^4) =	268077	277898	284104	282699	278495	288060	279402	282318	283281	286382	280505
Aver. I_x =		281,001		280,597		283,731		282,799		283,444	

Table 8.5 shows the computed I from Table 8.4 compared to I of a transformed section as well as the standard I of a AASHTO BT-54.

Table 8.5 Computed moment of inertia compared to standard

Girder	Computed I (in^4)	Transformed Computed I (in^4)	Standard I (in^4)	$\frac{\text{I Computed}}{\text{I Standard}}$
1	281,001	287,821	268,077	1.048
2	280,597	287,719	268,077	1.047
3	283,731	291,046	268,077	1.058
4	282,799	291,208	268,077	1.055
5	283,444	291,439	268,077	1.057
Average	282,314	289,858	268,077	1.053

The girders were found to have a 5% larger I than a standard BT-54. This increase in moment of inertia increases the stiffness of the girder. This larger moment of inertia also affects the strain calculations shown in Figure 8.14. Using the calculated moment of inertia, a new stiffness can be calculated as shown in Table 8.6.

Table 8.6 Load test stiffness compared to new calculated theoretical stiffness

Girder	Measured EI (kip ft^2)	Computed EI (kip ft^2)	$\frac{\text{EI Measured}}{\text{EI Computed}}$
1	7.883×10^6	7.316×10^6	1.08
2	8.258×10^6	7.479×10^6	1.10
3	8.671×10^6	7.442×10^6	1.17
4	8.899×10^6	7.332×10^6	1.21
5	1.387×10^7 **	7.584×10^6	1.83
Average	8.428×10^6	7.431×10^6	1.13

The stiffness is still 13% larger than anticipated. The increase in moment of inertia represents 8% of the difference from Table 8.4.

This final 13% increase in stiffness can be accounted for in two areas. First, the standard and computed I values both underestimate the true stiffness of the girder. The transformed section of the girder, which includes the stiffness of the steel strands, is the closest representation of the true stiffness of each girder. Standard practice is to not use transformed sections. Thus, most girders in use are stiffer than their design.

The second source for the stiffness increase is the set up of the girder stiffness test. As previously discussed, each end of the girder was resting on elastomeric bearing pads. This bearing condition was not a "pure" roller support. Horizontal movement is not restricted, but the internal shear stiffness of the elastomeric bearing pads would limit any horizontal movement that a "perfect" roller would allow. This now makes the setup

of the girders somewhere between that of a pin-pin condition and a pin-roller condition. Equation 8.2, which was used to find the stiffness from measured deflections, is only true on a pin-roller system.

Computer analysis in GTSTRUDL 29 was done to investigate what effect end conditions had on expected deflections. The data from this analysis are given in Appendix F. Two models were used: one for a pin-pin setup and one for a pin-roller setup. The cross-section and stiffness properties were set to that of each girder. Under the stiffness test load, the pin-roller model showed a deflection of 0.800 inches, a deflection greater than any of the measured deflections from the stiffness test. The pin-pin model under the same load gave a deflection of 0.409 inches, 49% less than the same load on a pin-roller setup. The average deflection for the girders of 0.64 inches falls between these two end conditions, showing that the actual end conditions were somewhere between these two models.

8.6 Conclusions

Several conclusions can be drawn from this field test. Firstly, it is recommended that the average girder stiffness of 8.428×10^6 kip ft^2 should be used by GDOT engineers when designing the deck to be used on the I-85 Ramp "B" Bridge. This should improve road profile design for this bridge, because the girders are stiffer than expected. Secondly, in future uses of HSLW concrete girders, it is suggested that the modulus of elasticity be measured from samples of concrete used in each girder. Full field tests of all beams would become a tedious and expensive process, but a modulus of elasticity test can be conducted fairly quickly and provide valuable data to bridge designers. Lastly,

forms used at precast plants need to be periodically checked to ensure that their dimensions match those specified. A larger cross-section appears to be a conservative approach to girder strength, but a larger section can affect deflections, deck profile, self-weight flexural stresses, and substructure loads.

CHAPTER 9

SILICA FUME BAG ISSUE

9.1 Background

Silica fume was called for in the mix design for these girders, and was used according to specifications. Standard Concrete Products (SCP) had not constructed many girders calling for silica fume, and had no need, up to this point, for a silica fume silo to feed directly into the mixer. Silica fume was supplied in bags and manually placed into the mixer according to the mix design.

Silica fume can be very harmful to the human body if inhaled or digested. Due to its powdery and lightweight nature, many particles of silica fume become airborne during movement of the product. To limit the amount of silica fume inhaled, Sika makes silica fume bags that are designed to dissolve during the batching process. This bag can be tossed whole into the mixer, keeping the silica fume particles contained during the entire process. These Sika silica fume bags were used in the construction of all 5 HSLW girders.

9.2 Bag Pieces in Concrete Specimens

During cylinder testing, pieces of bag were found inside some specimens, which had not fully dissolved during batching. The pieces of bag ranged in size from small pieces, approximately the size of a dime, up to very large pieces, some that even covered the entire cross-section of a 4”x8” cylinder. Cylinders with any visible bag pieces

present were photographed. Figures 9.1 through 9.5 are examples of some cylinders containing pieces of undissolved bag.

Figure 9.1 Medium piece of bag present across failure plane

Figure 9.2 Medium piece of bag in cylinder 2-5-4-2

Figure 9.3 Large piece of bag is folded inside 4”x 8” cylinder 3-1-4-3

Figure 9.4 The top and bottom pieces of cylinder 3-1-4-3 are shown side by side

Figure 9.5 Large piece of bag woven into specimen 2-5-4-3

The primary concerns are that the undissolved pieces of bag limit aggregate interlock across that surface, that the bag surrounds pockets of undissolved silica fume, which would also weaken the structure, and that the bag provides a weak plane which reduces both compressive and tensile strength.

There are no bag pieces along the surfaces of cylinders, or along the surface of any of the girders. The bag pieces were only found after breaking the cylinders. It is possible that there are more bag pieces inside the cylinders that were not along a failure plane, and therefore were not visible.

9.3 Data Analysis

Of the 224 cylinders broken on or before 56 days after pouring, 72 cylinders had visible bag pieces across failure planes. The visible bag pieces were divided into 3 categories based on approximate size. Small pieces were those ¼ inch or less in diameter. Medium pieces were ¼ to ¾ inch in diameter. Large pieces were ¾ inch or larger, with some pieces as large as 4 inches in diameter. Of the 72 cylinders with visible bag pieces, 24% were small pieces, 44% were medium pieces, and 32% were large pieces. 24% of 4in x 8in cylinders and 34% of 6in x 12in cylinders contained visible bag pieces.

To evaluate the effect the bag pieces had on the strength of the concrete, Figure 9.6 was created comparing the strength of the cylinders containing visible pieces of bag to those containing no visible bag. This figure highlights the low stress levels found in some cylinders containing bag pieces at all ages of testing.

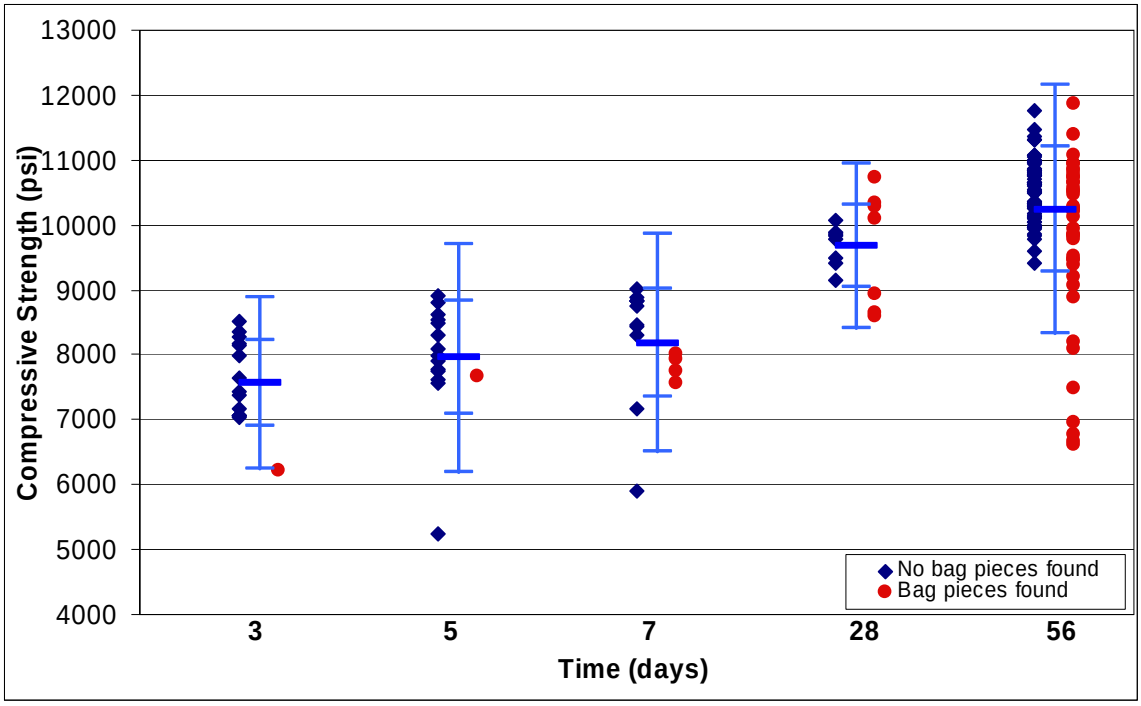

Figure 9.6 Compressive strength of cylinders with and without bag pieces

The size of the bag pieces had a strong effect in the strength of the cylinder. Figure 9.7 shows compressive strength test data from days 28 and 56, and also shows the sizes of the bag pieces when they were present. Figure 9.8 shows details of the 56 day tests with the average stress and standard deviation for each group.

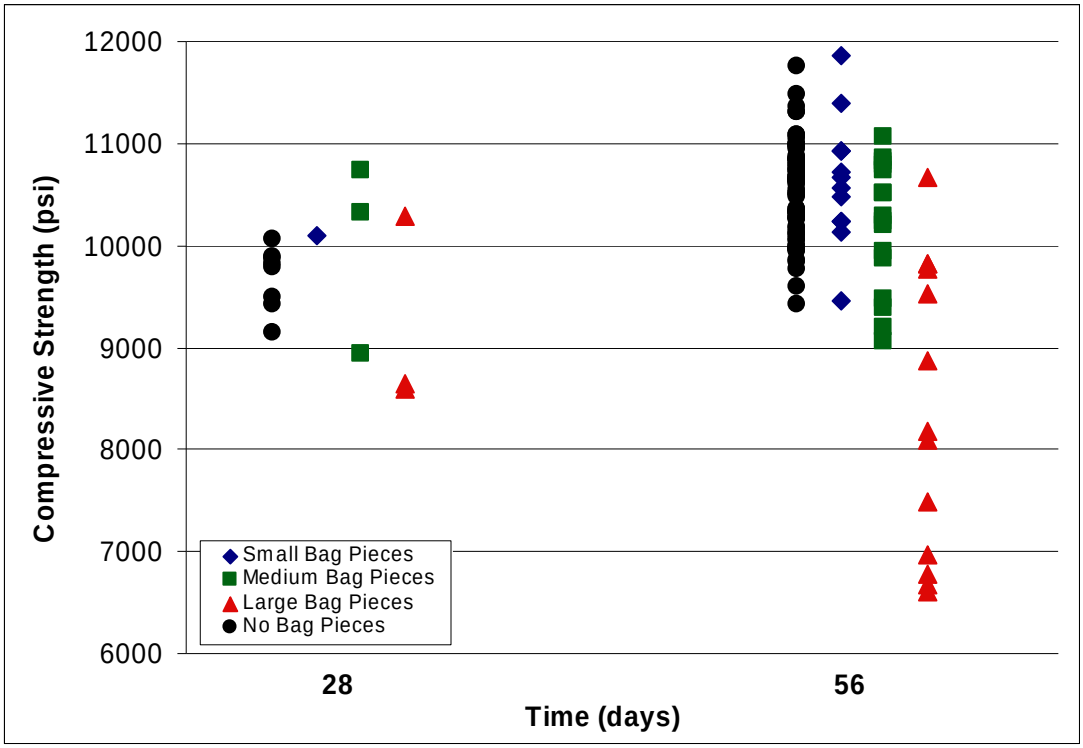

Figure 9.7 Compressive stress of cylinders containing various size bag pieces

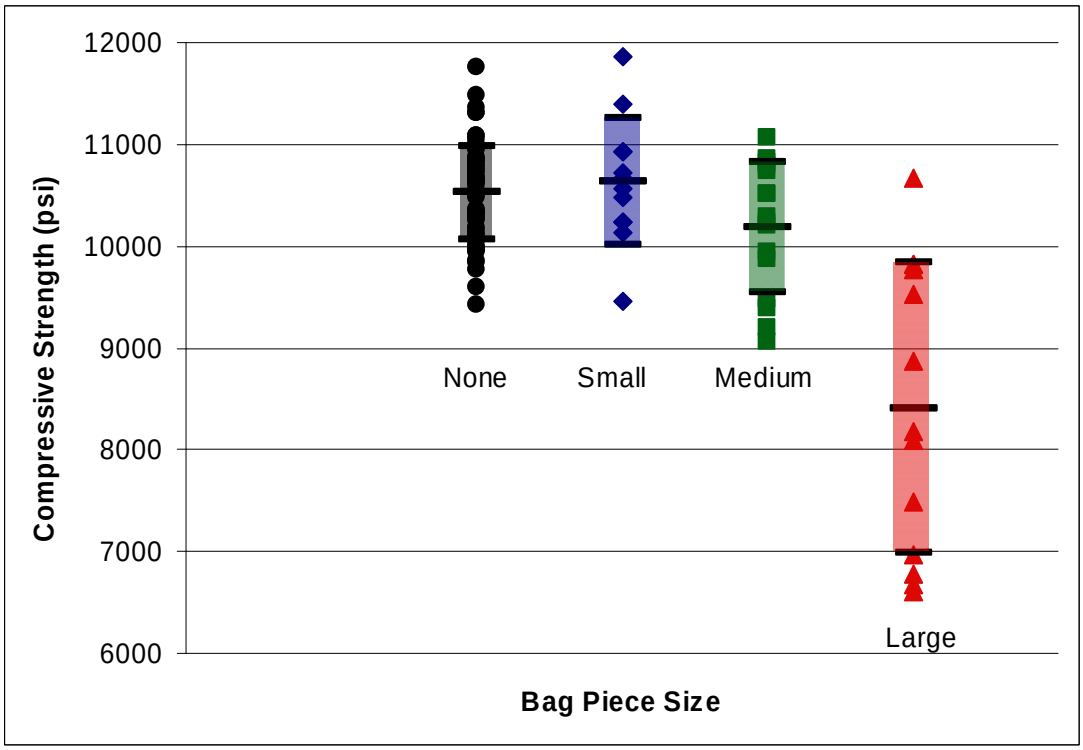

Figure 9.8 56 day tests showing average stress for each size category

Hypothesis testing was performed on the resulting data to try to determine the effect, if any, the bag pieces had on the girders. The results of the testing showed no statistical evidence that small pieces of bag affected the concrete strength. However, there was statistical evidence that both medium and large bag pieces significantly affected the concrete strength.

9.4 Conclusions

The bag pieces from the silica fume bags had negative effects on test cylinder strength. The impact was increased as the size of the bag piece was increased. Some cylinders containing large bag pieces only reached 65% of the required compressive strength. However, the compression tests were done on 4in x 8in cylinders with a cross-sectional area of 12.57 in^2. Bag pieces would affect a larger fraction of the cross-section of a cylinder than the same size piece of bag in an actual girder. Therefore, the piece of bag would be expected to have less effect on the girder than it would have on a cylinder.

9.5 Recommendations

It is recommended that the girders be accepted and used in the I-85 Ramp B Bridge. The impact of the bag pieces is apparent, however, a large piece of bag in a critical area would have become evident after the release of the prestressing strands, due to the amount of compressive force on the girder. Also, the effect of a possible bag piece must be considered at the smallest thickness of the girder, which would be the web. The web is 6 inches thick, and if a bag piece were to cover the entire width, it could severely diminish the strength at that point. However, the girders were reinforced vertically in the

web. The reinforcement in the middle of the web suggests that if bag pieces were present they would not cover the entire thickness of the web.

Although the recommendation is to accept the girders, it is also recommended that the girders be closely monitored during their use due to the unique nature of this problem. This research will be continued for approximately 2 years, during which time the girders will be monitored internally for strains in the girders and externally for the deflections of the girders. Careful attention will be paid to the appearance of any spalling that could represent a piece of bag near the surface. After the conclusion of this research, bridge inspectors should closely monitor the girders for unusual behavior and appearance.

CHAPTER 10

DISCUSSION OF RESULTS

10.1 Material Properties

Material tests found that the HSLW concrete had an average compressive strength of 10,238 psi at 56 days, with a standard deviation of 168 psi. The average strength was greater than the design strength of 10,000 psi. This average included cylinders that were found to have pieces of bag present. Had the silica fume bags all been dissolved into the mix the strength could have been higher. The average modulus of elasticity was 3,729 ksi at 56 days, with a standard deviation of 254 ksi. This average was less than the values predicted by AASHTO and Meyer (2002), and 2% less than the value predicted by ACI 363. Previous research showed that the elastic modulus was dependent on the type of lightweight aggregate used even when compressive strengths were the same. The elastic modulus from this concrete was well within the range found by previous researchers (Meyer, 2002). The average Poisson's ratio for the HSLW concrete was calculated to be 0.22. The average split cylinder strength was 679 psi at 56 days, which, as expected, was less than the modulus of rupture predicted by ACI 318-08. The average coefficient of thermal expansion was determined to be 3.24×10^{6} strain/˚F. The chloride ion permeability tests showed "very low chloride ion permeability" with an average of 318 coulombs.

The HSLW concrete met the strength requirement of 10,000 psi. Both the elastic modulus and Poisson's ratio were reasonable, and similar the findings from past research.

The chloride permeability at 56 days was well under the maximum value allowed of 3,000 coulombs. Overall, the material was found to be adequate and expected to perform well in the girders.

10.2 Girder Properties

The girders were tested for several properties. The camber and transfer lengths were monitored during storage of the girders at the precasting plant. Each girder was tested to determine its stiffness. Also, the moment of inertia was calculated based of end dimensions of each girder.

The camber measurements showed that on average the girders were cambering 4.26 inches at midspan at 56 days. This was very close to the camber of 4.20 inches predicted by WSDOT equations. The deflection of the girders will be monitored during their use in the bridge.

The average transfer length of the prestressing strands was determined as 27.6 inches, which was 23% less than the value predicted by AASHTO and ACI specifications. The measured transfer length is significantly higher than the values found by previous research (Meyer, 2002). One possible cause of this increase in transfer length could be the longer free ends of the strands on the girders. The longer free strand at the end of a girder may create longer transfer lengths at that end of the girder. The longer transfer lengths from the North ends of girders 3 and 5, which were the ends with free strands, raised the average significantly. Another possible cause is the weight of the girders. The subject girders were about 108-ft long compared with Meyer's test of 39 and 43-ft long girders; the subject girders weighed about 4.5 times more than Meyer's

largest girder. The larger friction force at the bearing ends of the girders on the prestressing bed after cut-down would have produced significantly higher tensile forces in the ends of the HPLC girders. It is known that these high friction and end bearing forces can induce cracking at the end of the girders with resulting increase in transfer length (Kelly and Kahn 2007). Therefore, end bearing details similar to those recommended by Kelly and Kahn (2007) should be considered for long girders.

The stiffness of the girders was calculated using the girder field stiffness tests discussed in Chapter 8. The stiffness (combined EI) of the girders was found to be 8.428 x 10^6 kip ft^2. This is the stiffness recommended for use by GDOT engineers in designing the road profile. However, this value was not equivalent to the experimental modulus of elasticity multiplied by the standard I for a BT-54. This discrepancy led to the computation of the moment of inertia.

Using the end dimensions of each girder, the moment of inertia, I, was computed for each girder. The average I was found to be 5.3% higher than the PCI bulb-tee standard. This larger moment of inertia is a significant factor in the stiffness of the girders. Since a stiffness test was performed, the stiffness values given in this report are considered dependable, and are recommended to be used over typical calculations. However, the increase in moment of inertia raises the question about the stiffness of other beams that were not manually tested.

If a larger cross-section is a common occurrence among precast girders, then many bridges have stiffer girders than expected, which may result in road profiles different from the design. If a beam does not deflect as much as expected under the load of the deck, then the road will have an arching shape in each span. For a multi-span

bridge this means an automobile encounters a low point at each bent, which can lead to an undesirable ride.

CHAPTER 11

CONCLUSIONS AND RECOMMENDATIONS

11.1 Conclusions

Five BT-54 precast prestressed girders were constructed using HSLW concrete. Each of these girders were instrumented with five vibrating wire strain gages (VWSG) at midspan to monitor the strains in the concrete during the service life of the bridge. Concrete samples were taken to measure material properties: compressive strength, modulus of elasticity, Poisson's ratio, split cylinder strength, coefficient of thermal expansion, and rapid chloride ion permeability.

Short term deflections were measured using a taut wire system, and short term internal strains were monitored while the girders were in storage at the precast concrete supplier (Standard Concrete Products, Atlanta). The stiffness of each girder was measured using a field test; the average stiffness (EI) was 8.428×10^6 kip ft^2 which was reported to GDOT bridge division for design of the deck profile.

All long term information, such as creep and shrinkage tests and long term girder deflections, will be presented in a later report.

The HSLW girders satisfied the GDOT strength and durability requirements. The precaster was able to develop the required design strength of 10,000 psi and to provide a concrete with a chloride ion permeability at 56-days less than 3,000 Coulombs and a unit weight less than 120 lbs/ft^3.

11.2 Recommendations

It is recommended that HSLW concrete be used for future applications, provided that several quality control procedures are followed. Addition of silica fume must be closely monitored to ensure that it is mixed well within the batch, and that no foreign materials are present in the concrete, such as paper bags from the silica fume packaging. Precast forms should be periodically checked for correct dimensions and alignment. The moisture content of the lightweight aggregate should be frequently measured as well to ensure mixture consistency.

For future use of HSLW concrete, the modulus of elasticity should be measured in batches using lightweight aggregates other than Stalite. Assuming the forms are to standard size, the modulus of elasticity can assist road profile engineers in design of the profile. Because the elastic modulus has been shown to vary based on aggregate source and type, tests need to be performed for each type of aggregate in use.

APPENDIX A

SCP BATCH REPORTS FROM TRIAL BATCHES

PRODUCER: Standard Concrete — MIX CODE: 10000 LtWt HPC

ADDRESS: Atlanta — MIX DESIGN: 12,000 PSI @ 28 DAYS

CITY: Atlanta — STATE: GA. — LAB BATCH SIZE: 27.00 CU.FT.

SIKA-RWH

MATERIA	SOURCE	TYPE
CEMENT	LaFarge	III (II)
FLY ASH	Boral	F
S.Fume	Sika SF	Silica Fume
STONE 1	Vulcan	LS Granite
STONE 2	Stalite	ES
SAND 1	Vulcon LS	GRANITE
SAND 2	Vulcon LS	GRANITE
WATER	COUNTY	

ADMIXTURES

	SOURCE	NAME	OZ/CWT
AEA	SIKA	AEA-14	0.20
ADMIX 1	SIKA	V-2100	6.00
ADMIX 2	SIKA	Plastiment	3.00
ADMIX 3	SIKA	RAPID 1	15.00

MIX RATIOS

W/C	0.36	0.63	AGG/PASTE
W/(C+FA)	0.27		
GAL/SACK	3.04	7.87	BAG FACTOR
SAN/AGG	0.35	10.53	EQUIV (C+FA) BAG FACTOR

AGGREGATE INFORMATION

STONE 1	Vulcan	LS Granite
SIZE		#67
DRW		100.00
FM		
SP.GR.		2.60
STONE 2	Stalite	ES
SIZE		#7
DRW		
FM		
SP.GR.		1.50
SAND 1	Vulcon LS	GRANITE
FM		2.57
SP.GR.		2.60
SAND 2	Vulcon LS	GRANITE
FM		2.80
SP.GR.		2.63

Date Printed 01-Apr-09

12000 PSI MIX — LAB BATCH INFORMATION

1 YARD — 27.00 CUBIC FT

SSD WEIGHTS				VOLUME	AGG MOISTURE CONTENTS		BATCH WTS	
LaFarge	740.0	LBS	75%	3.76			740.00	LBS
Boral	150.0	LBS	15%	0.85			150.00	LBS
Sika SF	100.0	LBS	10%	0.73			100.00	LBS
Vulcan	0.0	LBS	0%	0.00	0.0	%	0.00	LBS
Stalite	980.0	LBS	100%	10.47	4.0	%	1019.20	LBS
Vulcon LS	931.6	LBS	100%	5.74	7.6	%	1002.77	LBS
Vulcon LS	0.0	LBS	0%	0.00	0.0	%	0.00	LBS
WATER	32.0	GAL	% AIR	4.27			156.19	LBS
AEA-14	2.0	OZS	4.00	1.08			58.56	ML
V-2100	59.4	OZS		0.06			1756.70	ML
Plastiment	29.7	OZS		0.03			878.35	ML
							0.00	ML

THEORETICAL YIELD 27.00 CU FT

SIKA-RWH TARGET UNIT WG 117.60 LBS/CU FT

MIX DATA

ATE BATCHED	8-Oct-07		
IME BATCHED	2:55 PM		
IME SAMPLED	3:16 PM		
/ATER ADDED	41.50	LBS	0 ML's
WATER LEFT	0.00	LBS	0 ML's
SLUMP/FLOW	5.00	INCHES	
MBIENT TEMP	78.00	*F	
CONCRETE TEMP	83.00	*F	
AIR%	3.00	%	
ACTUAL UNIT WEIGHT	122.00	LBS PER CU FT	
CTUAL YIELD	26.37	CU FT PER YARD	
ACTUAL W/C+FA) RATIC	0.31		

TIME TO INITIAL SET — HOURS & MINUTES

CYLINDERS MKD_____ — STEAM Yes No

LAB ID. NO._____

CYLINDERS BROKEN BY

SIKA-RWH PREPARED BY: RH MM LC

BREAK INFORMATION

BRAKE DATE & TIME		AGE
10/9/07 4:55 AM	9,410	PSI @18 HOU
10/9/07 4:55 AM	7,908	PSI @18 HOURS
-----	8,659	-18 HOUR AVG
1/7/00 12:00 AM	10,500	PSI @7 DAYS
1/7/00 12:00 AM	10,476	PSI @7 DAYS
-----	10,488	7 DAY AVG
05-Nov-07	11,519	PSI@28DAYS
05-Nov-07	11,040	PSI@28DAYS
------	11,280	-28DAY AVG
12/3/07 12:00 AM	11,050	PSI@56DAYS
12/3/07 12:00 AM	12,131	PSI@56DAYS
12/3/07 12:00 AM	11,020	PSI@56DAYS
12/3/07 12:00 AM	11,340	PSI@56DAYS
	11,385	56 Day avg

PRODUCER: Standard Concrete — MIX CODE: 10000 LtWt HPC

ADDRESS: Atlanta — MIX DESIGN: 12,000 PSI @ 28 DAYS

CITY: Atlanta — STATE: GA. — LAB BATCH SIZE: 27.00 CU.FT.

SIKA-RWH

MATERIA	SOURCE	TYPE
CEMENT	LaFarge	III (II)
FLY ASH	Boral	F
S.Fume	Sika SF	Silica Fume
STONE 1	Vulcan	LS Granite
STONE 2	Stalite	ES
SAND 1	Vulcon LS	GRANITE
SAND 2	Vulcon LS	GRANITE
WATER	COUNTY	

ADMIXTURES

	SOURCE	NAME	OZ/CWT
AEA	SIKA	AEA-14	0.25
ADMIX 1	SIKA	V-2100	6.00
ADMIX 2	SIKA	Plastiment	3.00
ADMIX 3	SIKA	RAPID 1	15.00

MIX RATIOS

W/C	0.36	0.63	AGG/PASTE
W/(C+FA)	0.27		
GAL/SACK	3.04	7.87	BAG FACTOR
SAN/AGG	0.35	10.53	EQUIV (C+FA) BAG FACTOR

AGGREGATE INFORMATION

STONE 1	Vulcan	LS Granite
SIZE	#67	
DRW	100.00	
FM		
SP.GR.	2.60	
STONE 2	Stalite	ES
SIZE	#7	
DRW		
FM		
SP.GR.	1.50	
SAND 1	Vulcon LS	GRANITE
FM	2.57	
SP.GR.	2.60	
SAND 2	Vulcon LS	GRANITE
FM	2.80	
SP.GR.	2.63	

Date Printed 01-Apr-09

12000 PSI MIX — LAB BATCH INFORMATION

1 YARD — 27.00 CUBIC FT

SSD WEIGHTS				VOLUME	AGG MOISTURE CONTENTS	BATCH WTS	
LaFarge	740.0	LBS	75%	3.76		740.00	LBS
Boral	150.0	LBS	15%	0.85		150.00	LBS
Sika SF	100.0	LBS	10%	0.73		100.00	LBS
Vulcan	0.0	LBS	0%	0.00	0.0 %	0.00	LBS
Stalite	980.0	LBS	100%	10.47	2.5 %	1004.50	LBS
Vulcon LS	931.6	LBS	100%	5.74	7.6 %	1002.77	LBS
Vulcon LS	0.0	LBS	0%	0.00	0.0 %	0.00	LBS
WATER	32.0	GAL	% AIR	4.27		170.89	LBS
AEA-14	2.5	OZS	4.00	1.08		73.20	ML
V-2100	59.4	OZS		0.06		1756.70	ML
Plastiment	29.7	OZS		0.03		878.35	ML
						0.00	ML

THEORETICAL YIELD 27.00 CU FT

SIKA-RWH TARGET UNIT WG 117.60 LBS/CU FT

MIX DATA

ATE BATCHED	8-Oct-07		
IME BATCHED	5:15 PM		
IME SAMPLED	5:30 PM		
/ATER ADDED	8.00	LBS	0 ML's
WATER LEFT	0.00	LBS	0 ML's
SLUMP/FLOW	4.50	INCHES	
MBIENT TEMP	82.00	*F	
CONCRETE TEMP	88.00	*F	
AIR%	4.00	%	
ACTUAL UNIT WEIGHT	120.00	LBS PER CU FT	
ACTUAL YIELD	26.53	CU FT PER YARD	
ACTUAL W/C+FA) RATIC	0.28		

TIME TO INITIAL SET — HOURS & MINUTES

CYLINDERS MKD_____ — STEAM Yes No

LAB ID. NO._____

CYLINDERS BROKEN B\ MM

SIKA-RWH PREPARED BY: RH MM LC

BREAK INFORMATION

BRAKE DATE & TIME		AGE
10/9/07 5:15 AM	7,455	PSI @18 HOURS
10/9/07 5:15 AM	8,465	PSI @18 HOURS
	7,960	-18 HOUR AVG
1/7/00 12:00 AM	10,673	PSI @ 7 DAYS
1/7/00 12:00 AM	10,700	PSI @ 7 DAYS
-----	10,687	7 DAY AVG
05-Nov-07	11,520	PSI@28DAYS
05-Nov-07	11,670	PSI@28DAYS
	11,595	-28DAY AVG
12/3/07 12:00 AM	12,820	PSI@56DAYS
12/3/07 12:00 AM	11,801	PSI@56DAYS
12/3/07 12:00 AM	10,995	PSI@56DAYS
12/3/07 12:00 AM	11,010	PSI@56DAYS
	11,657	56 DAY AVG.

APPENDIX B

LOAD CELL READINGS

Table B.1(a) Load cell readings and resulting forces for Pour 1

		08/06 8:15a		08/06 5:37pm		08/07 10:01am	
	Zero	After Stressing		After Pour		After Pour	
	Reading	Reading	kips	Reading	kips	Reading	kips
1	-1902	8637	37.855	8278	36.566	8884	38.742
2	-428	-12190	39.096	-12318	39.521	-12904	41.469
3	-16	-11634	38.242	-11570	38.031	-12183	40.049
4	2194	-9170	38.673	-9272	39.020	-9880	41.089
5	5572	17061	40.604	17128	40.841	17699	42.859
6	-2723	8725	37.857	8844	38.251	9404	40.103
7	1958	13211	40.110	13245	40.231	13794	42.188
8	-7	11993	37.945	12066	38.176	12602	39.871

Table B.1(b) Load cell readings and resulting forces for Pour 1 (cont.)

	08/08 8:50am		08/09 9:45am	
	After Pour		After Pour	
	Reading	kips	Reading	kips
1	8882	38.735	8222	36.364
2	-12903	41.466	-12190	39.096
3	-12150	39.940	-11634	38.242
4	-9862	41.028	-9170	38.673
5	17720	42.933	17061	40.604
6	9422	40.162	8725	37.857
7	13779	42.135	13211	40.110
8	12598	39.858	11993	37.945

Table B.2 Load cell readings and resulting forces for Pour 2

		08/07 10:11am		08/08 9:01am		08/09 9:41am	
	Zero	Initial		Before Pour		After Pour	
	Reading	Reading	kips	Reading	Kips	Reading	Kips
5	-174	-11878	39.98	-10190	34.21	-11651	39.20
6	-1019	8322	31.52	8448	31.95	8232	31.22
7	1410	-10092	38.02	-10066	37.93	-9774	36.97
8	-2357	-13390	37.05	-13458	37.28	-13284	36.70

APPENDIX C

BATCH REPORT SUMMARY FOR EACH GIRDER

Table C.1 Girder 1 batch quantities

		Batch							
Ingredient	units	1-1	1-2	1-3	1-3	1-5	1-6	1-7	Average
Cement	lbs	2581	2585	2585	2581	2592	2590	2612	2589.43
Flyash	lbs	528	521	532	521	524	522	524	524.571
Lightweight Aggregate	lbs	3441	3436	3445	3429	3424	3449	354	2996.86
Manufactured Sand	lbs	3349	3295	3327	3278	3269	3245	3272	3290.71
Water	gallons	85	88	88	87	88	88	88	87.4286
AEA	ozs	7	6	7	8	7	6	7	6.85714
Water Reducer	ozs	126	126	124	126	126	126	126	125.714
HRWR		158	156	158	158	158	158	156	157.429
Silica Fume	lbs	350	350	350	350	350	350	350	350
Total Volume	yd^3	3.5	3.5	3.5	3.5	3.5	3.5	3.5	3.5
Time		2:20 pm	2:32 pm	2:43 pm	2:53 pm	3:03 pm	3:22 pm	3:32 Pm	

Table C.2 Girder 2 batch quantities

		Batch						
Ingredient	units	2-1	2-2	2-3	2-4	2-5	2-6	Average
Cement	lbs	2587	2587	2587	2583	2592	2590	2587.67
Flyash	lbs	521	543	525	522	526	525	527
Lightweight Aggregate	lbs	3432	3411	3425	3419	3414	3429	3421.67
Manufactured Sand	lbs	3280	3265	3254	3283	3239	3235	3259.33
Water	gallons	85	84	87	87	87	87	86.17
AEA	ozs	8	6	8	6	7	8	7.17
Water Reducer	ozs	126	126	128	126	126	126	126.33
HRWR		158	156	158	158	158	156	157.33
Silica Fume	lbs	350	350	350	350	350	350	350
Total Volume	yd^3	3.5	3.5	3.5	3.5	3.5	3.5	3.5
Time		12:47pm	1:02pm	1:09pm	1:28pm	1:35pm	1:45pm	

Table C.3 Girder 3 batch quantities

		Batch						
Ingredient	units	3-1	3-2	3-3	3-4	3-5	3-6	Average
Cement	lbs	2610	2614	2607	2597	2600	2594	2603.67
Flyash	lbs	527	521	521	526	523	526	524
Lightweight Aggregate	lbs	3603	3565	3531	3496	3479	3472	3524.33
Manufactured Sand	lbs	3316	3233	3246	3269	3279	3251	3265.67
Water	gallons	89	82	84	84	83	84	84.33
AEA	ozs	7	8	8	7	6	7	7.17
Water Reducer	ozs	126	126	126	126	128	126	126.33
HRWR		156	158	158	156	158	158	157.33
Silica Fume	lbs	350	350	350	350	350	350	350
Total Volume	yd^3	3.5	3.5	3.5	3.5	3.5	3.5	3.5
Time		11:48 am	12:05 pm	12:13 pm	12:22 pm	12:30 pm	12:39 pm	

Table C.4 Girder 4 batch quantities

		Batch							
Ingredient	units	4-1	4-2	4-3	4-4	4-5	4-6	4-7	Average
Cement	lbs	2589	2577	2591	2583	2585	2585	2585	2584.33
Flyash	lbs	527	533	526	522	530	520	525	526
Lightweight Aggregate	lbs	3412	3419	3419	3454	3463	3457	3437	3441.50
Manufactured Sand	lbs	3279	3305	3325	3269	3281	3279	3254	3285.50
Water	gallons	87	89	89	90	89	90		89.40
AEA	ozs	8	6	8	6	7	8	7	7
Water Reducer	ozs	124	128	124	126	126	128	124	126
HRWR		156	158	158	158	156	158	160	158
Silica Fume	lbs	350	350	350	350	350	350	350	350
Total Volume	yd^3	3.5	3.5	3.5	3.5	3.5	3.5	3.5	3.5
Time		5:17 pm	5:27 pm	5:41 pm	6:07 pm	6:24 pm	6:40 pm	6:54 pm	

Table C.5 Girder 5 batch quantities

		Batch						
Ingredient	units	5-1	5-2	5-3	5-4	5-5	5-6	Average
Cement	lbs	2581	2587	2595	2585	2567	2590	2584.17
Flyash	lbs	521	521	529	528	526	525	525
Lightweight Aggregate	lbs	3481	3480	3463	3430	3431	3134	3403.17
Manufactured Sand	lbs	3259	3235	3236	3230	3233	3242	3239.17
Water	gallons	87	89	87	88	89	88	88
AEA	ozs	8	6	7	8	6	7	7
Water Reducer	ozs	126	124	128	124	126	128	126
HRWR		158	158	156	160	156	158	157.67
Silica Fume	lbs	350	350	350	350	350	350	350
Total Volume	yd^3	3.5	3.5	3.5	3.5	3.5	3.5	3.5
Time		3:58pm	4:13pm	4:24pm	4:40pm	4:46pm	5:03pm	

APPENDIX D

RECOMMENDATIONS FOR MOISTURE CONDITIONING OF STALITE EXPANDED LIGHTWEIGHT COARSE AGGREGATE PRIOR TO BATCHING

Recommendations for Moisture Conditioning of Stalite Expanded Lightweight Coarse Aggregate Prior to Batching

The fundamentals of handling aggregate and batching concrete described in ACI 304 and ASTM C 94 (which are followed by most ready mixed concrete plants) apply to Stalite expanded slate lightweight aggregate. However, because of the cellular nature of lightweight aggregates, the absorption is higher than most normalweight aggregates. Therefore, we recommend the following procedures to address the increased absorption of lightweight aggregate.

Stalite expanded slate lightweight aggregate may be moisture conditioned by sprinkling with water to reduce the absorption of mix water from concrete, which can result in loss of slump during mixing and delivery. This is of particular importance when concrete is to be placed by pumping. The 24 hour immersed absorption (from an oven-dry condition) of Stalite is approximately 6%. Because aggregate storage arrangements and water delivery and distribution systems are so variable, it is difficult to give specific recommendations regarding the duration of aggregate preparation by water sprinkling. However, when concrete is to be placed by pumping, we recommend that Stalite have a minimum absorbed moisture content of approximately 6% by mass. The absorbed moisture content is determined by oven drying after removing the visible film of water from the aggregate surface with an absorbent cloth. We recommend that sprinkling be discontinued and the prepared stockpiles then be allowed to drain prior to batching (usually overnight) to avoid excessive surface moisture and to provide more uniform moisture content. It has been our experience that adequate aggregate conditioning by sprinkling with water can usually be achieved in 2 to 4 days.

APPENDIX E

TRANSFER LENGTH GRAPHS

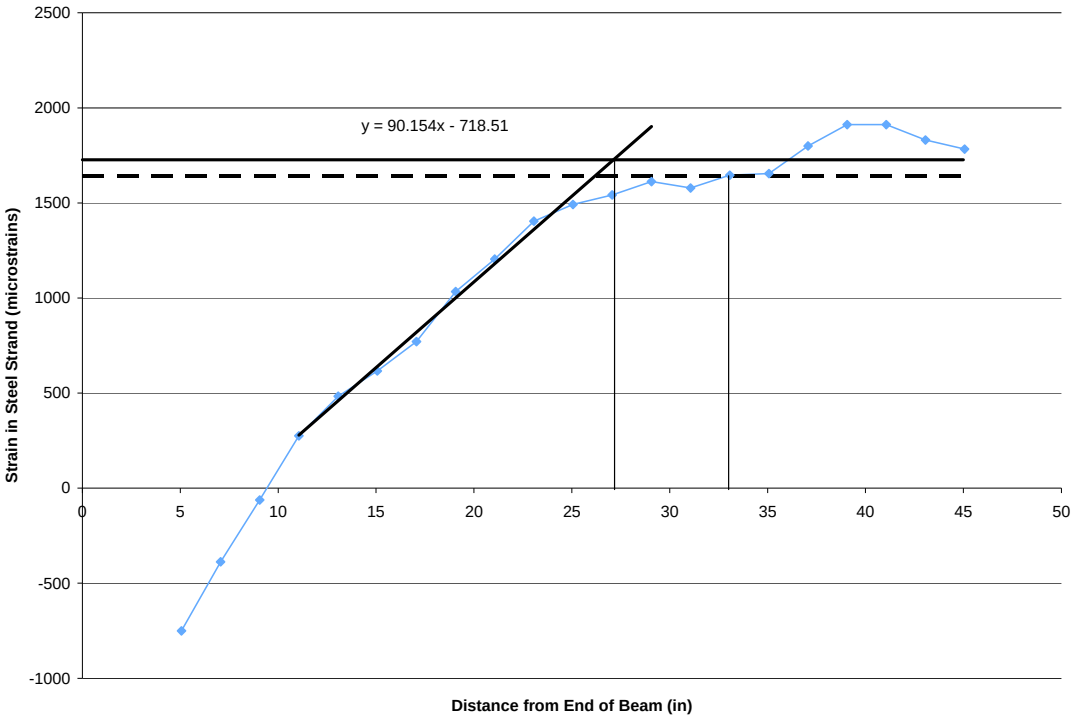

Figure E.1. Transfer length graph of the South end of Girder 1 at 5 days.

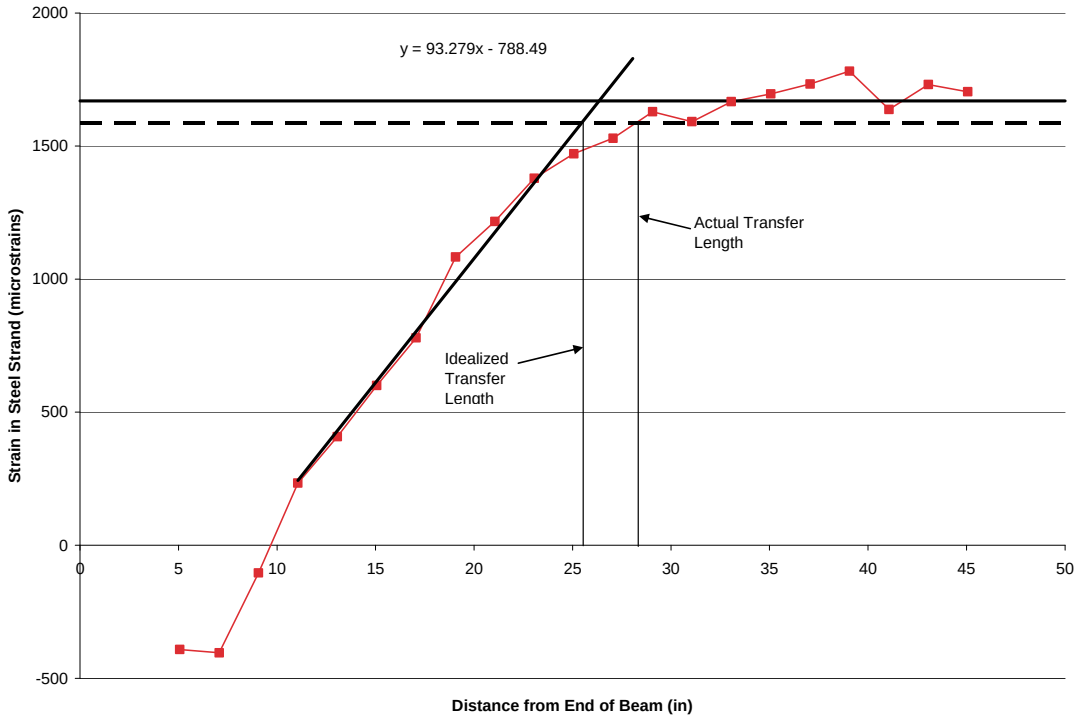

Figure E.2. Transfer length graph of the South end of Girder 1 at 8 days.

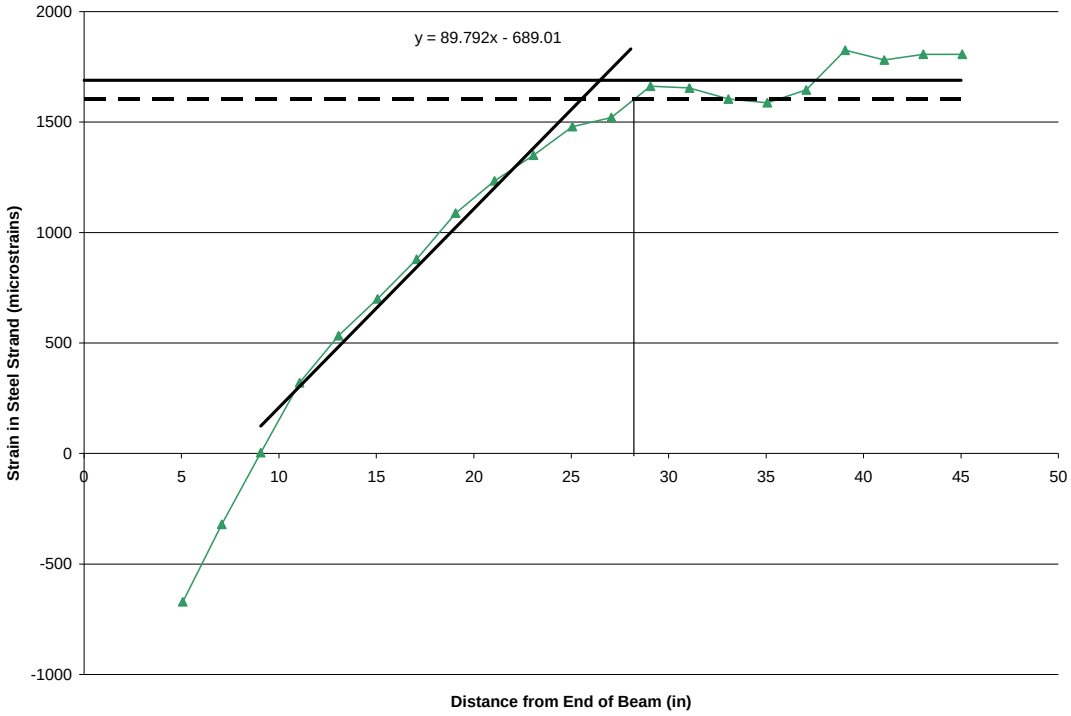

Figure E.3. Transfer length graph of the South end of Girder 1 at 14 days.

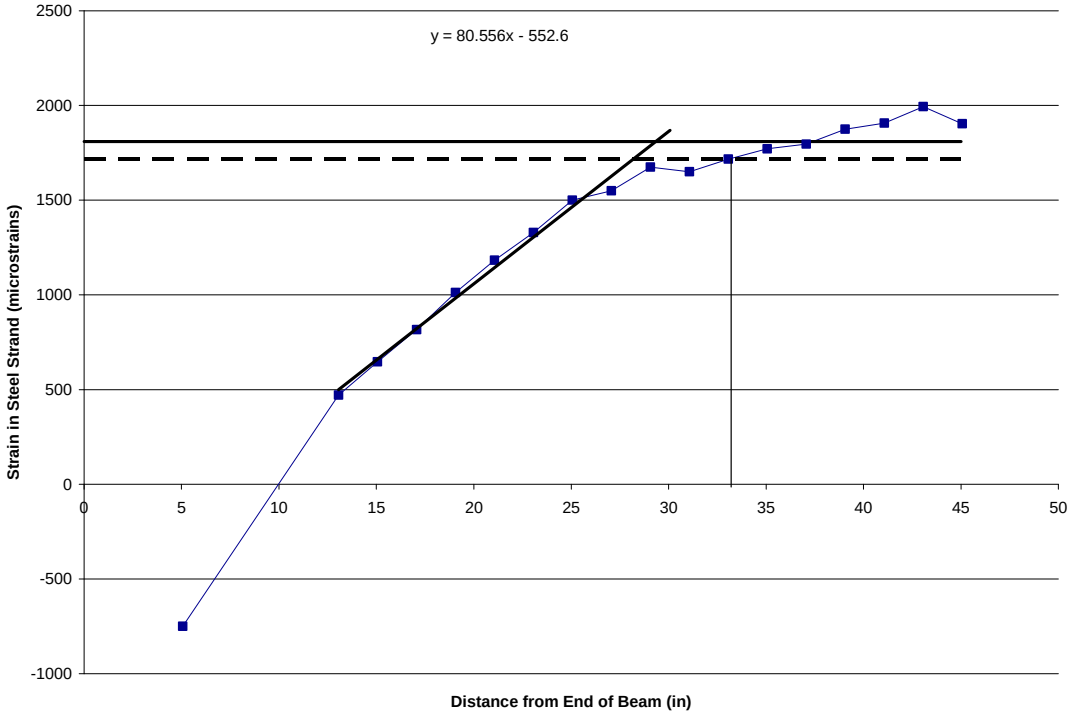

Figure E.4. Transfer length graph of the South end of Girder 1 at 28 days.

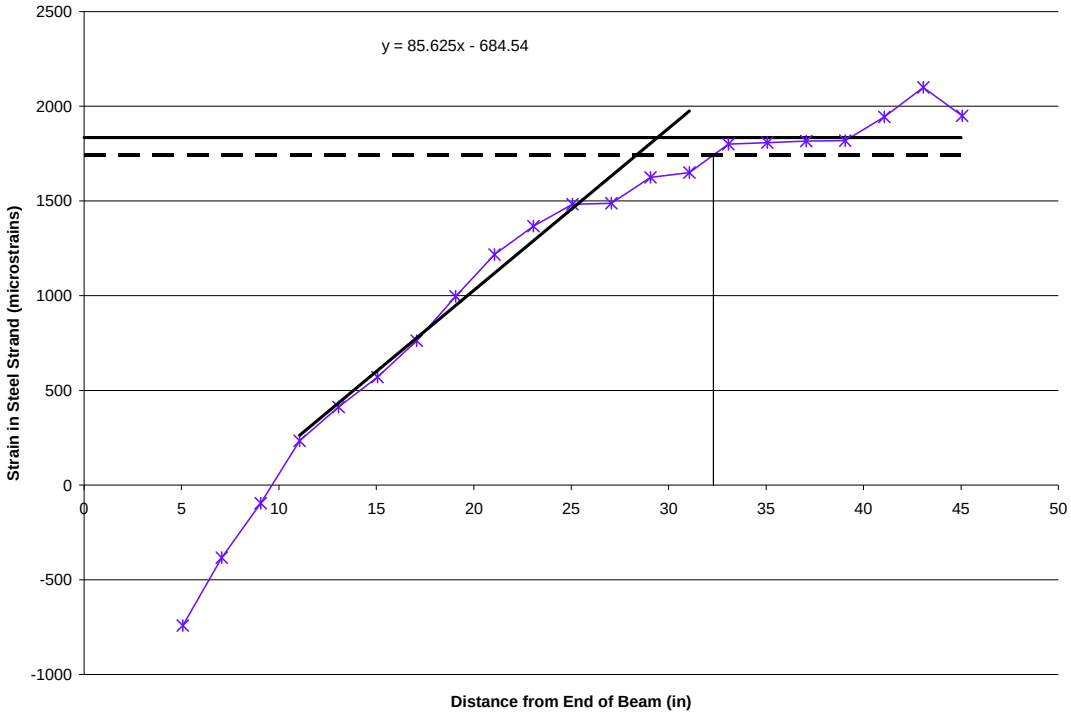

Figure E.5. Transfer length graph of the South end of Girder 1 at 80 days.

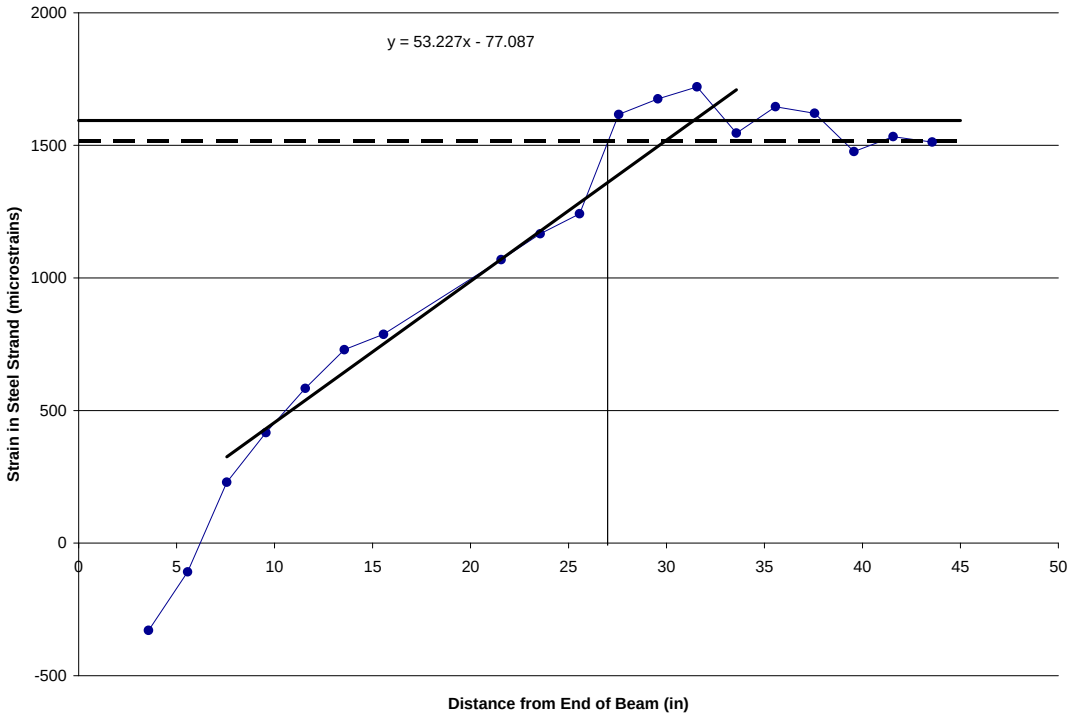

Figure E.6. Transfer length graph of the North end of Girder 1 at 5 days.

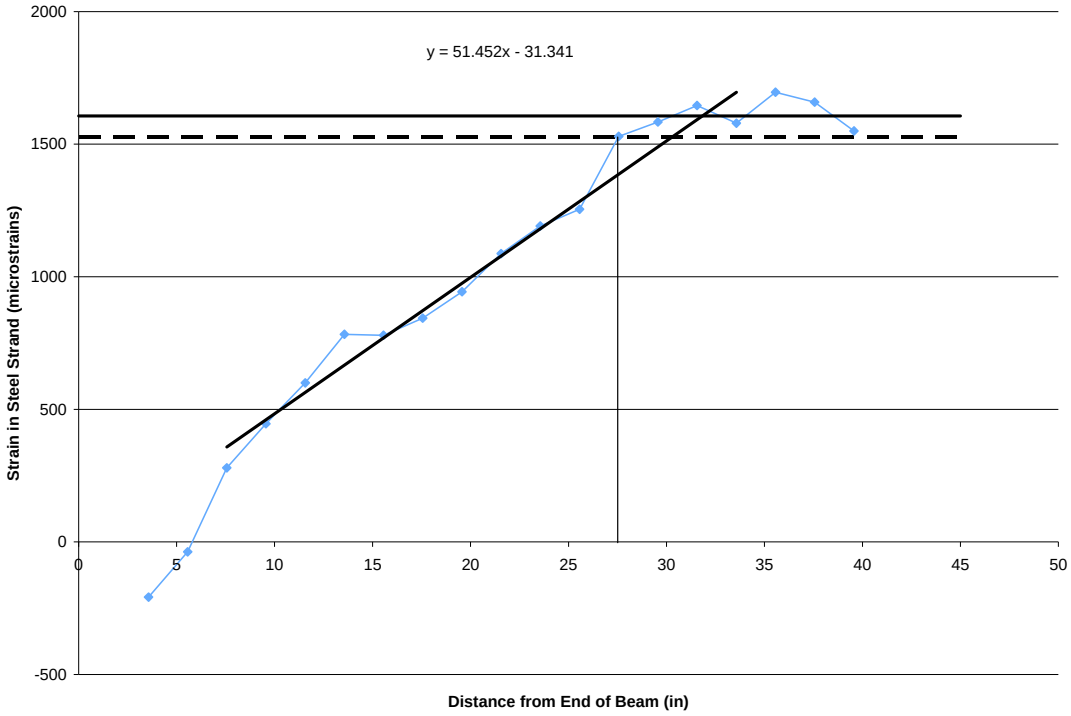

Figure E.7. Transfer length graph of the North end of Girder 1 at 8 days.

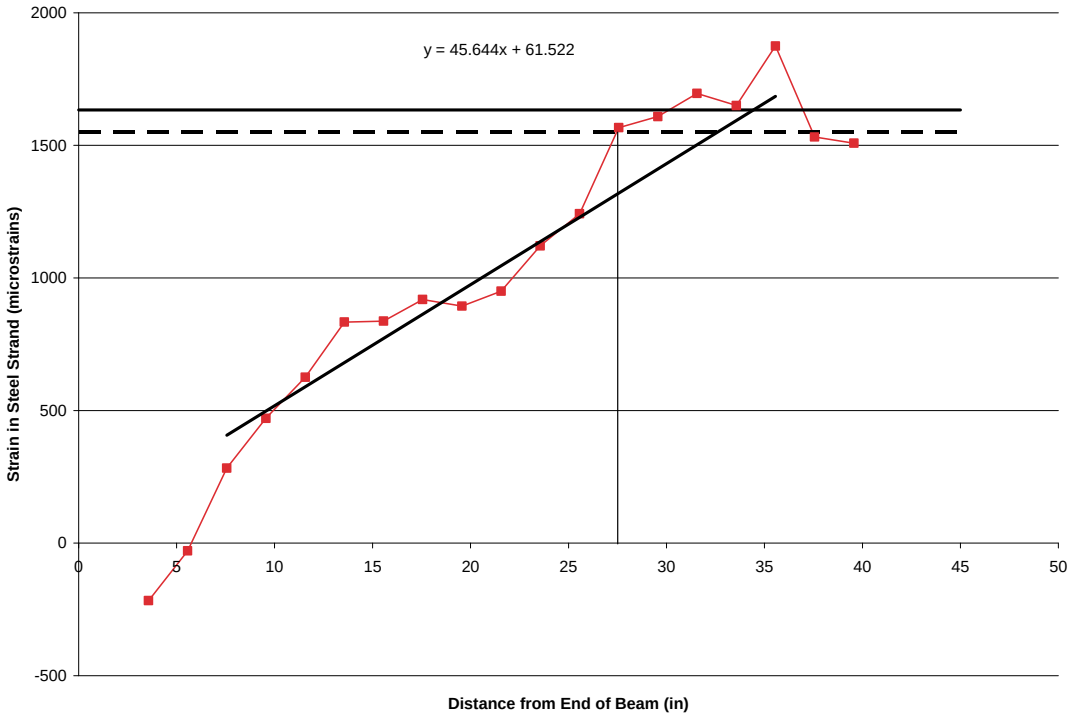

Figure E.8. Transfer length graph of the North end of Girder 1 at 14 days.

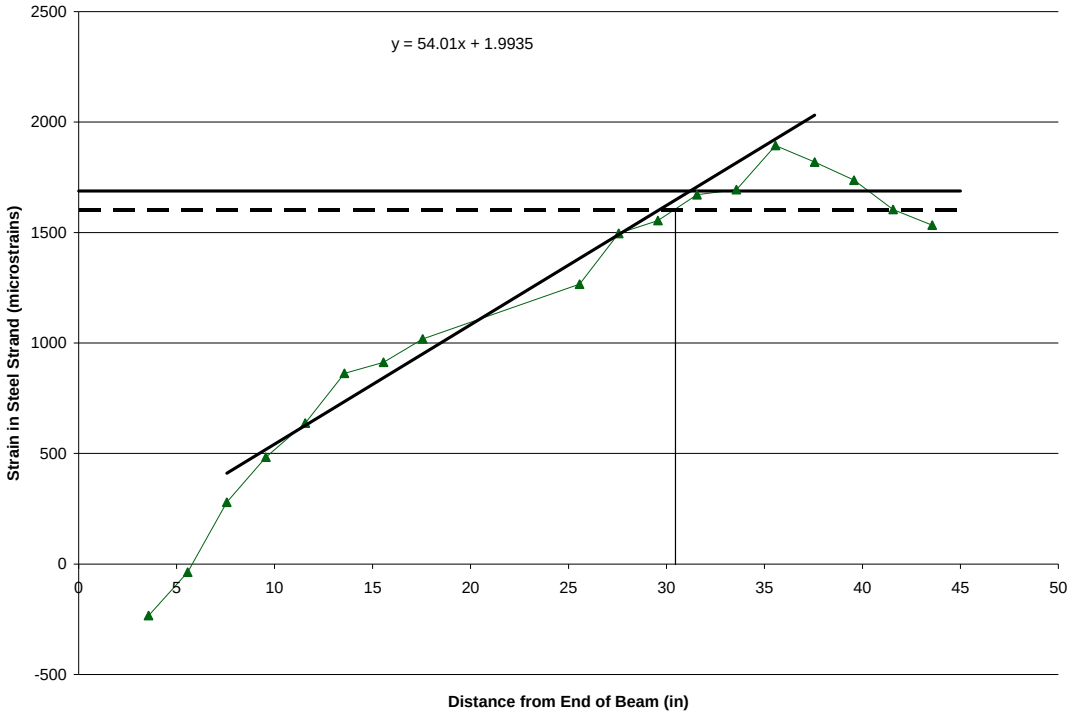

Figure E.9. Transfer length graph of the North end of Girder 1 at 28 days.

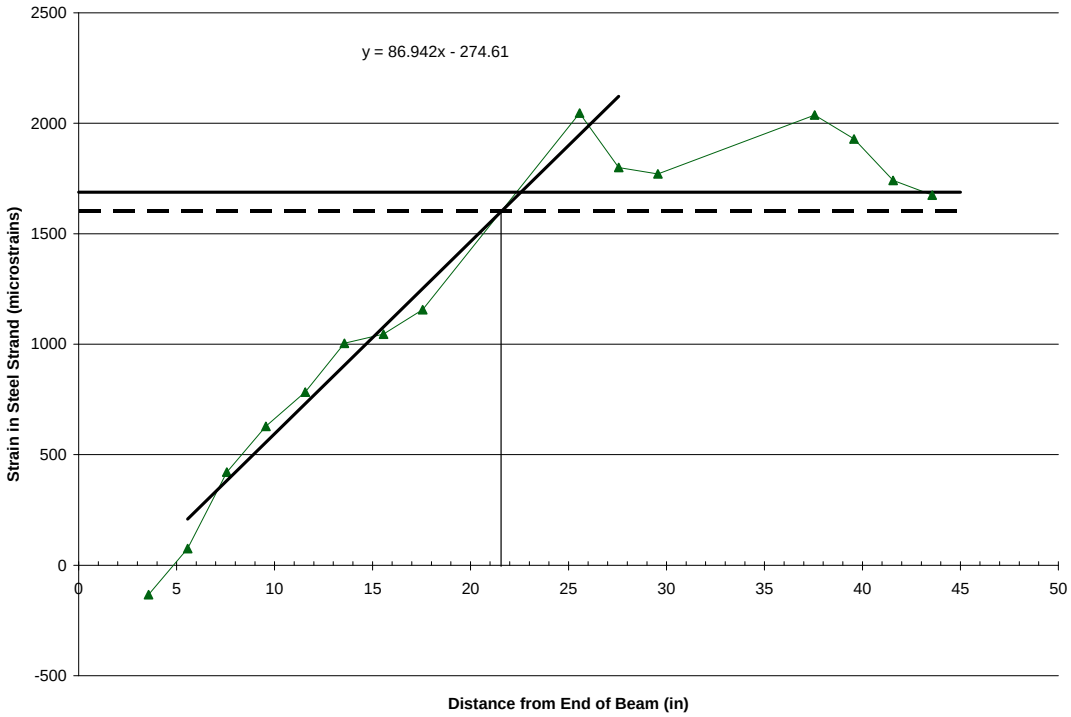

Figure E.10. Transfer length graph of the North end of Girder 1 at 80 days.

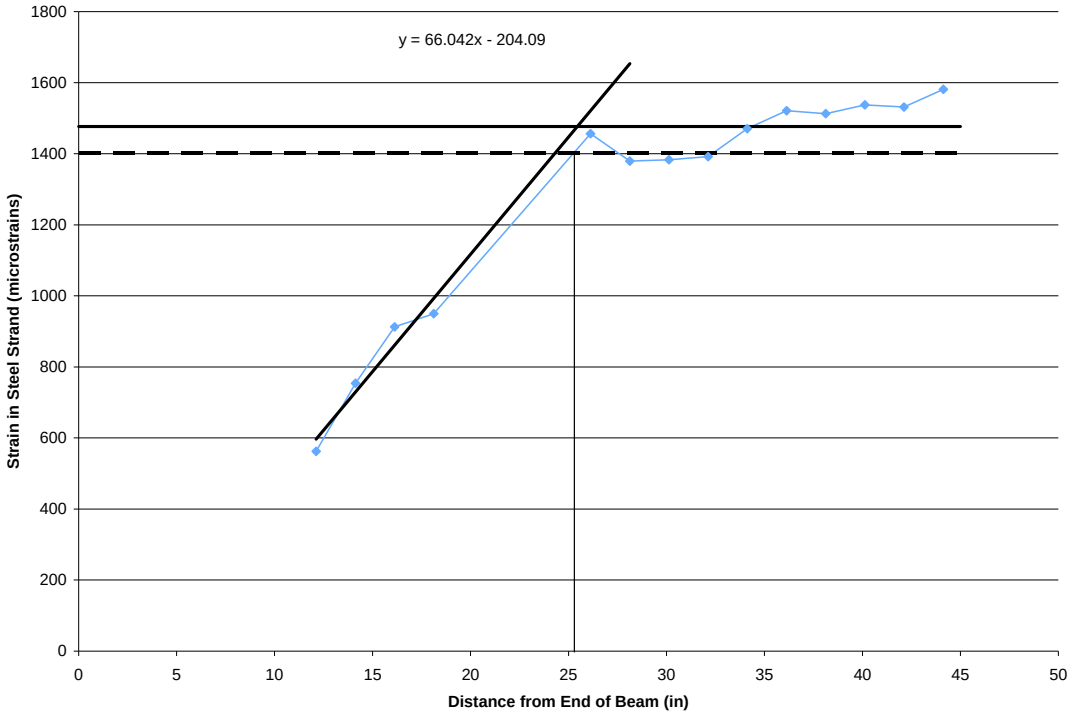

Figure E.11. Transfer length graph of the South end of Girder 2 at 5 days.

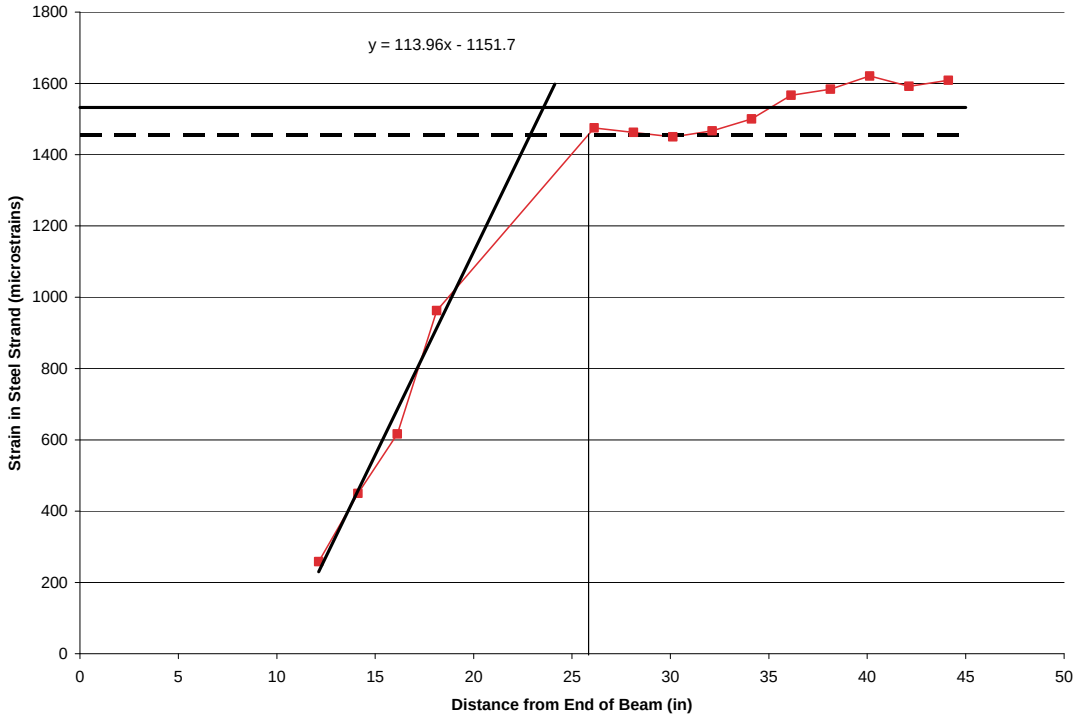

Figure E.12. Transfer length graph of the South end of Girder 2 at 8 days.

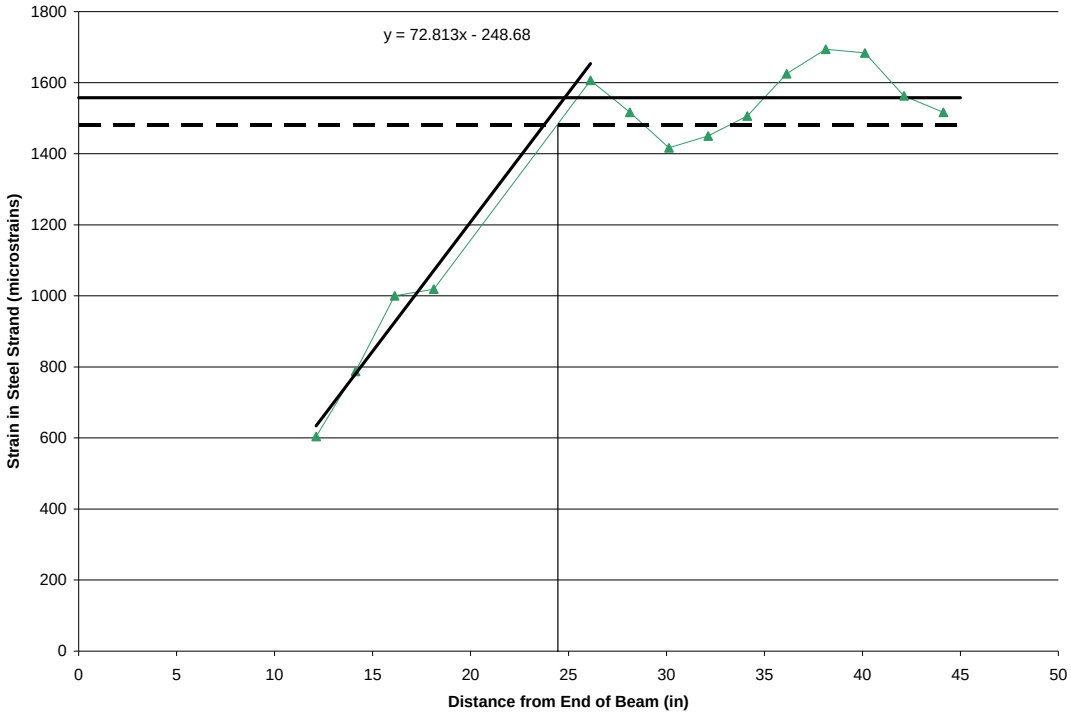

Figure E.13. Transfer length graph of the South end of Girder 2 at 14 days.

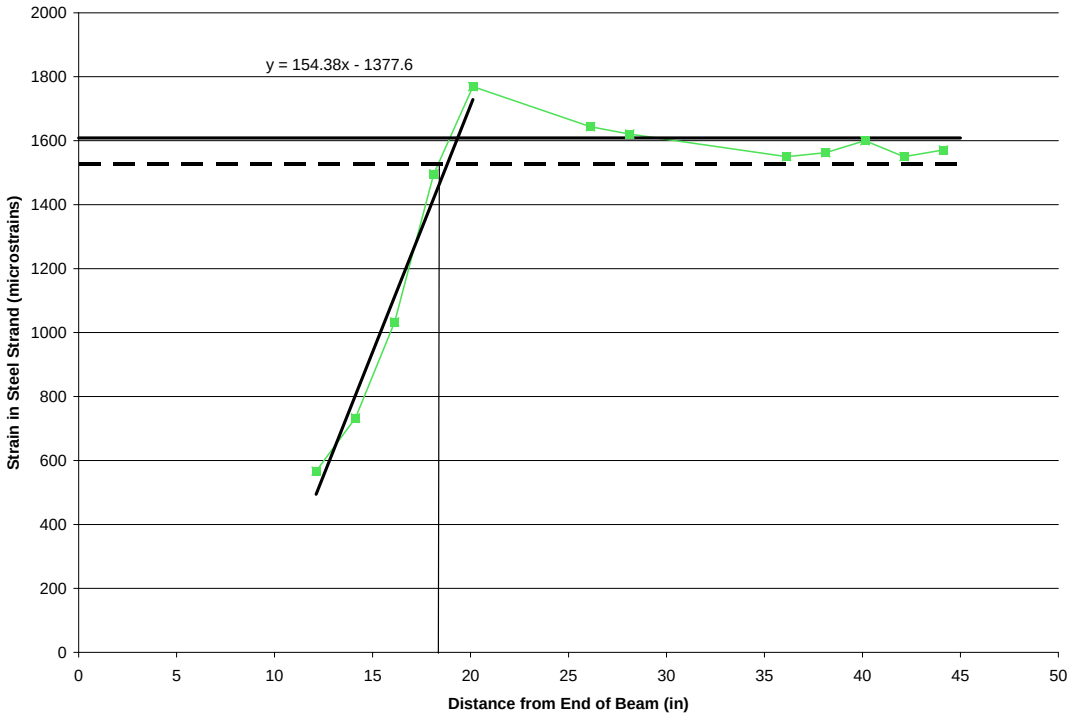

Figure E.14. Transfer length graph of the South end of Girder 2 at 28 days.

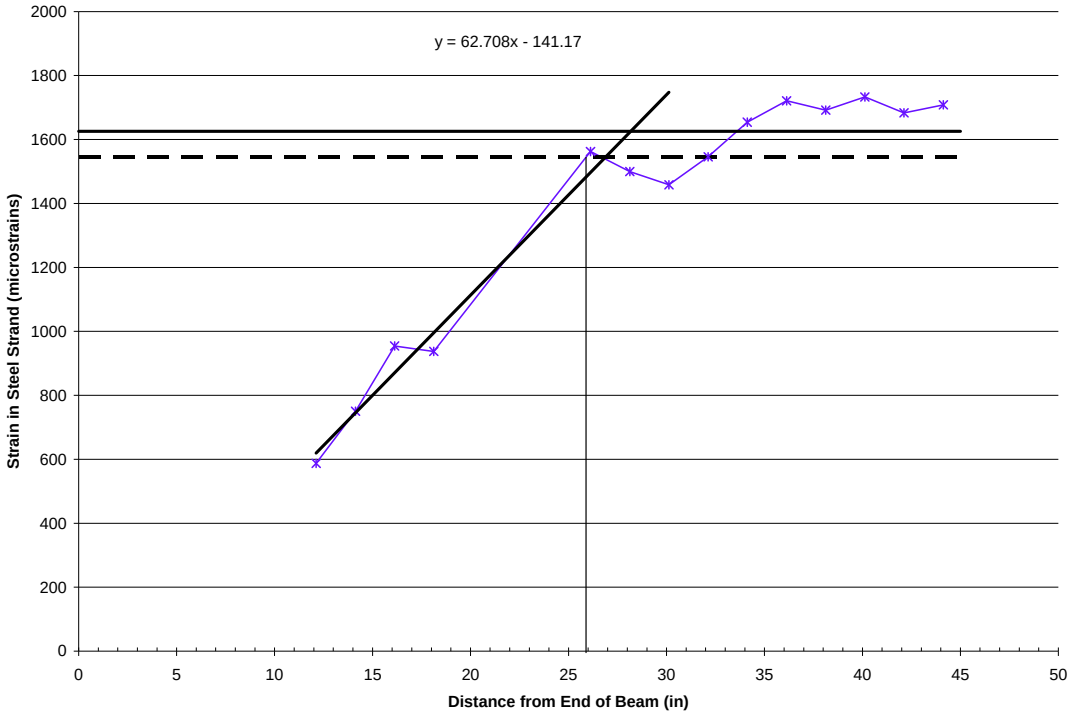

Figure E.15. Transfer length graph of the South end of Girder 2 at 80 days.

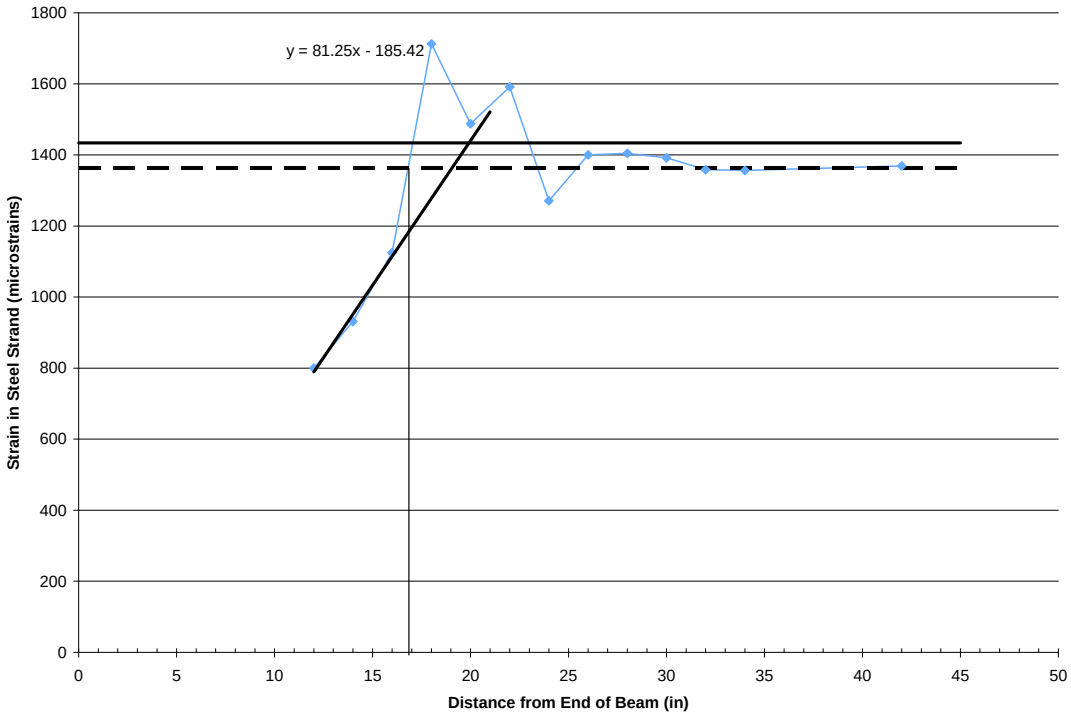

Figure E.16. Transfer length graph of the North end of Girder 2 at 5 days.

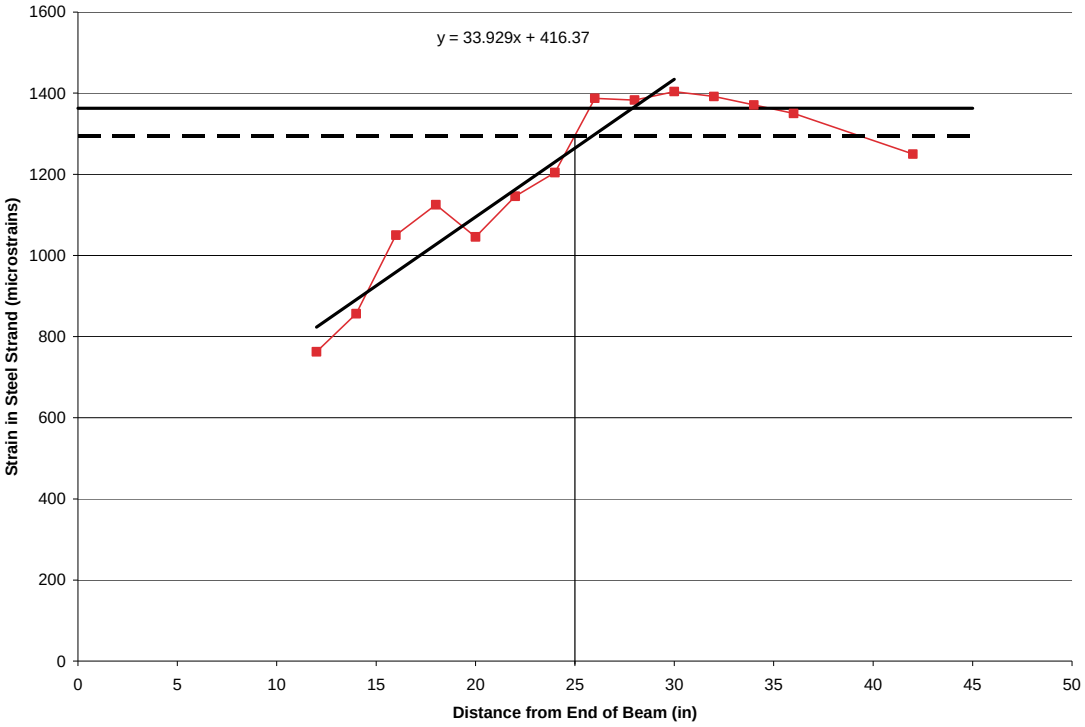

Figure E.17. Transfer length graph of the North end of Girder 2 at 8 days.

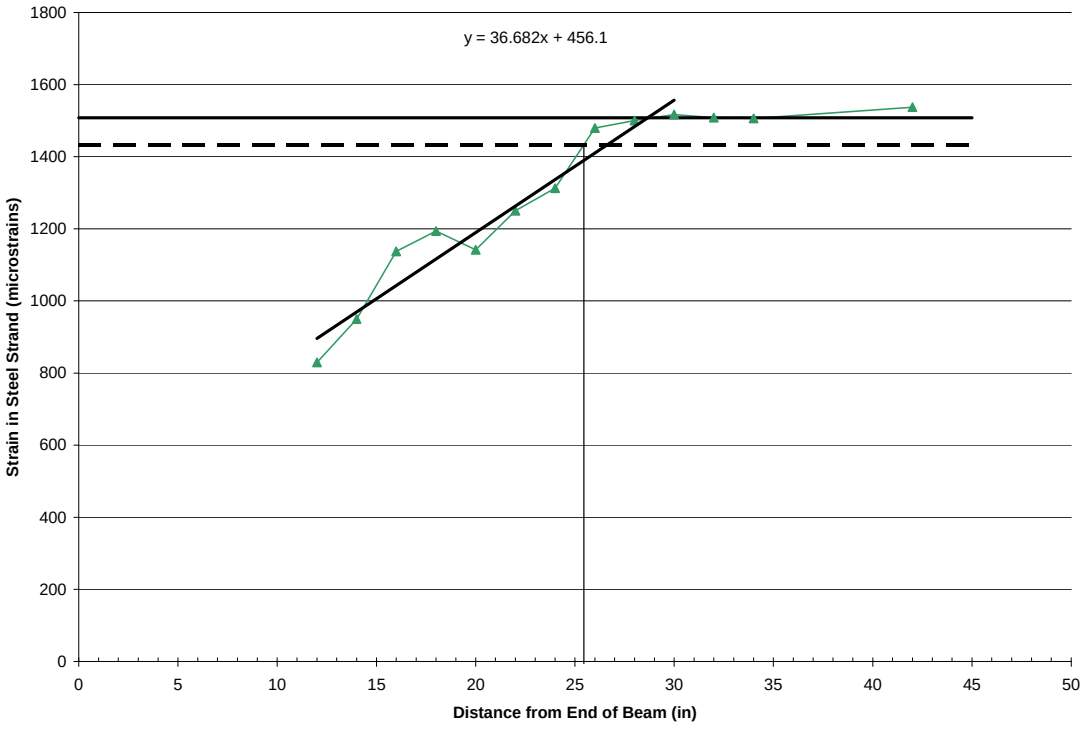

Figure E.18. Transfer length graph of the North end of Girder 2 at 14 days.

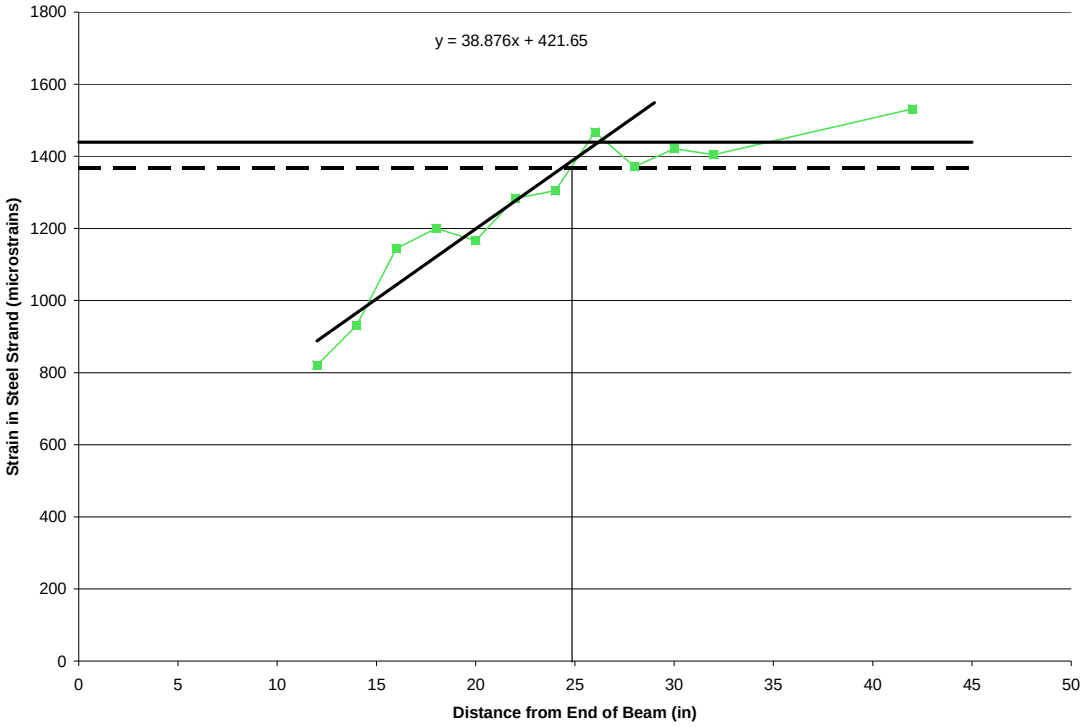

Figure E.19. Transfer length graph of the North end of Girder 2 at 28 days.

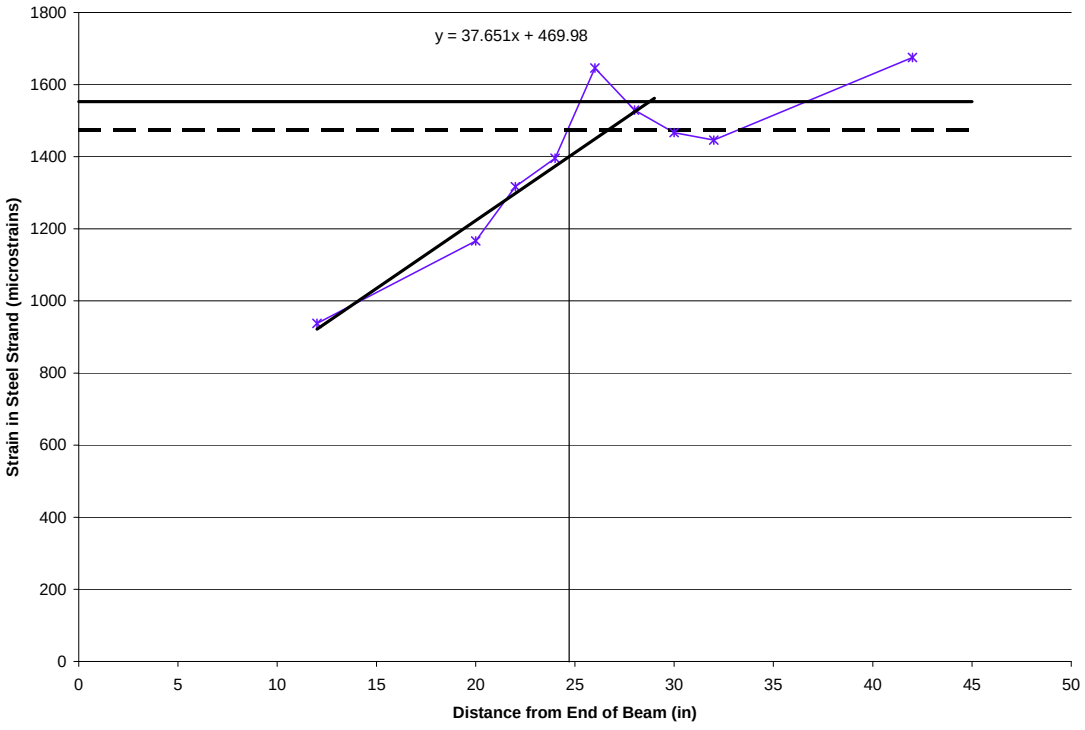

Figure E.20. Transfer length graph of the North end of Girder 2 at 80 days.

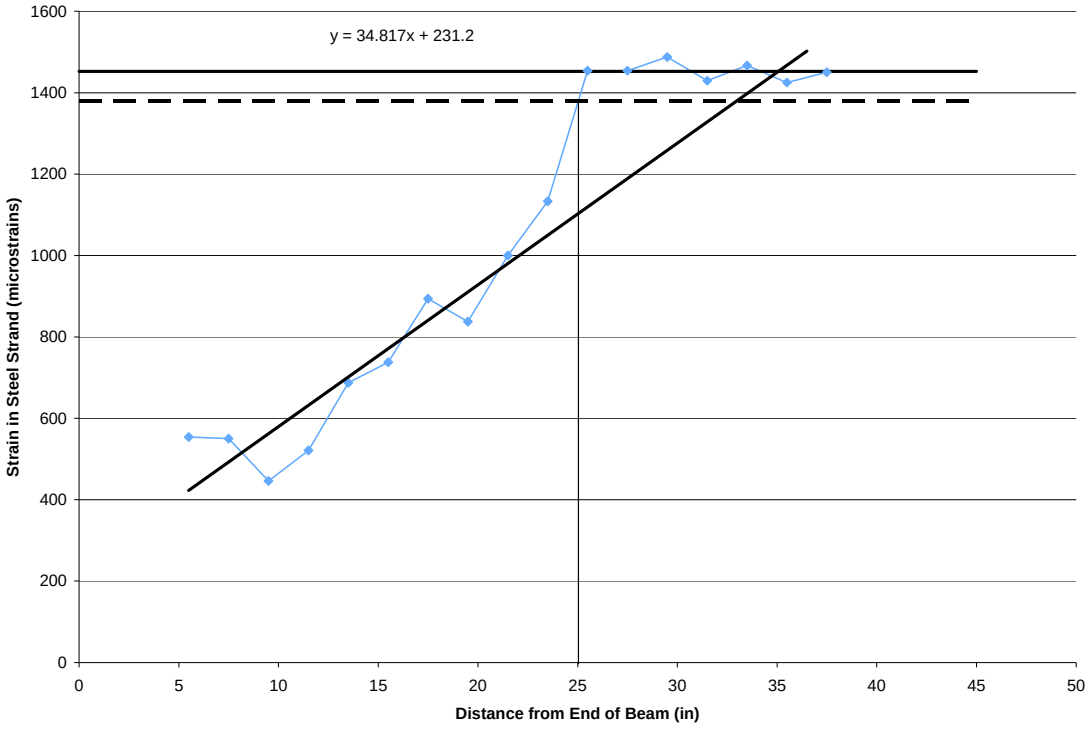

Figure E.21. Transfer length graph of the South end of Girder 3 at 5 days.

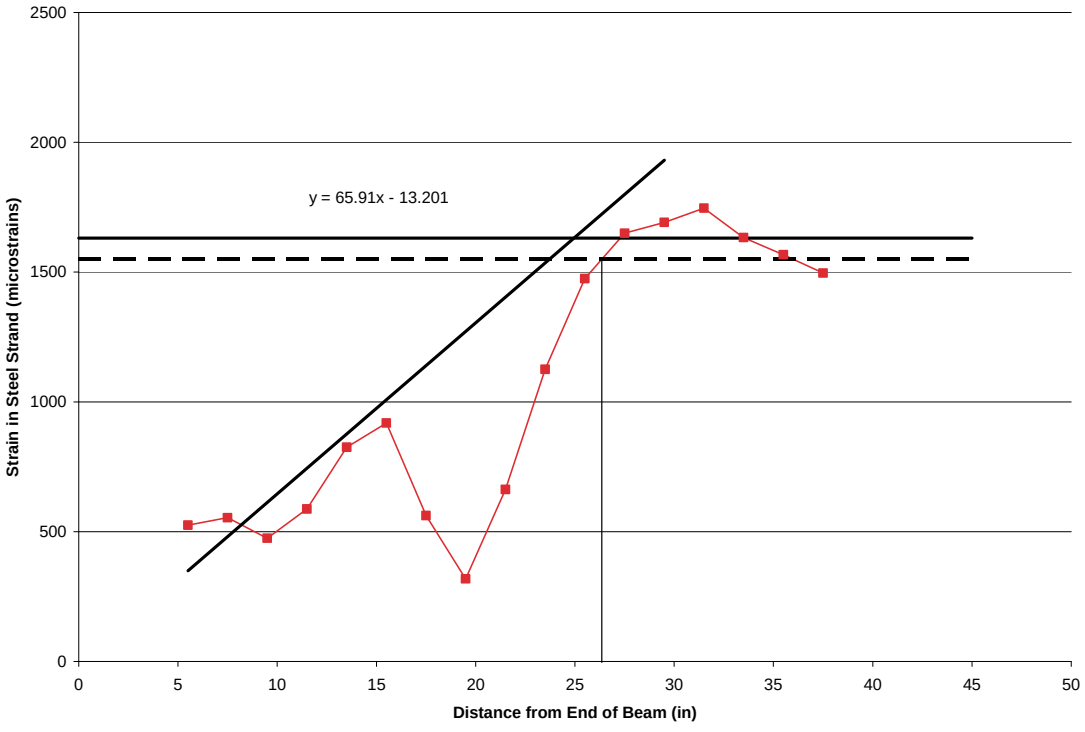

Figure E.22. Transfer length graph of the South end of Girder 3 at 8 days.

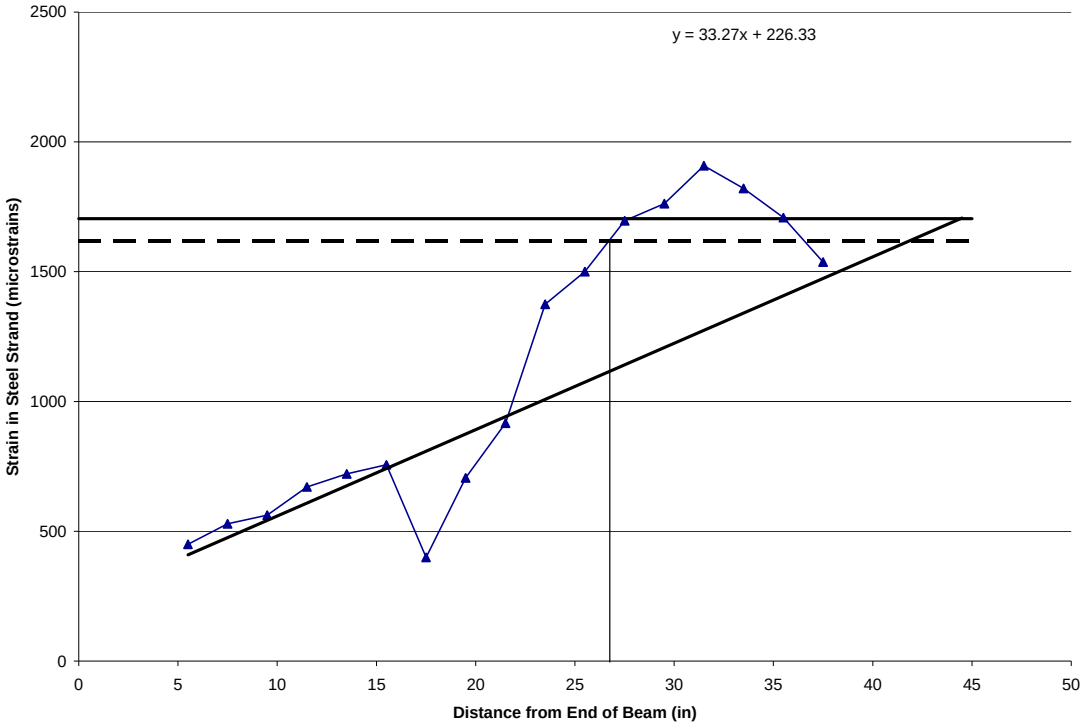

Figure E.23. Transfer length graph of the South end of Girder 3 at 14 days.

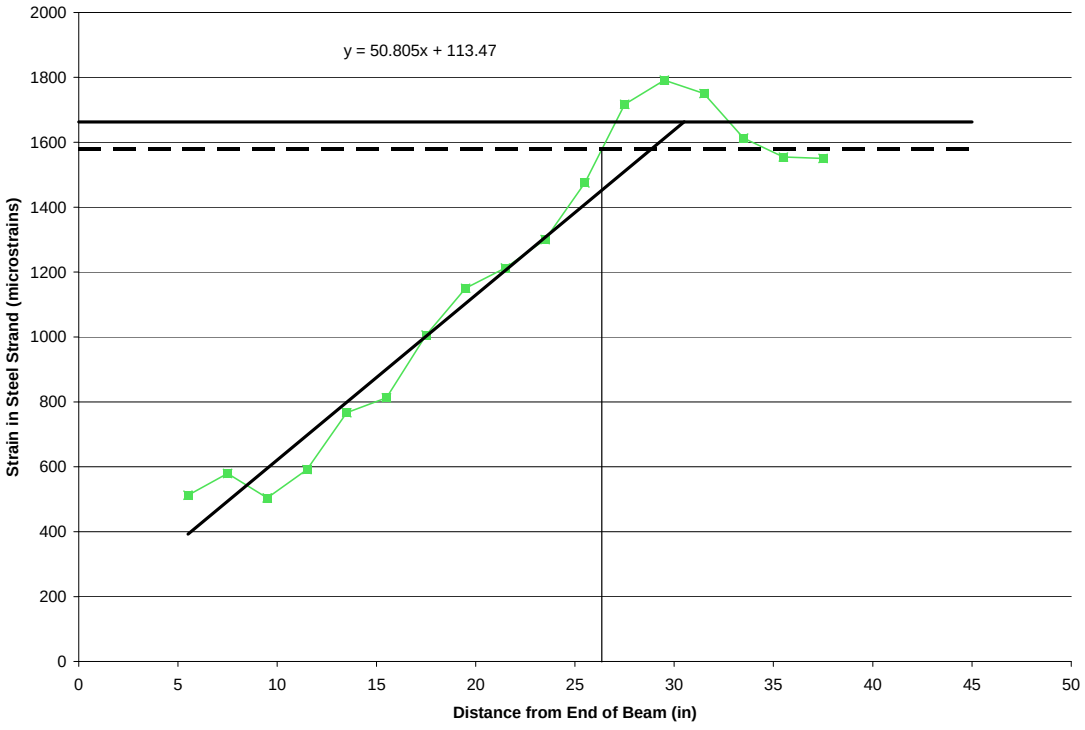

Figure E.24. Transfer length graph of the South end of Girder 3 at 28 days.

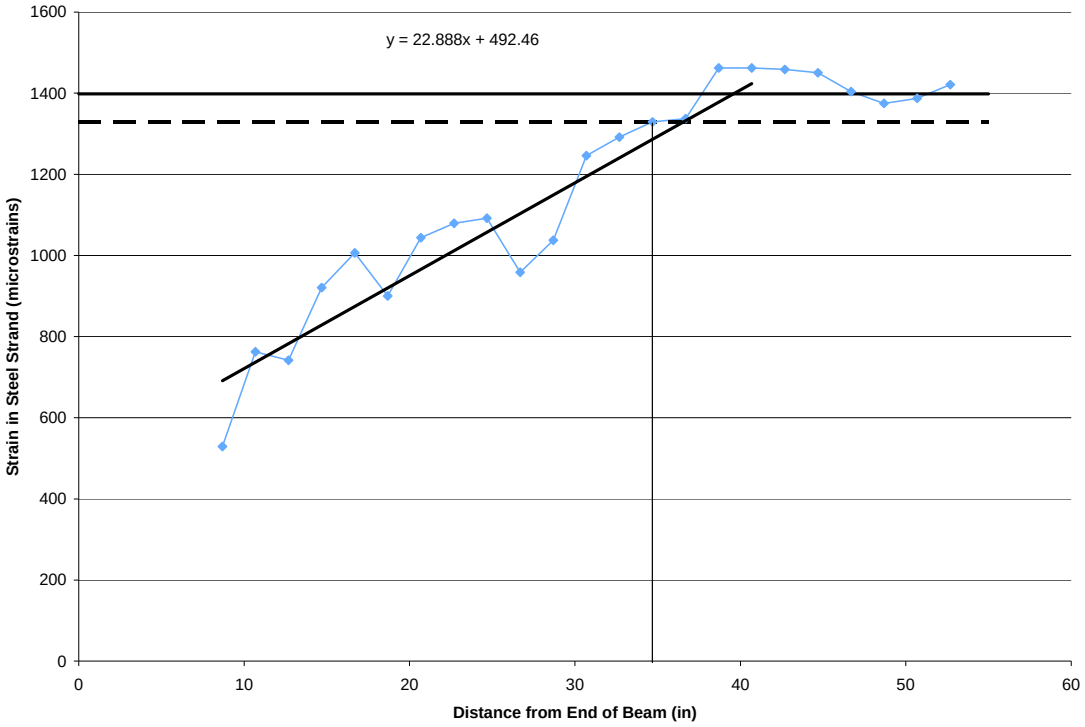

Figure E.25. Transfer length graph of the North end of Girder 3 at 5 days.

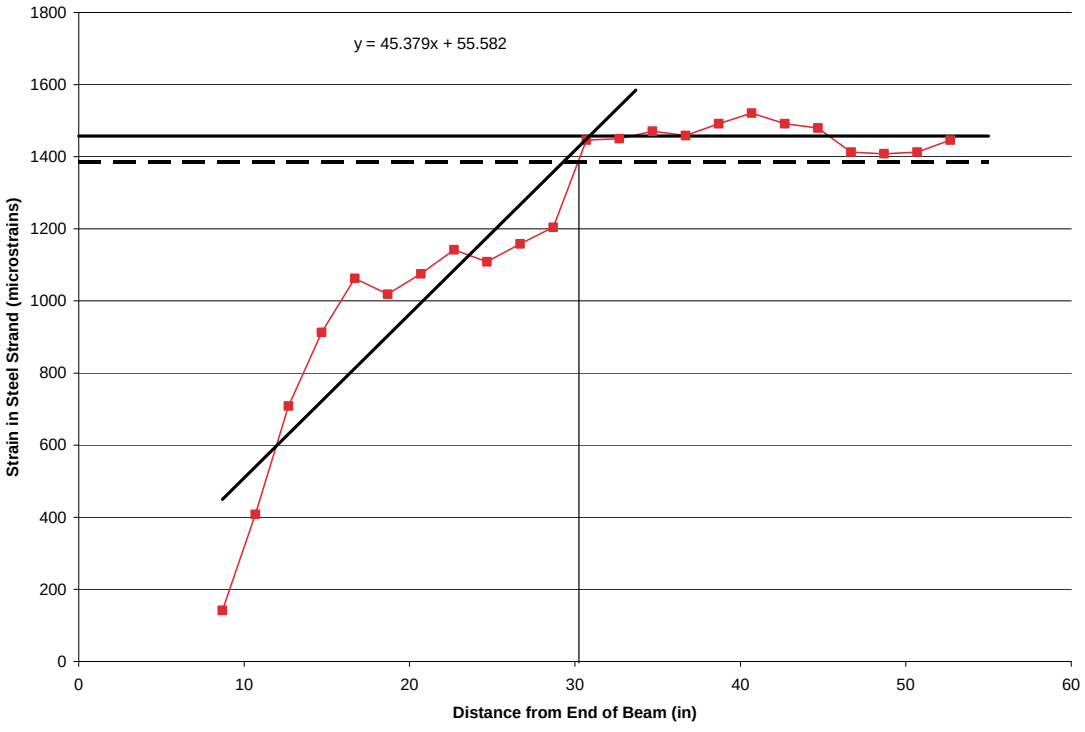

Figure E.26. Transfer length graph of the North end of Girder 3 at 8 days.

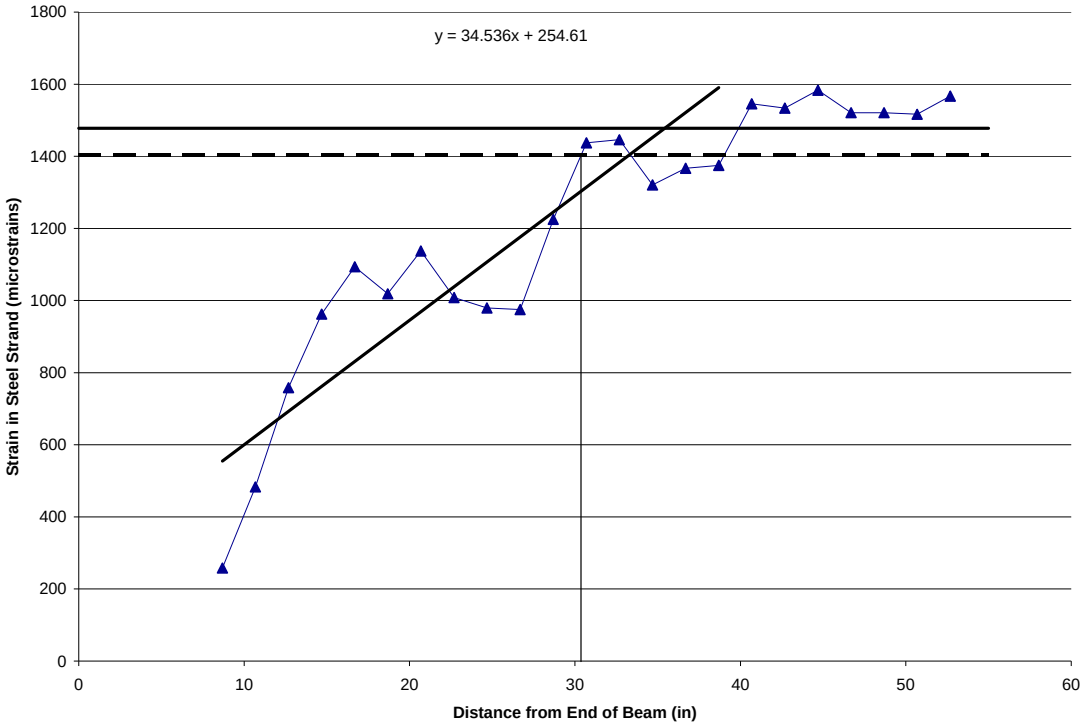

Figure E.27. Transfer length graph of the North end of Girder 3 at 14 days.

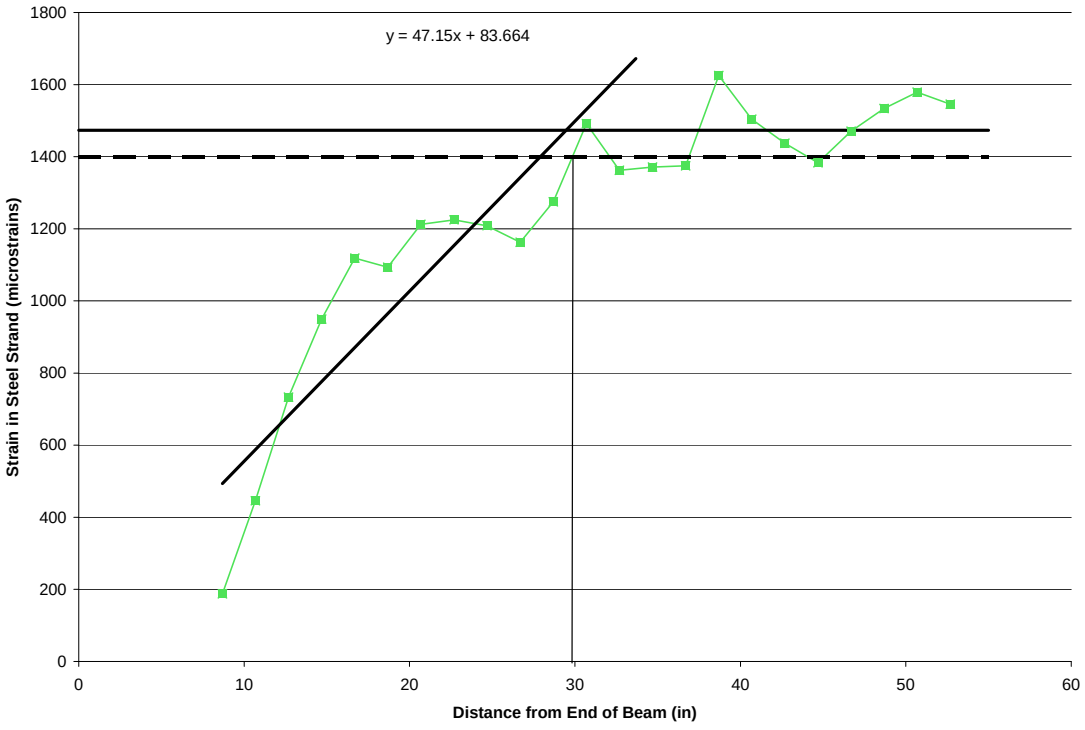

Figure E.28. Transfer length graph of the North end of Girder 3 at 28 days.

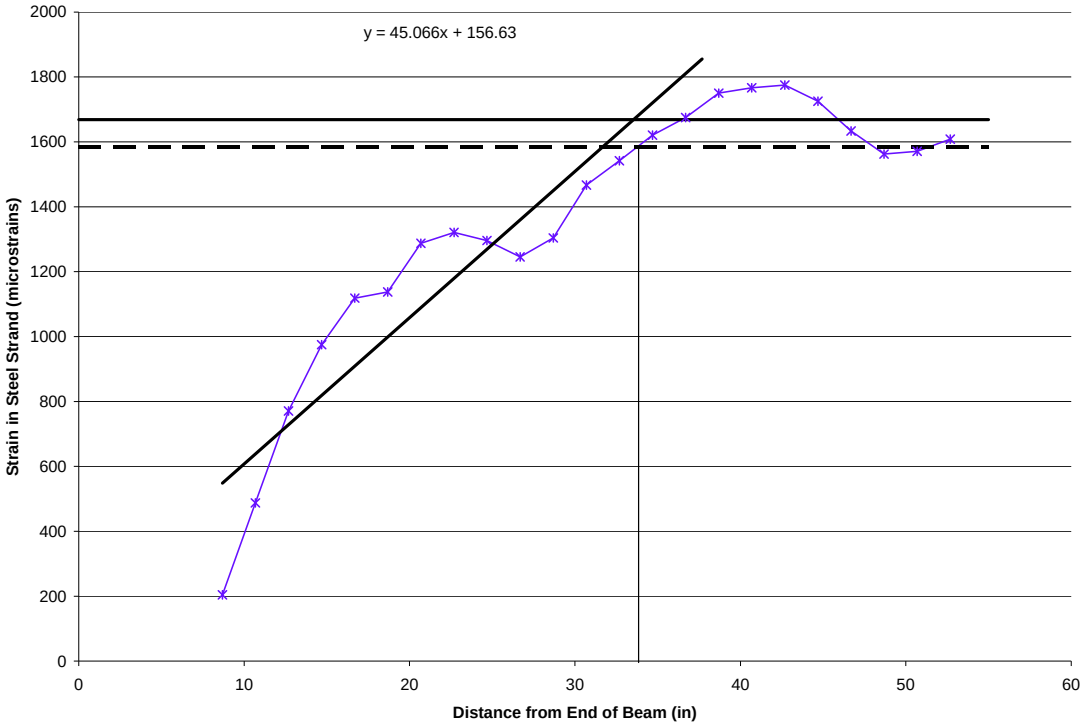

Figure E.29. Transfer length graph of the North end of Girder 3 at 80 days.

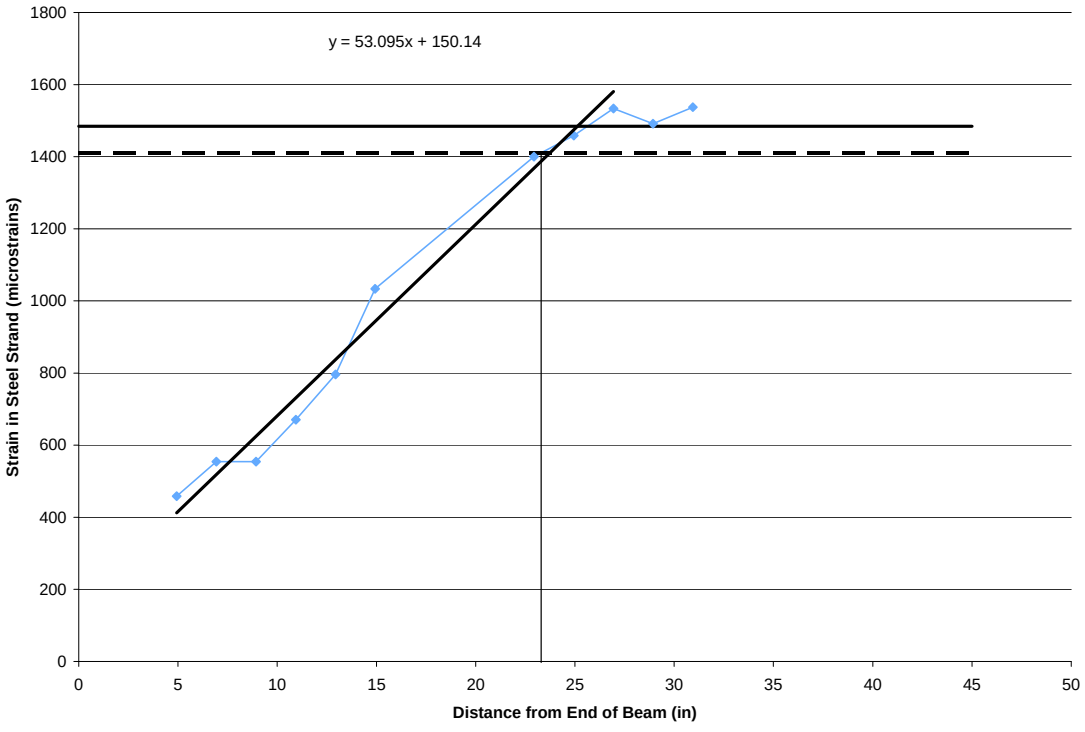

Figure E.30. Transfer length graph of the South end of Girder 4 at 5 days.

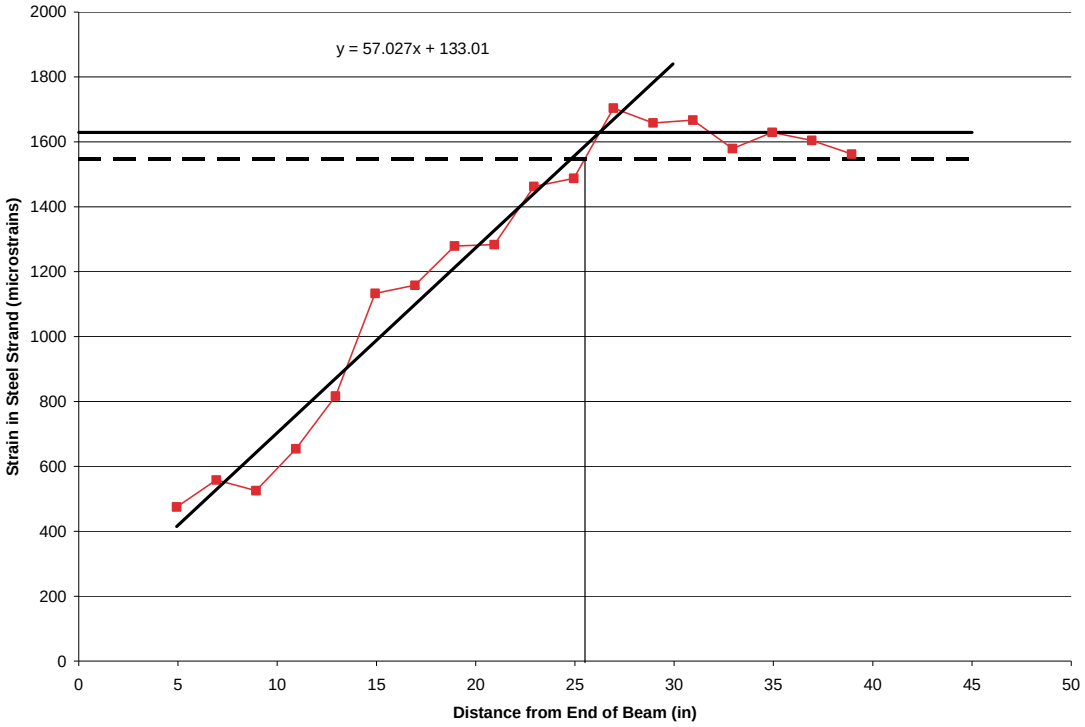

Figure E.31. Transfer length graph of the South end of Girder 4 at 8 days.

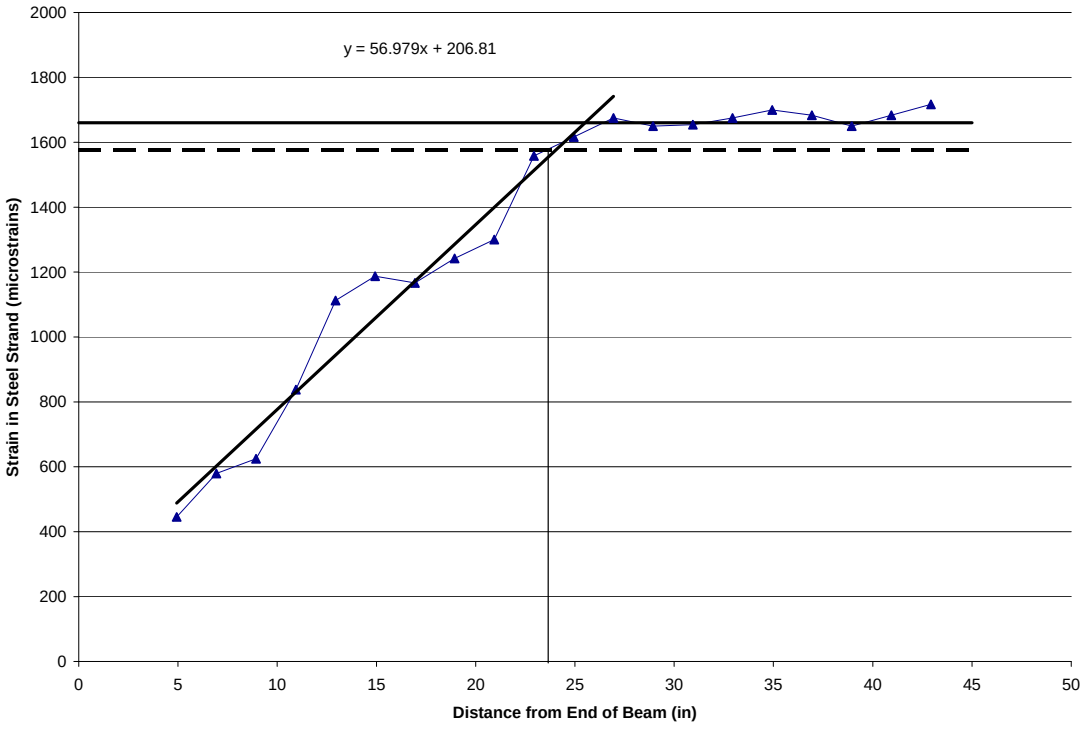

Figure E.32. Transfer length graph of the South end of Girder 4 at 14 days.

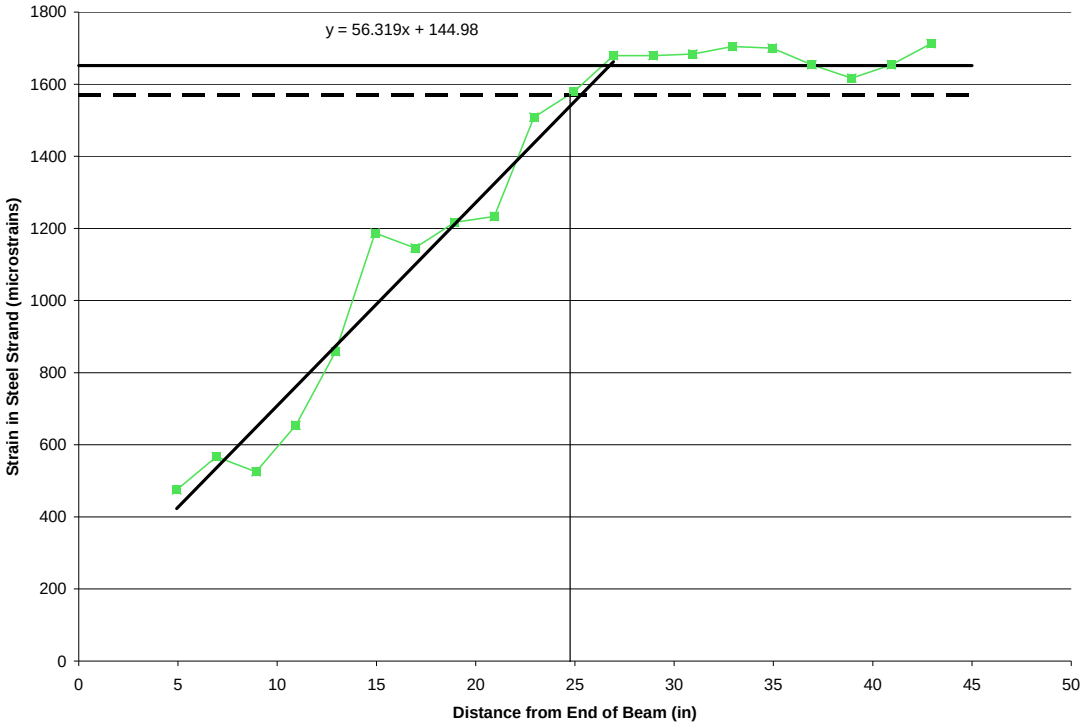

Figure E.33. Transfer length graph of the South end of Girder 4 at 28 days.

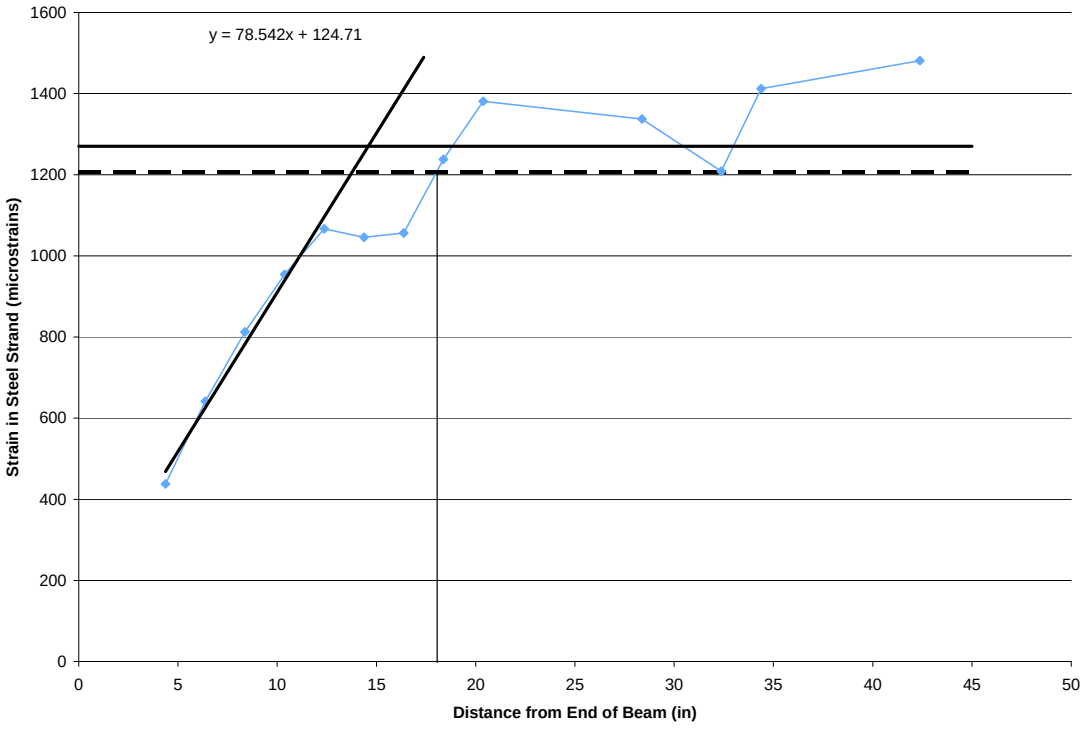

Figure E.34. Transfer length graph of the South end of Girder 2 at 5 days.

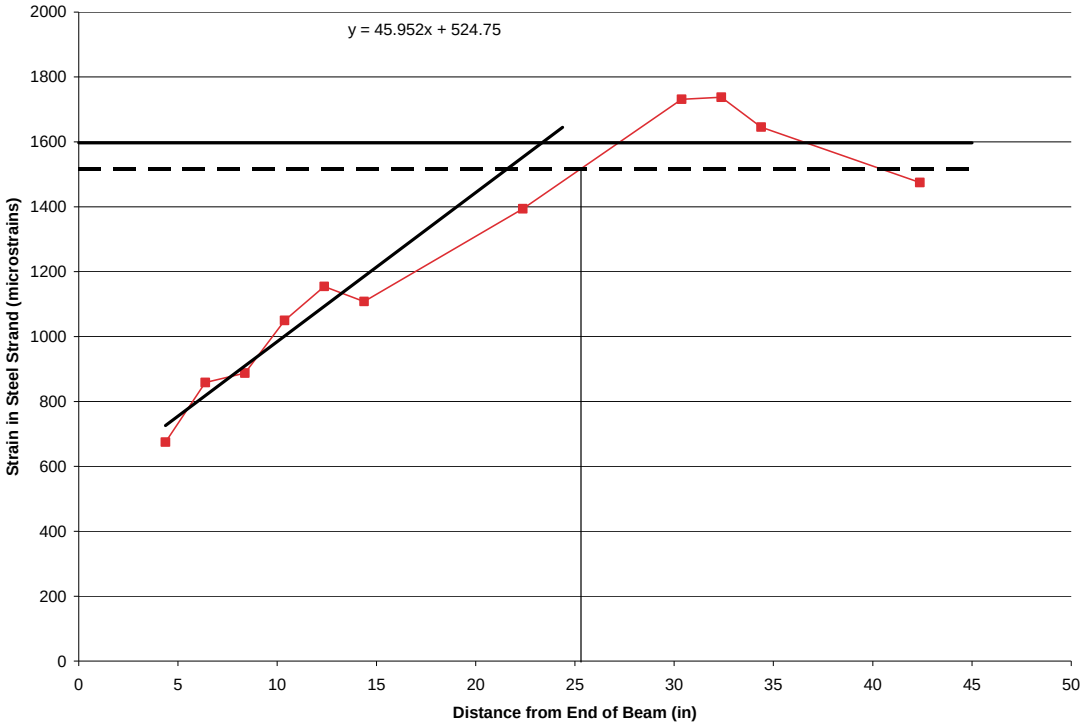

Figure E.35. Transfer length graph of the South end of Girder 2 at 8 days.

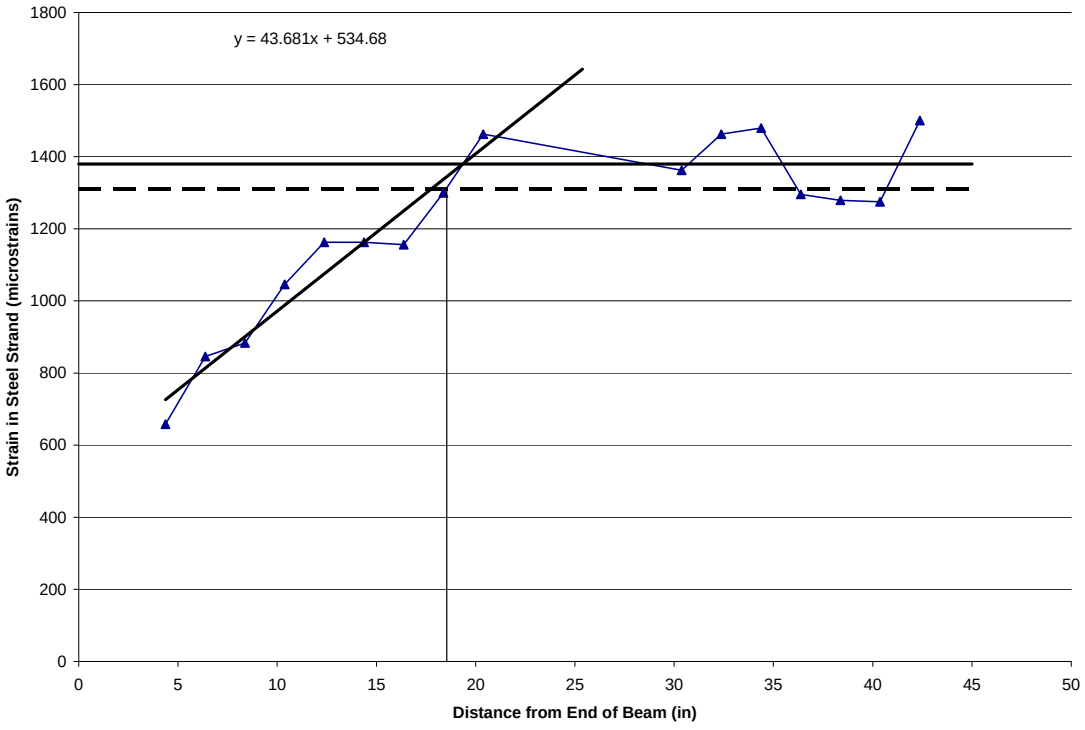

Figure E.36. Transfer length graph of the South end of Girder 2 at 14 days.

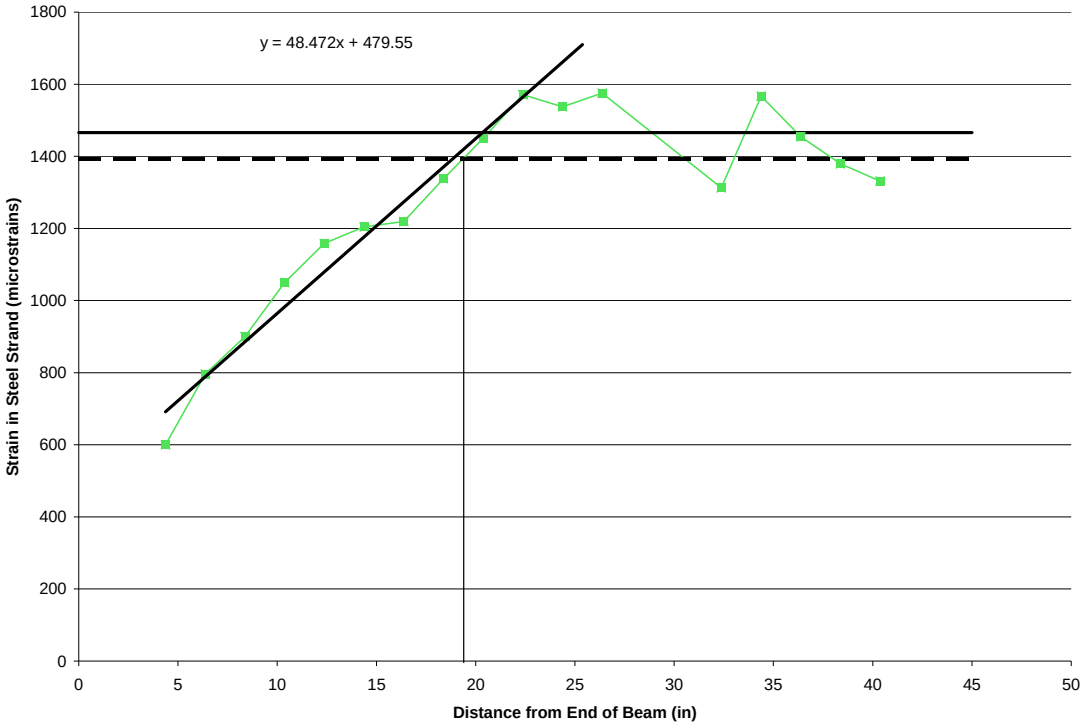

Figure E.37. Transfer length graph of the South end of Girder 2 at 28 days.

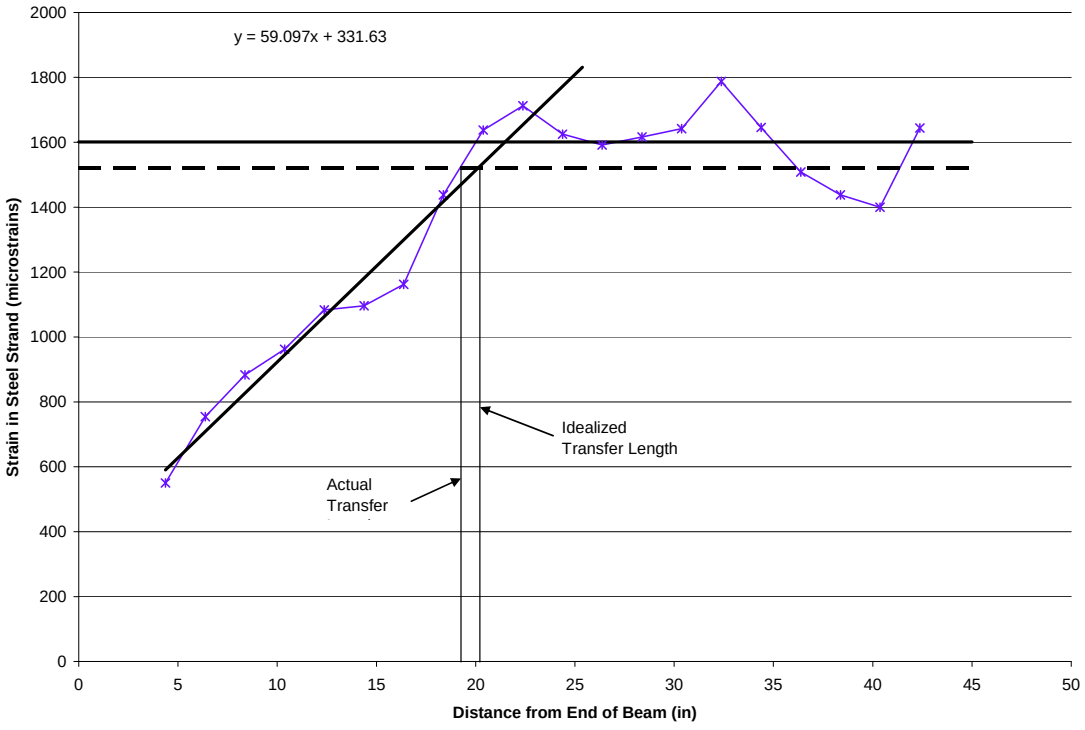

Figure E.38. Transfer length graph of the South end of Girder 2 at 80 days.

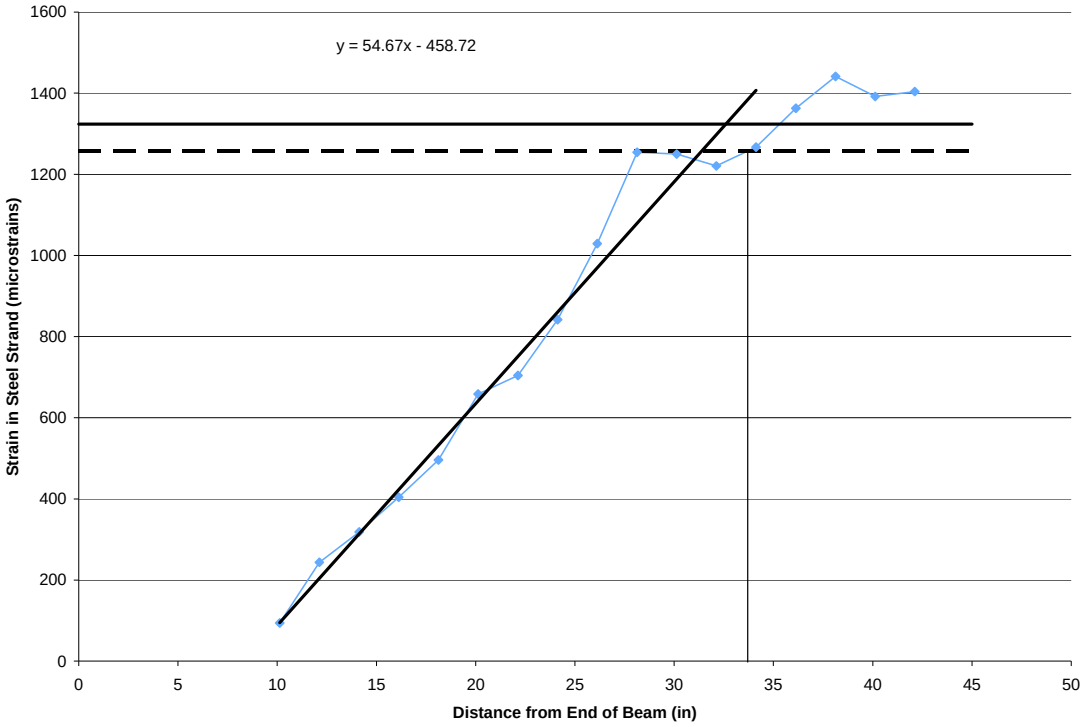

Figure E.39. Transfer length graph of the North end of Girder 2 at 5 days.

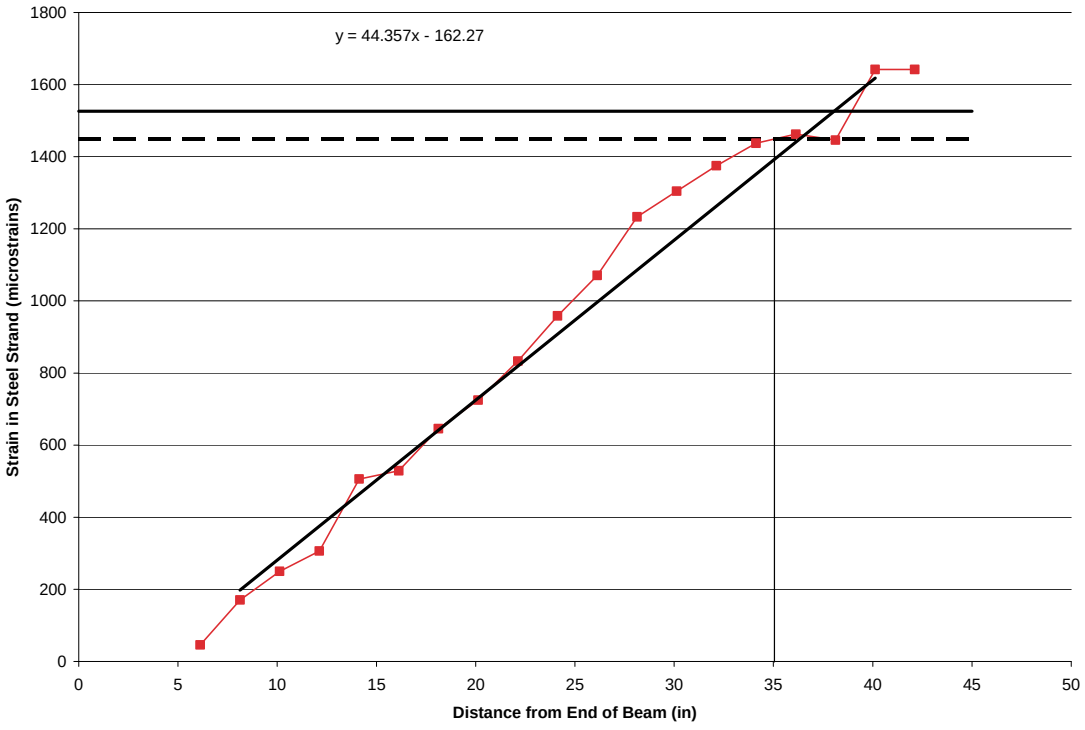

Figure E.40. Transfer length graph of the North end of Girder 2 at 8 days.

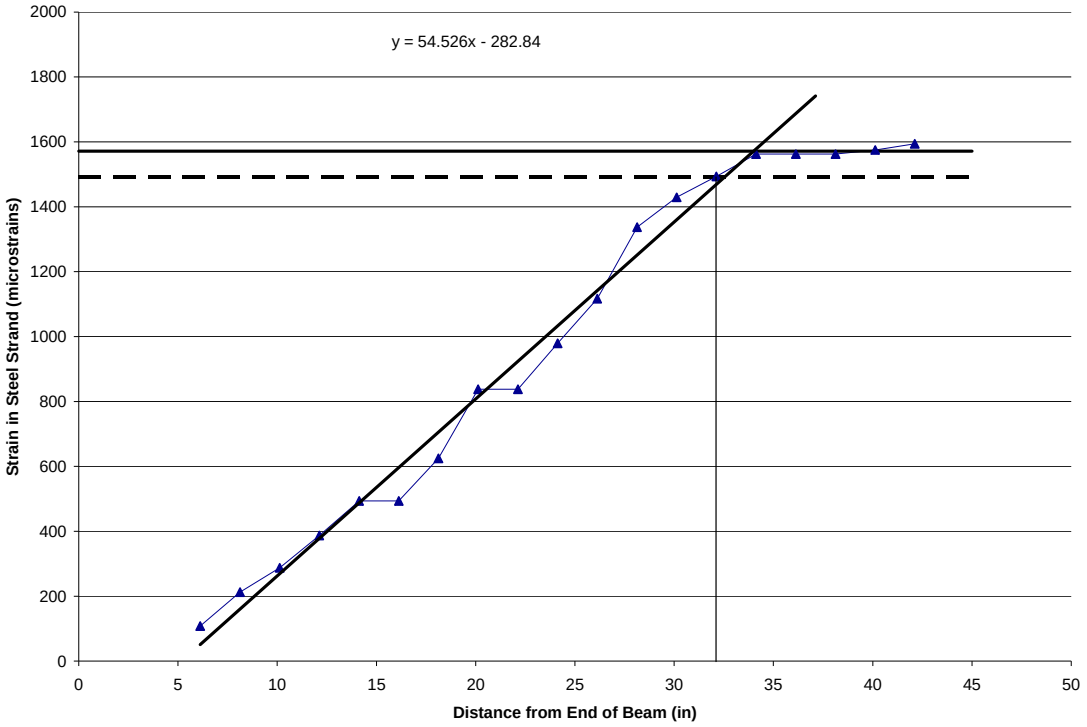

Figure E.41. Transfer length graph of the North end of Girder 2 at 14 days.

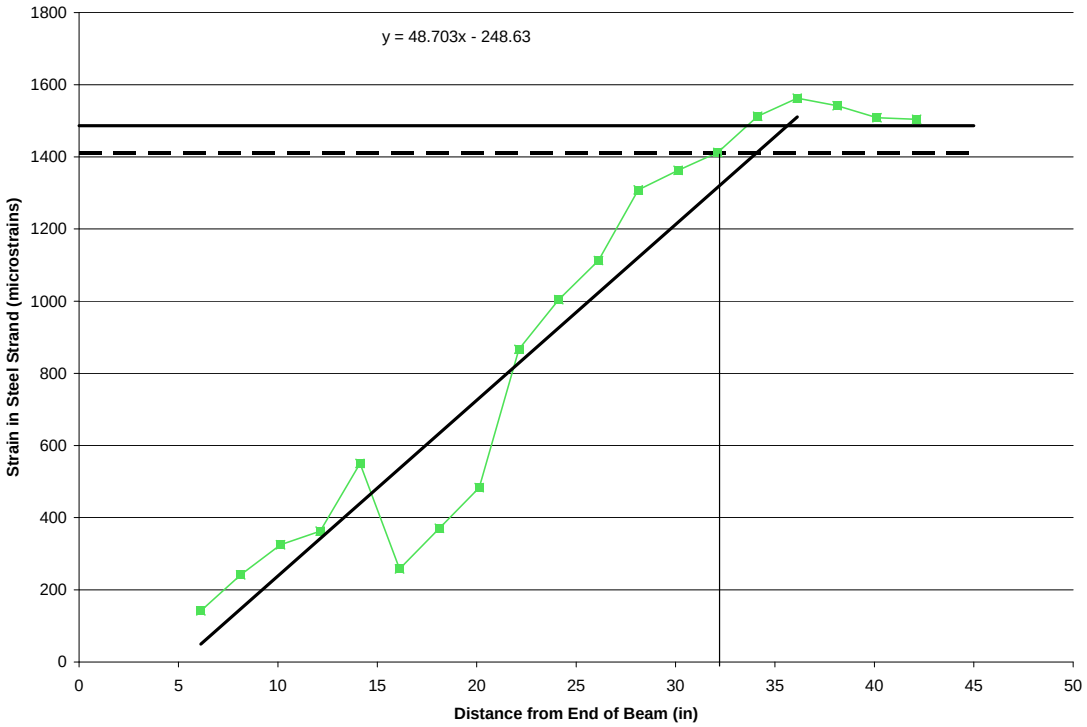

Figure E.42. Transfer length graph of the North end of Girder 2 at 28 days.

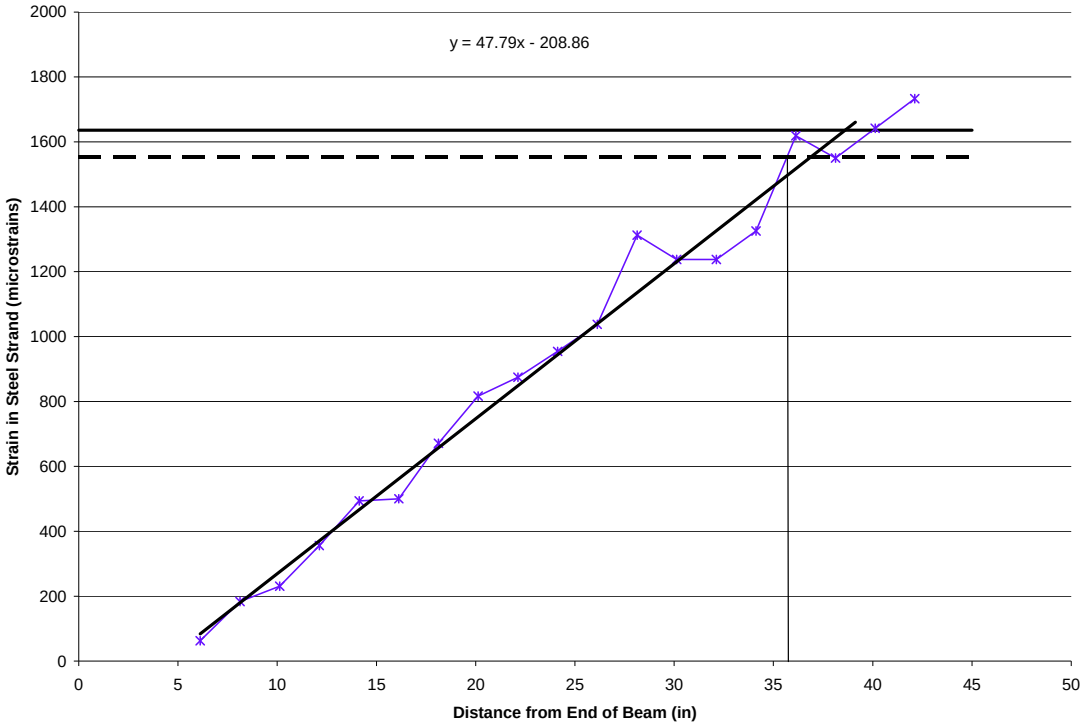

Figure E.43. Transfer length graph of the North end of Girder 2 at 80 days.

APPENDIX F

GTSTRUDL INPUT AND OUTPUT FOR LOAD TEST ANALYSIS

GTSTRUDL model of Pin-Pin supports:

INPUT:

```
STRUDL 'Pinned'
$$
$$    This   GTSTRUDL file created from GTMenu on  2/28/2009
$$

UNITS  INCH  KIPS  DEG   FAH
JOINT COORDINATES GLOBAL
   1            0.0000000E+00  0.0000000E+00  0.0000000E+00
   2            1.2960000E+03  0.0000000E+00  0.0000000E+00

TYPE  PLANE FRAME XY
MEMBER INCIDENCES
  1          1          2

UNITS  INCH  KIPS  DEG   FAH
MEMBER ECCENTRICITIES GLOBAL
   1          -
 START  0.0000000E+00  2.7629999E+01  0.0000000E+00  -
  END   0.0000000E+00  2.7629999E+01  0.0000000E+00

UNITS  INCH  KIPS  DEG   FAH
MEMBER PROPERTIES   PRISMATIC   AX  6.5900006E+02   IZ  2.6807703E+05
   1

STATUS SUPPORT  -
   1          2

UNITS  INCH  KIPS  DEG   FAH
JOINT RELEASES
   1          2          -
     MOM  Z

UNITS  INCH  KIPS  DEG   FAH
CONSTANTS
    E    3.7900005E+03  ALL
    G    1.4400002E+03  ALL
    POI  2.1850000E-01  ALL
    DEN  8.6800013E-05  ALL
    CTE  5.5000000E-06  ALL

UNITS  INCH  KIPS  DEG   FAH
```

LOADING 'Test'
MEMB LOADS FOR Y GLO CON FRA P -1.7940001E+01 L 5.0000000E-01
1

OUTPUT FROM STIFFNESS ANALYSIS:

INTERNAL MEMBER RESULTS

MEMBER DISPLACEMENTS - Relative to member chord

--- Member 1 ---
---

* Maximum and Minimum Section Displacements for Member 1 *					
* Relative to member chord Units = INCH *					
*	Displacement	Disp/length	Loading	FR Location	*
*	---	---	---	---	*
* X	Max: 0.00000	0.00000	Test	1.000	*
*	Min: 0.00000	0.00000	Test	0.500	*
*					*
* Y	Max: 0.00000	0.00000	Test	0.000	*
*	**Min: -0.40896**	0.00032	Test	0.500	*
*					*
* Z	Max: 0.00000	0.00000	Test	0.000	*
*	Min: 0.00000	0.00000	Test	0.000	*

GTSTRUDL model of Pin-Roller supports:

INPUT:

```
STRUDL 'Roller'
$$
$$    This   GTSTRUDL file created from GTMenu on  2/27/2009
$$

UNITS  INCH  KIPS  DEG   FAH
JOINT COORDINATES GLOBAL
   1            0.0000000E+00  0.0000000E+00  0.0000000E+00
   2            1.2960000E+03  0.0000000E+00  0.0000000E+00

TYPE  PLANE FRAME XY
MEMBER INCIDENCES
  1          1          2

UNITS  INCH  KIPS  DEG   FAH
MEMBER PROPERTIES   PRISMATIC   AX  6.5900000E+02   IZ  2.6807700E+05
   1

STATUS SUPPORT  -
   1          2

UNITS  INCH  KIPS  DEG   FAH
JOINT RELEASES
   1          -
     MOM  Z
   2          -
     FOR  X  MOM  Z

UNITS  INCH  KIPS  DEG   FAH
CONSTANTS
    E    3.7900002E+03  ALL
    G    1.4400001E+03  ALL
    POI  2.1850000E-01  ALL
    DEN  8.6800006E-05  ALL
    CTE  5.5000000E-06  ALL

UNITS  INCH  KIPS  DEG   FAH
LOADING 'Test'
  MEMB LOADS  FOR Y GLO CON FRA  P  -1.7940001E+01 L   5.0000000E-01
   1
```

OUTPUT FROM STIFFNESS ANALYSIS:

INTERNAL MEMBER RESULTS

MEMBER DISPLACEMENTS - Relative to member chord

--- Member 1 ---

==========
* Maximum and Minimum Section Displacements for Member 1 *
* Relative to member chord Units = INCH *

==========

		Displacement	Disp/length	Loading	FR Location
* X	Max:	0.00000	0.00000	Test	0.000 *
*	Min:	0.00000	0.00000	Test	0.000 *
*					*
* Y	Max:	0.00000	0.00000	Test	1.000 *
*	**Min:**	**-0.80075**	0.00062	Test	0.500 *
*					*
* Z	Max:	0.00000	0.00000	Test	0.000 *
*	Min:	0.00000	0.00000	Test	0.000 *

==========

REFERENCES

ACI Committee 318 (2008). "Building Code Requirements for Structural Concrete (ACI 318-08) and Commentary" American Concrete Institute. Farmington Hills, Michigan, 2008.

ACI Committee 363R-92 (1997). "Report on High-Strength Concrete" American Concrete Institute. Farmington Hills, Michigan, 2005.

ASTM C 31, *Standard Test Method for Making and Curing Concrete Test Specimens in the Field*, American Society for Testing and Materials, West Conshohocken, PA, 2008, 6pp.

ASTM C 39, *Standard Test Method for Compressive Strength of Cylindrical Concrete Specimens*, American Society for Testing and Materials, West Conshohocken, PA, 2005, 7pp.

ASTM C 469, *Standard Test Method for Static Modulus of Elasticity and Poisson's Ration of Concrete in Compression*, American Society for Testing and Materials, West Conshohocken, PA, 2002, 5pp.

ASTM C 496, *Standard Test Method for Splitting Tensile Strength of Cylindrical Concrete Specimens*, American Society for Testing and Materials, West Conshohocken, PA, 2004, 5pp.

ASTM C 1202, *Standard Test Method for Electrical Indication of Concrete's Ability to Resist Chloride Ion Penetration*, American Society for Testing and Materials, West Conshohocken, PA, 2007, 6pp.

Buchberg, Brandon S., "Investigation of Mix Design and Properties of High-Strength/High-Performance Lightweight Concrete," Masters Thesis, Georgia Institute of Technology, 2002, 453pp.

Castrodale, Reid W. and Kenneth S. Harmon, "Recent Projects Using Lightweight and Specified Density Concrete for Precast Bridge Elements," *Proceedings*, 2007 National Bridge Conference, Phoenix, AZ, PCI, October 22-24, 2007.

CRD C 39. "Method of Test for Coefficient of Linear Thermal Expansion of Concrete," Handbook Concrete and Cement, U.S. Army Engineer Waterways Experiment Station, Vicksburg, MS, 2pp.

Kelly, Patrick J., and Lawrence F. Kahn, "Bearing Zone Cracking of Precast Prestressed Concrete Bridge Girders," Final Report, Georgia Department of Transportation, Project No. 05-14, February 2007, 237pp.

Lopez, Mauricio, "Creep and Shrinkage of High Performance Lightweight Concrete: A Multi-scale Investigation," Doctoral Thesis, Georgia Institute of Technology, 2005, 530pp.

Meyer, Karl F., "Transfer Length and Development of 0.6-inch Diameter Prestressing Strand in High Strength Lightweight Concrete," Doctoral Thesis, Georgia Institute of Technology, 2002, 616pp.

Meyer, Karl F., and Lawrence F. Kahn, "Lightweight Concrete Reduces Weight and Increases Span Length of Pretensioned Concrete Bridge Girders," PCI JOURNAL V. 47, No.1, January-February 2002, pp. 68-75.

National Cooperative Highway Research Program, Report 595: Application of the LRFD Bridge Design Specifications to High-Strength Structural Concrete: Flexure and Compression Provisions, Transportation Research Board, Washington D.C., 2007.

Rosa, Michael A., John F. Stanton, and Marc O. Eberhard, "Improving Predictions for Camber in Precast, Prestressed Concrete Bridge Girders", Research Report Task 68, Washington State Department of Transportation, April 2007, 323pp.

Russell, Bruce W., "Design Guidelines for Transfer, Development and Debonding of Large Diameter Seven Wire Strands in Pretensioned Concrete Girders," Doctoral Thesis, University of Texas at Austin, 1992, 464pp.

AASHTO LRFD Bridge Design Specifications, 4th ed., American Association of Highway and Transportation Officials, Washington D.C., 2007.